5-1979

Evaluation of a Welded Wire Retaining Wall

Jerold Albert Bishop
Utah State University

EVALUATION OF A WELDED WIRE RETAINING WALL

by

Jerold Albert Bishop

A thesis submitted in partial fulfillment
of the requirements for the degree

of

MASTER OF SCIENCE

in

Engineering

UTAH STATE UNIVERSITY

Logan, Utah

1979

ACKNOWLEDGMENTS

I would like to express my appreciation to Mr. Bill Hilfiker of the Hilfiker Pipe Company for his personal interest and assistance as well as for the financial assistance provided by his company. Appreciation is also expressed to his son, Art, for assistance during the instrumentation of the wall in California.

I express appreciation to Southern California Edison Company for their cooperation and assistance during the instrumentation of the Welded Wire Wall.

Appreciation is expressed to Mr. Rene Winward for his expert assistance and advice in devising and installing the instruments. Thanks is also given to the students in the USU Department of Civil Engineering who rendered much diverse and timely assistance throughout the project.

Appreciation is expressed to Dr. I. S. Dunn and Dr. F. W. Kiefer for serving on my graduate committee.

And finally a very special thanks is extended to Dr. Loren R. Anderson for his influence and patience in undertaking and completing this project.

Jerold A. Bishop

TABLE OF CONTENTS

Page

ACKNOWLEDGMENTS ii

LIST OF TABLES v

LIST OF FIGURES vi

ABSTRACT viii

Chapter

I. INTRODUCTION 1

Problem 1
Purpose of Study 5

II. REVIEW OF LITERATURE 8

Introduction 8
Mechanism of Reinforced Soil 8
Reinforced Soil Retaining Walls 12

III. METHODOLOGY 29

Introduction 29
Instrumentation and Monitoring Program 29
Laboratory Studies 40

IV. RESULTS 48

Welded Wire Wall 48
Pullout Tests 58
Model Wall 61

V. CONCLUSIONS AND RECOMMENDATIONS 65

Introduction 65
Evaluation of Results 65
Conclusions 69
Recommendations 70

LITERATURE CITED 78

APPENDICES 78

Appendix A. Soil Data 81
Appendix B. Field Data 87

TABLE OF CONTENTS (Continued)

		Page
Appendix C.	Pullout Tests Data	93
Appendix D.	Laboratory Test Wall Data	98
Appendix E.	Hypothetical Design Problem	101

LIST OF TABLES

Table		Page
1.	Schedule of pullout tests	45
2.	Sand cone density tests for San Gabriel wall	83
3.	Settlement plate data	87
4.	Strain gage data, S1 - S12	88
5.	Strain gage data, S13 - S24	90
6.	Extensometer data (relative movements)	91
7.	Survey monument data	92
8.	Pullout test data, preliminary tests	93
9.	Pullout test data, varied mesh sizes	95
10.	Single wire pullout tests	97
11.	Laboratory test wall data	98

LIST OF FIGURES

Figure		Page
1.	Reinforced earth wall, California Highway 39	3
2.	Welded wire wall: pictorial sketch showing general plan of construction	4
3.	Welded wire retaining wall, San Gabriel Mountains of Southern California	6
4.	Reinforcement/soil interaction	10
5.	Mohr's circles for cohesionless soils (after Dunn, Anderson, and Kiefer, 1976)	13
6.	Active zone for a wall of finite height (after Dunn, Anderson, and Kiefer, 1976)	14
7.	Cross-section of reinforced earth wall showing symbols and dimensions used in analysis	16
8.	Isometric view of reinforced soil construction with longitudinal reinforcement only--typical of Reinforced Earth structures	19
9.	Comparison of different methods of analyzing pullout	22
10.	Plan and elevation sketches of constructed welded wire wall	31
11.	Cross-section of wall showing location of instrumentation	33
12.	Strain gage load cell distribution for the first of two instrumented layers of wire mesh (placed at the top of lift #2)	35
13.	Load cell design and installation	36
14.	Wheatstone Bridge schematic	37
15.	Plan and elevation sketches of earth pressure cell	41
16.	Pullout tests in earth pressure cell	43
17.	Laboratory test wall	47
18.	Height of backfill versus force in longitudinal wires	50

LIST OF FIGURES (Continued)

Figure		Page
19.	Height of fill versus force in longitudinal wires	51
20.	Height of fill versus force in longitudinal wires	52
21.	Height of fill versus force in longitudinal wires	53
22.	Force in longitudinal wires versus depth into wall	54
23.	Force in longitudinal wires versus depth into wall	55
24.	Extensometer displacement as a function of wall height	56
25.	Settlement plate displacement	57
26.	Single wire pullout force	59
27.	Pullout force as a function of NWσ	60
28.	Pullout force as a function of NbW	62
29.	Force in the longitudinal wires versus height of backfill above instrumented mat--laboratory test wall	63
30.	Force in wires versus depth into wall - laboratory test wall	64
31.	Generalized cross-section of welded wire wall showing the Coulomb failure plane	72
32.	Upper mats shown cut off inside Coulomb failure plane	74
33.	Proposed construction sequence	75
34.	Moisture/density relationships (AASHTO T-99 Method C) for soil used in construction of California wall	82
35.	Grain size distribution-sample 1 (GP)	84
36.	Grain size distribution-sample 2 (SM)	85
37.	Direct shear tests, S1 and S2	86
38.	Plan view of instrumentation layout on wire mat for test wall.	100
39.	Freebody Diagram of Wall	101
40.	Cross-section for hypothetical design problem (N.T.S.)	102

ABSTRACT

An Evaluation of a Welded Wire Retaining Wall

by

Jerold A. Bishop, Master of Science

Utah State University, 1979

Major Professor: Dr. Loren Anderson
Department: Civil Engineering

The purpose of this paper is to evaluate the performance of a Welded Wire Retaining Wall and present design recommendations for its future use. Field data from the instrumentation of a Welded Wire Retaining Wall as well as laboratory data from a study of welded wire fabric as a reinforcing agent for soil was gathered. A study of the theory and practice of reinforced soil construction was made. On the basis of this study and the experimental data obtained, the wall is evaluated and design recommendations presented.

(115 pages)

CHAPTER I

INTRODUCTION

Problem

Background of the study

During the past two decades the strengthening of soil for engineering purposes has received increasing attention. This concept, however, has a well established history. Biblical records state that in ancient Egypt straw was mixed with clay to improve the properties of brick. Fortifications built by the ancient Gauls used alternating layers of earth and logs. There are additional examples of using an earth and logs construction technique in building dikes, highway embankments (Amesbury, 1935), and roads over swampy areas (corduroy roads). Stabilization of soil along river banks by roots or branches (known as faggoting) is another reinforcing technique (Doran, 1948). Sandbags or a variation of sandbags called gabions (coarse gravel or cobbles held together in a cage of wire mesh) are also used to strengthen soil.

In the 1960's a French engineer, Mr. Henri Vidal, introduced a rational method of design for a particular scheme of soil reinforcement, known as Reinforced Earth (Vidal, 1966, 1969). This process, which is patented, reinforces soil embankments with metal strips embedded in the soil. Friction between the narrow metal strips and the surrounding soil gives substantial tensile reinforcement to the soil mass. This technique is now commonly used for constructing retaining walls. Since Vidal's reintroduction of reinforcing earth, a great deal of theoretical and experimental work has been done on this and similar reinforcing schemes. Studies

by Dr. Kenneth Lee at UCLA have made a significant advancement in the state of the art (Lee, Adams, and Vagneron, 1972).

The first Reinforced Earth construction in the United States was a retaining wall used as part of a landslide correction scheme (Figure 1) located near Los Angeles on California Highway 39 (Chang, Forsyth, and Smith, 1972). Construction of Reinforced Earth structures has subsequently experienced growing popularity.

Definition of soil reinforcement

A broad definition of soil reinforcement would include any technique for strengthening soil from anchor bars and piles to Vidal's Reinforced Earth. For the purpose of this study, reinforced soil is considered to be "a construction material composed primarily of soil or earth, which is strengthened by the action of small quantities of bars, rods, or fibers" (Lee, Adams, and Vagneron, 1972, p. 1). This easily encompasses Vidal's concept of Reinforced Earth and essentially means that earth itself is made stronger and is thus a much more formidable structural unit.

Welded wire retaining wall

Another technique known as a welded wire retaining wall has recently been used to reinforce earth embankments. Welded wire retaining walls consist of two components, earth and a 9 gage wire mesh. The mesh is constructed of high strength galvanized steel wires laid in a 2-inch by 6-inch grid and spot welded at the joints. The retaining wall is constructed in 18 inch lifts with a mat of wire mesh on the foundation and between each lift as shown in Figure 2. The length of

Figure 1. Reinforced earth wall, California Highway 39.

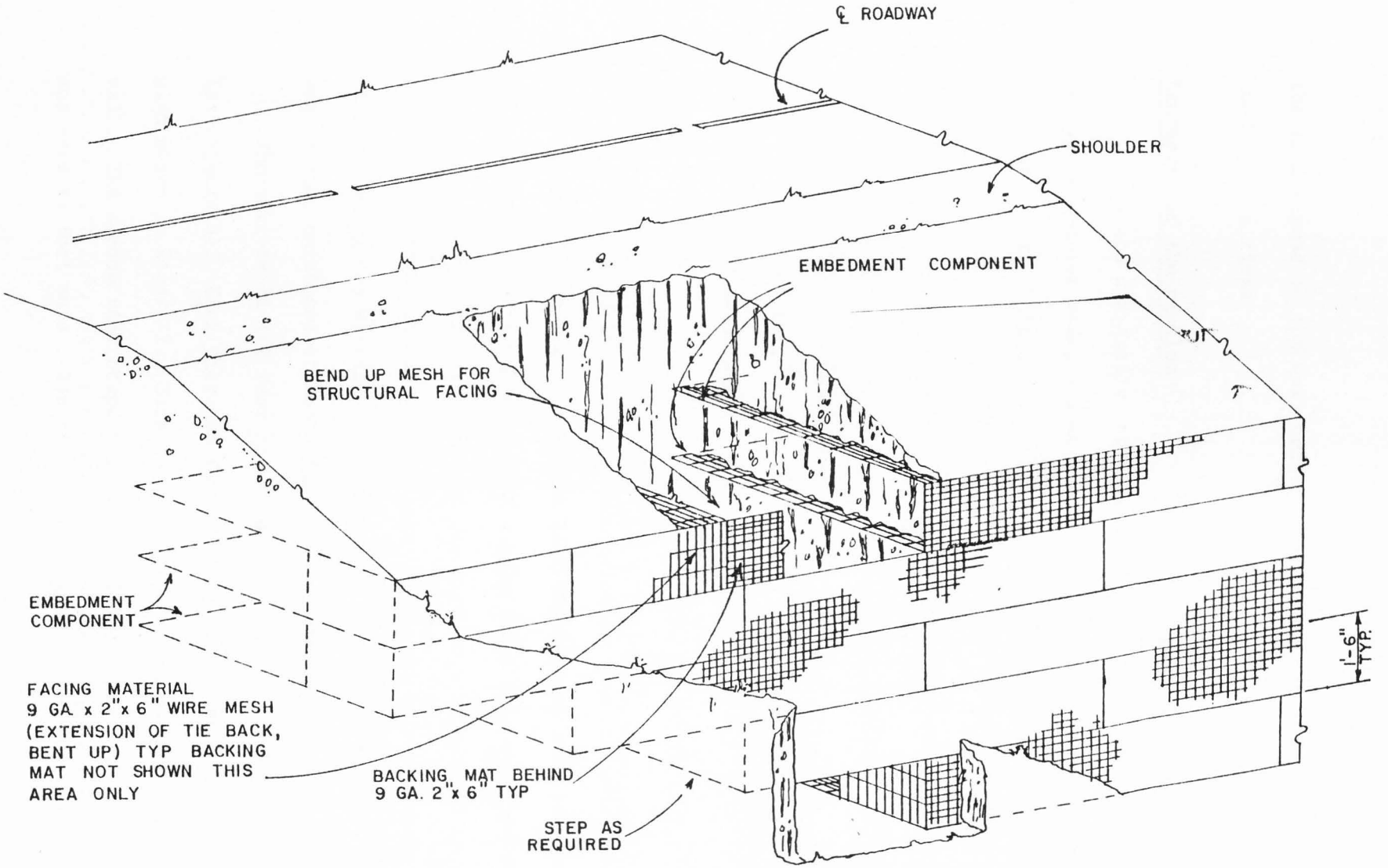

Figure 2. Welded wire wall: pictorial sketch showing general plan of construction.

the mats depend on the wall height, the soil conditions, and the surcharge loading conditions.

Statement of the problem

Due to the comparative newness of the use of welded wire mesh as a reinforcement for soil, a comprehensive analysis of its adequacy had not been performed. This study is the beginning of the needed analysis.

Purpose of Study

Objectives

The objectives of this study are twofold:

1. To evaluate the performance of the welded wire retaining wall.
2. To develop design recommendations.

Scope

In the fall of 1978 an instrumentation program was undertaken to monitor the performance of a 22 1/2 foot high welded wire retaining wall. This wall was built as a correction scheme for a slip out that occurred on a power line access road. The road was part of a network of improved dirt roads built and maintained by Southern California Edison Company for routine and emergency service of high tension transmission lines. The project was located northeast of Los Angeles in the rugged San Gabriel Mountains.

The wall is 22 1/2 feet high and was built in three 7 1/2 foot tiers (see Figure 3). Each tier has five 18 inch lifts, built from the basic plan shown in Figure 2. Mats for the first tier extend 16 feet into the wall. The second tier steps back 3 feet from the face of the first tier, and uses 13 foot mats. The third tier steps back 4 feet and uses 10 foot

Under construction

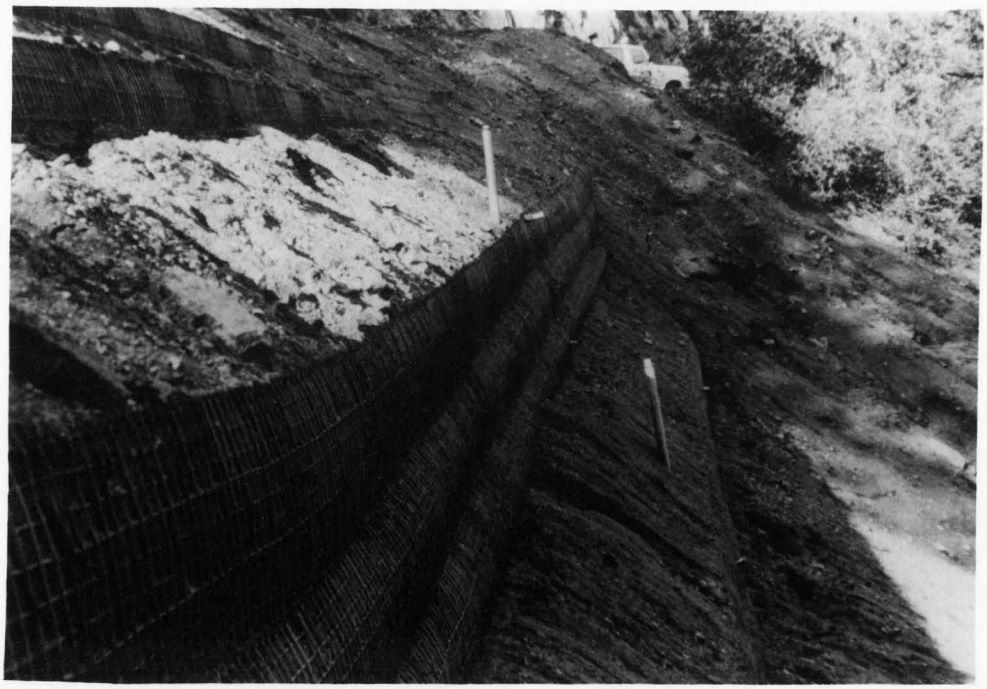

Upon completion

Figure 3. Welded wire retaining wall, San Gabriel Mountains of Southern California.

mats. The top three lifts have additional stepbacks to allow for the decreasing slope of the mountain as the level of the roadway is approached. The length of the wall is 32 feet at the bottom and 96 feet across the top.

As the wall was constructed, instrumentation was placed to monitor its performance. Wire mats were instrumented to measure the stresses in the longitudinal wires. Just above these mats a series of mechanical extensometers were placed to measure soil strain. Settlement plates were installed at the base of each tier to indicate overall and differential settlement. Survey monuments were mounted on the face to allow observation of the wall's overall movement.

Evaluation of the wall was accomplished using the data obtained from the instrumentation systems. Standard soil tests were performed in the field and in the laboratory to determine the engineering properties of the backfill material used in the construction. Laboratory tests were made with sections of wire mesh to determine the pullout resistance of the mat. These tests were performed in a large earth pressure cell capable of simulating up to 100 feet of overburden pressure. Finally, a small welded wire retaining wall was constructed and observed in the earth pressure cell. The field and laboratory data were used to evaluate the performance of the wall and to develop design recommendations.

CHAPTER II

REVIEW OF LITERATURE

Introduction

In reviewing the literature on reinforced soil, it is pertinent to realize that artificially strengthened soil has many applications. The most common of these applications is with regard to retaining walls. Since this study concerns a type of retaining wall, this review of literature will be restricted to the theory of reinforced soil and its application to retaining walls.

Reinforced soil is a highly complex theoretical problem for which many answers have not yet been determined. However, by using good experimental techniques this problem can be easily and profitably studied in the laboratory and the field. Several such studies have been made, and have contributed significantly to the understanding and use of reinforced soil. The most important of these studies in concert with the important theoretical papers will be reviewed in this chapter.

Mechanism of Reinforced Soil

Construction of reinforced soil retaining walls consists of placing successive lifts of soil with a layer of reinforcement between each lift. This gives a layered effect of soil/reinforcement/soil/reinforcement. The basis of reinforced soil is the ability of this reinforcement to withstand tensile stresses which the earth alone cannot resist. To do this, the reinforcement must be bonded to the soil. Understanding the nature of this

bond between the soil and the reinforcement is fundamental to understanding reinforced earth.

Soil/reinforcement interaction--friction

Vidal (1969, p. 1) has stated that in the case of longitudinal reinforcement only (such as the narrow steel straps used by Reinforced Earth), bond is derived from friction between the soil and the reinforcement. A granular soil with a sufficient internal friction angle (greater than 25° for Reinforced Earth structures) is generally required to produce sufficient friction. Vidal (1969) and Lee (1976) indicate that the reinforcement introduces a 'cohesion' to the granular non-cohesive soil. This added 'cohesion' raises the Mohr failure envelope and allows the stress condition to remain below the envelope. Vidal (1969, pp. 1-4) states that this 'cohesion' is exhibited because the reinforcing holds the soil essentially in place by the friction bond. This friction bond is thus, of necessity, a non-slipping bond.

The contact force of a grain adjacent to the reinforcement makes an angle α with the perpendicular to the reinforcement (Figure 4a). To maintain equilibrium without slipping

$$\tan \alpha \leq f$$

where f is the friction coefficient between grains and reinforcement.

Vidal (1969, p. 1) states that if the tension in a reinforcing member is constant (such as anchored tie rods) transmission of stress to the soil is impossible. Consequently the contact angle and adjacent grains are unaffected. If, however, the tension varies along the reinforcing member, different forces will be transmitted to two adjacent grains (Figure 4b).

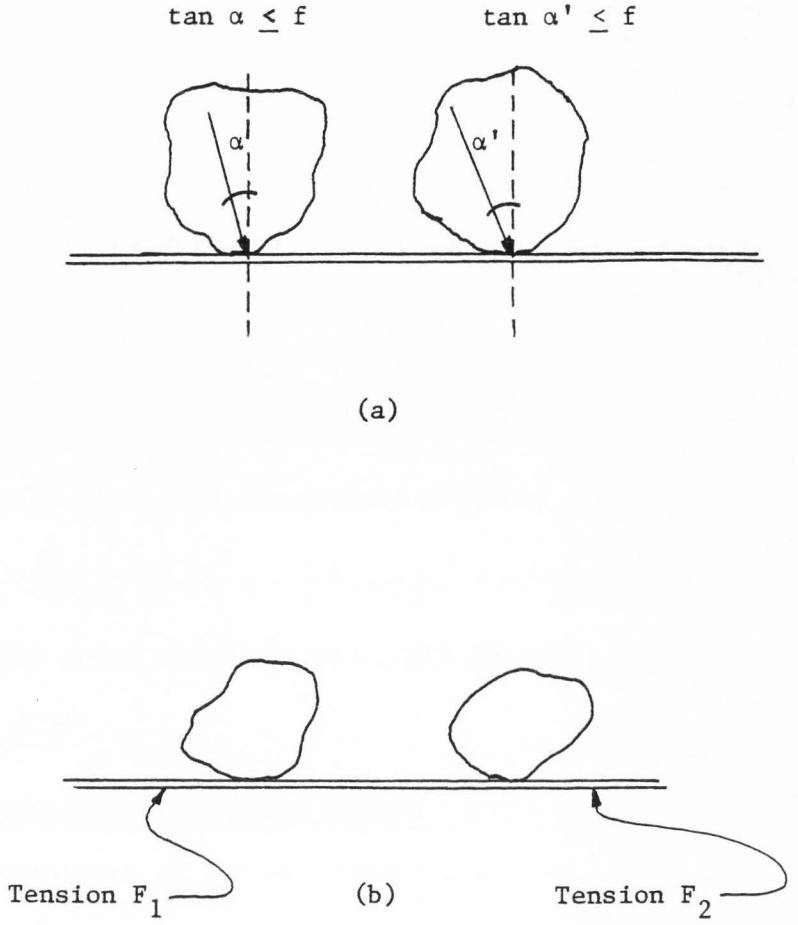

Figure 4. Reinforcement/soil interaction.

The contact angle α will then be different for both grains (Figure 4a). This results in a force pushing the two grains together, which is equal to the difference between the two forces transmitted by contact with the reinforcement. Thus a "connection" will be made between the two grains by the differential force, dF. For this to occur, the force dF distributed over the contact length of the grains with the reinforcement, $d\ell$ (Figure 4c), must be less than the maximum friction force fN, or:

$$\frac{dF}{d\ell} < fN$$

N being the total normal force. This is, by definition, a non-slipping friction bond.

Action between reinforcement layers

Transmission of forces outward into the soil matrix is less understood. Vidal (1969, p. 4) presumes an arching action to occur between layers of reinforcement. He concludes that the material between the reinforcement is contained and acts as a "sack" of earth, bounded by the reinforcement and the arching action. He further states that if there really were sacks between reinforcement layers, it would be of little importance to know exactly what occurs within the sacks. All calculations concerning the reinforcement would still be fully justified. Tearing the sacks open along the edge perpendicular to the reinforcement would result only in local stress changes, while the overall picture would remain the same.

Vidal (1969) suggests that these actions of bonding and arching have been achieved in all the numerous Reinforced Earth structures designed and built.

Reinforced Soil Retaining Walls

Lateral soil pressure in retaining walls

Coulomb (1776) and later Rankine (1857) studied lateral pressures against earth retaining walls and they each developed classical theories of earth pressure against retaining walls. Both theories indicate two limiting equilibrium states for the soil behind a retaining wall. These two states are the active and the passive states of lateral soil pressure. Intermediate between these two limiting conditions the soil is in a state of elastic equilibrium referred to as an at-rest condition. The Mohr's circles and the failure envelope of Figure 5 illustrate these stress states.

Consider an element of soil in a horizontal deposit that extends indefinitely in the horizontal direction. This element is not subject to lateral yielding. This is the at-rest condition, and the relationship of the horizontal to the vertical intergranular pressures is shown by the at rest circle in Figure 5. If the horizontal soil deposit is cut, providing a free standing face, and allowed to yield outward, the horizontal effective pressure is decreased while the vertical effective pressure remains constant. The horizontal stress will drop to a limiting value, at which time Mohr's circle is tangent to the failure envelope. This is shown by the active circle in Figure 5. When this limiting active pressure is reached unless the soil is restrained, it will no longer remain in equilibrium. The face of the soil will fail and slump until it can no longer flow. The soil will slide along a failure plane oriented at approximately an angle of $45 + \phi/2$ to the horizontal (Figures 5 and 6). The third case of equilibrium can be illustrated by considering pressure being placed

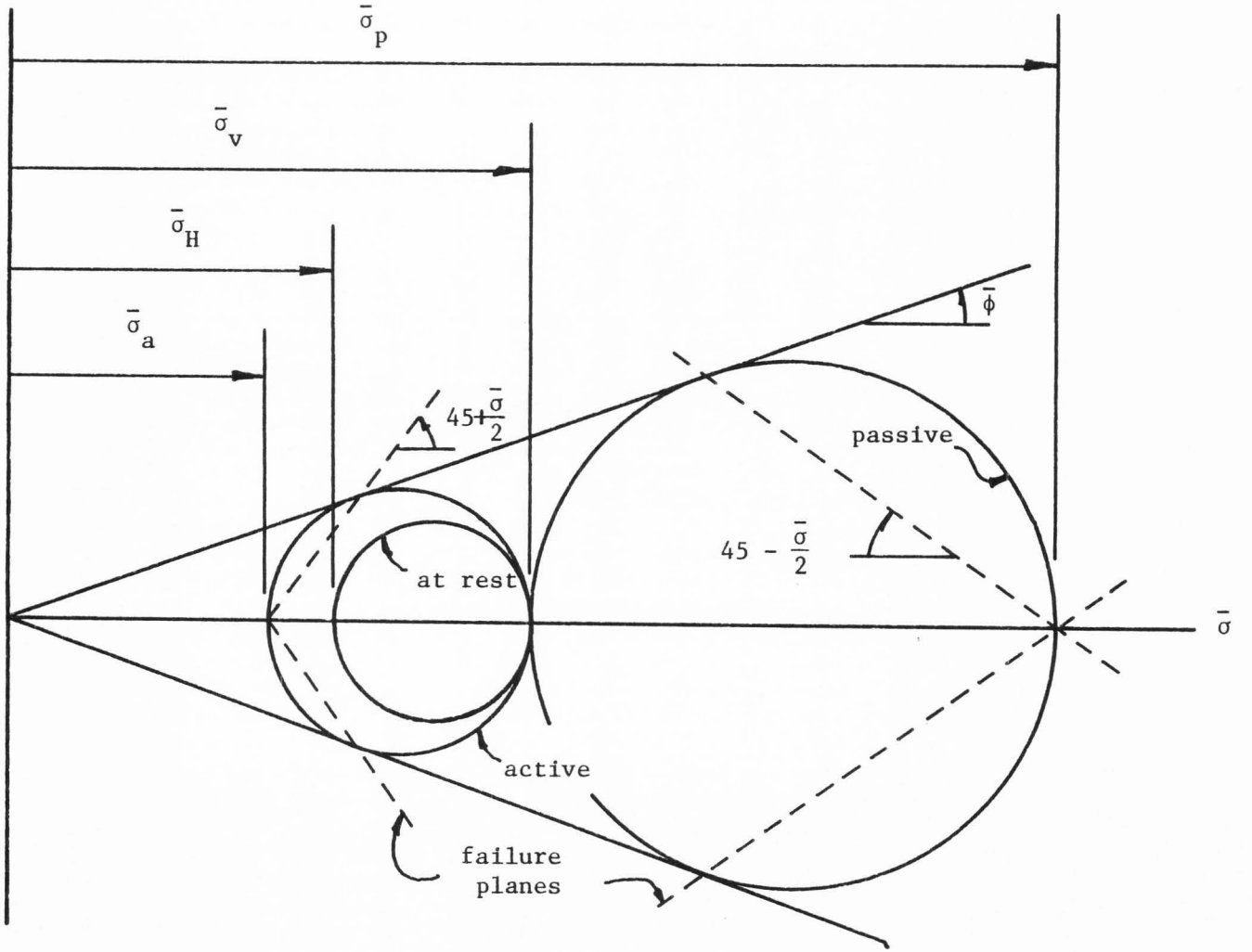

Figure 5. Mohr's circles for cohesionless soils (after Dunn, Anderson, and Kiefer, 1976).

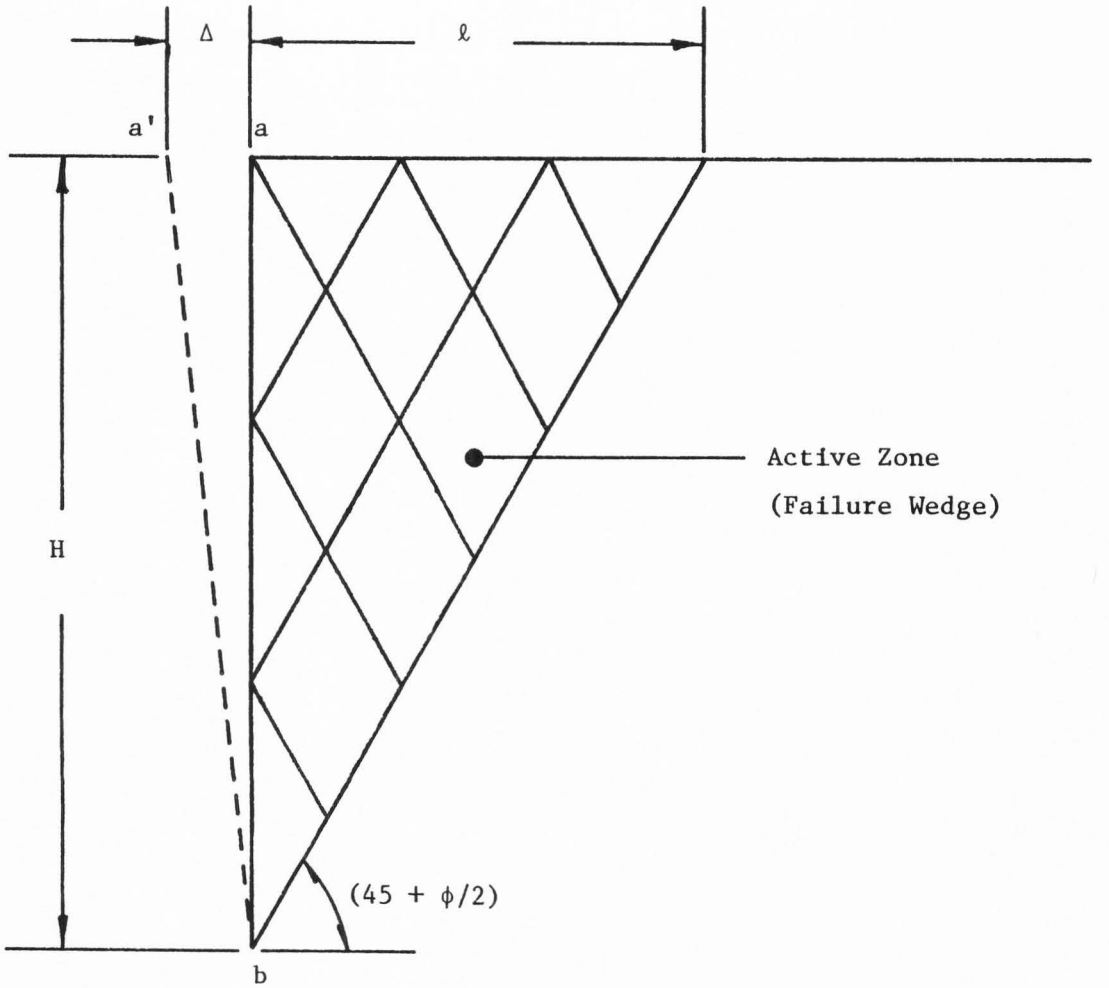

Figure 6. Active zone for a wall of finite height (after Dunn, Anderson, and Kiefer, 1976).

placed against the cut face of soil (as in the action of a thrust block). Here the horizontal effective pressure is increased while the vertical effective pressure is held constant. This pressure will continue to increase to a value much greater than the vertical pressure. This final limiting value (called the passive pressure) again places the Mohr's circle tangent to the failure plane (Figure 5). This is known as the passive state (Dunn, Anderson, and Kiefer, 1976).

The mechanism of a retaining wall is to yield outward due to the horizontal pressures. This allows the soil to strain and the limiting horizontal pressure of the active case is reached (Figure 6). Thus most retaining walls are designed to resist active pressures, provided the wall can yield.

Reinforced soil applied to retaining walls

Rather than use a retaining wall to stablilize a soil embankment, the concept of reinforced soil is to artificially strengthen the soil embankment itself. As has been discussed, the procedure is one of placing alternating layers of soil and reinforcement in a multiple sandwich effect (Figure 7). The bonding between these layers provides substantial reinforcement.

As the reinforced soil structure is constructed the face is considered to yield to the active state (Schlosser and Vidal, 1969). The active earth pressures, therefore, are used to design the reinforcement. They determine the sizing and spacing of the reinforcing material required to maintain the stability of the wall.

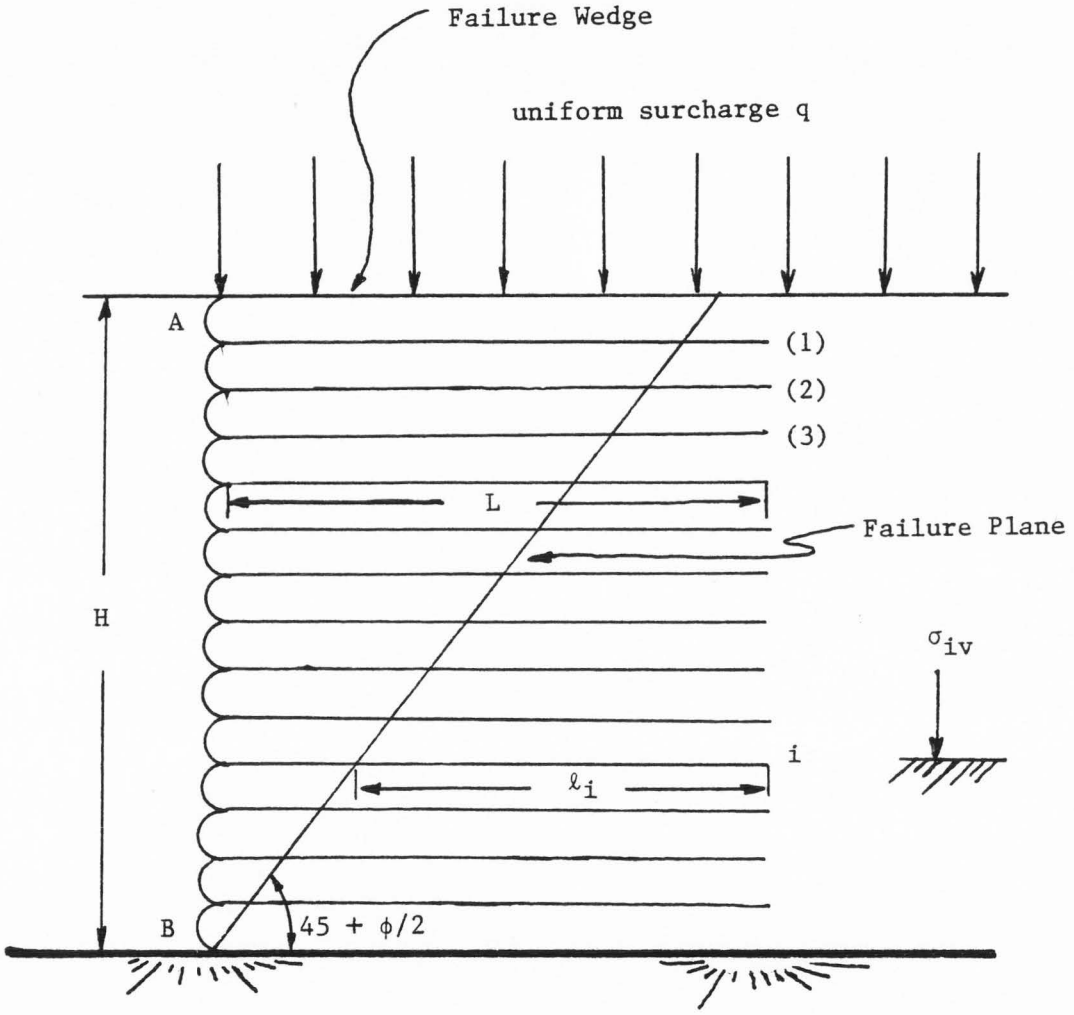

Figure 7. Cross-section of reinforced earth wall showing symbols and dimensions used in analysis.

Internal failure modes

Two basic modes of internal failure for a reinforced soil retaining structure have been established (Schlosser and Vidal, 1969, pp. 11-15):

1. Tension failure in the reinforcement;

2. Pull out of the reinforcement.

A tension failure of the reinforcement is comparatively straight forward. This occurs when the lateral pressures exceed the yield strengh of the reinforcement. Insufficient reinforcement, higher lateral pressures, or a very high live load could cause tension failure.

The problem of reinforcement pulling out is also relatively simple, in principle. Within the wall, the total wall force per unit of reinforcement must be resisted by the drag or anchoring of the reinforcement in the soil backfill. For the longitudinal steel straps used by Reinforced Earth, this drag is wholly frictional. There are differing opinions, however, as to the length of strap that can be considered effective in providing this resistance to pullout. Schlosser and Vidal (1969) consider the entire length to be effective. However, Dr. Kenneth Lee, in a detailed study of Reinforced Earth, stated (Lee, Adams, and Vagneron, 1972, pp. 19-31) that as the face of the wall yields to the active case and the soil within the failure wedge moves out (Figure 7), the soil and the reinforcement move in concert. Thus the reinforcement within the failure wedge would not act as a frictional anchor resisting pullout and only the reinforcement beyond the wedge could be considered effective against pullout. Lee further proposes that the sum of all straps resisting pullout can be considered as a single resisting force and produces the same stabilizing effect as the combination of all the individual straps resisting their respective unit pullout force.

This implies that resistance to pullout for a Reinforced Earth retaining wall can be attained without using each and every strap. Thus the entire pullout resistance for the wall can be achieved in the lower portion of the wall, where shorter strap lengths are needed to extend to the failure plane. The upper ties, therefore, need only be long enough to maintain the structural integrity of the upper portion of the wall.

Failure mode analysis

To understand the two internal modes of failure, tension and pull-out, it is necessary to consider their analysis.

Analysis of tension failure has been approached by both the Rankine and Coulomb earth pressure theories (Lee, Adams, and Vagneron, 1973). From Rankine's theory:

$$\sigma_H = K_a \sigma_v \tag{1}$$

where σ_H is the horizontal pressure, σ_v is the vertical pressure and K_a is the coefficient of active lateral pressure. Each piece of reinforcing is responsible for its surrounding area of wall (Figure 8). Thus the tensile force, F_t, in a given section of reinforcement will be:

$$F_t = K_a \sigma_v a z \tag{2}$$

with a and z defined as shown in Figure 8. Based on the yield stress of the reinforcement (σ_Y), an expression for the factor of safety against reinforcement breaking (FS_B) can be obtained:

$$FS_B = \frac{\sigma_Y A_R}{K_a \sigma_v a z} \tag{3}$$

where A_R is the area of reinforcement. Lee (1972) also approaches the tension failure analysis by considering the Coulomb earth pressure theory. This is a more general approach because it considers wall friction, sloping

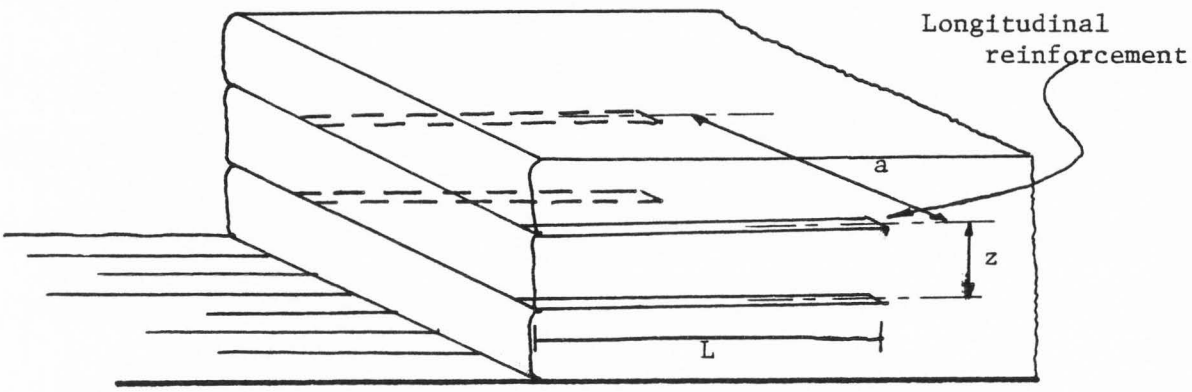

Figure 8. Isometric view of reinforced soil construction with longitudinal reinforcement only--typical of Reinforced Earth structures.

walls and backfill, and it evaluates overall rather than local stability. His resulting equations, the first considering force equilibrium and the second moment equilibrium, are:

$$F_t = \frac{N}{N+1} K_a \sigma_v a z \qquad \text{(Coulomb force method)} \qquad (4)$$

$$F_t = \frac{N^2}{N^2 - 1} K_a \sigma_v a z \qquad \text{(Coulomb moment method)} \qquad (5)$$

where N is the number of layers of reinforcement. For large walls (consequently large N), equations 3, 4, and 5 provide the same results.

In considering failure of the reinforcement by pullout an estimate of the friction force (F_r) developed by the strap to resist pullout is needed (Schlosser and Vidal, 1969). This can be expressed as

$$F_r = 2 \ell w \sigma_v \tan \phi_u, \qquad (6)$$

where ℓ is the length of reinforcement considered effective against pullout, w is the width of reinforcement, and ϕ_u is the angle of sliding friction between the soil and the reinforcement. If the entire length of the strap is considered to resist pullout then the factor of safety against pullout (FS_p) is found by dividing Equation 6 by Equation 2:

$$FS_{p1} = \frac{2 Lw \tan \phi_u}{K_a z a} \qquad (7)$$

where L is the total length of the strip. This indicates that the factor of safety is independent of the overburden pressure. If only that portion of the strip beyond the Coulomb failure wedge is considered effective against pullout (Lee, Adams, and Vagneron, 1969), then:

$$FS_{p2} = \frac{2 w \tan \phi_u}{K_a a z} (L - H \tan (45 - \phi/2)) \qquad (8)$$

where H is the height of the wall (Figure 7). When overall stability is considered it is not necessary to have all levels of reinforcement extend beyond the failure plane. For this case, the maximum frictional resisting force for reinforcement of constant length, L, is:

$$F_r = 2 \gamma z W \tan \phi_u \sum_{i=N}^{n} i \left[L - (n - i) z \tan (45 - \phi/2)\right] \quad (9)$$

where i is the summation index counting the number of reinforcement layers beginning from i=1 at the top to i=n at the bottom and N is the value of i for the first layer to extend past the failure wedge.. The factor of safety against pullout is the ratio of the resisting force behind the failure plane to the total active force,

$$FS_{p3} = \frac{4 W z \tan \phi_u}{K_z H^2 a} \sum_{i=N}^{n} i \left[L - (n - i) z \tan (45 - \phi/2)\right] \quad (10)$$

The Coulomb moment method follows a similar approach and gives:

$$FS_{p4} = \frac{12 W z^2 \tan \phi_u}{K_a H^3 a} \sum_{i=N}^{n} (n-i) i \left[L - (n - i) z \tan (45 - \phi/2)\right] \quad (11)$$

with the wall height, H, and the strap length, L, determined by trial and error.

Figure 9 presents a comparison of the four methods of computing the factor of safety against a pullout failure. In Figure 9, strap length anomalies near a wall height of zero are due to integer arithmetic only.

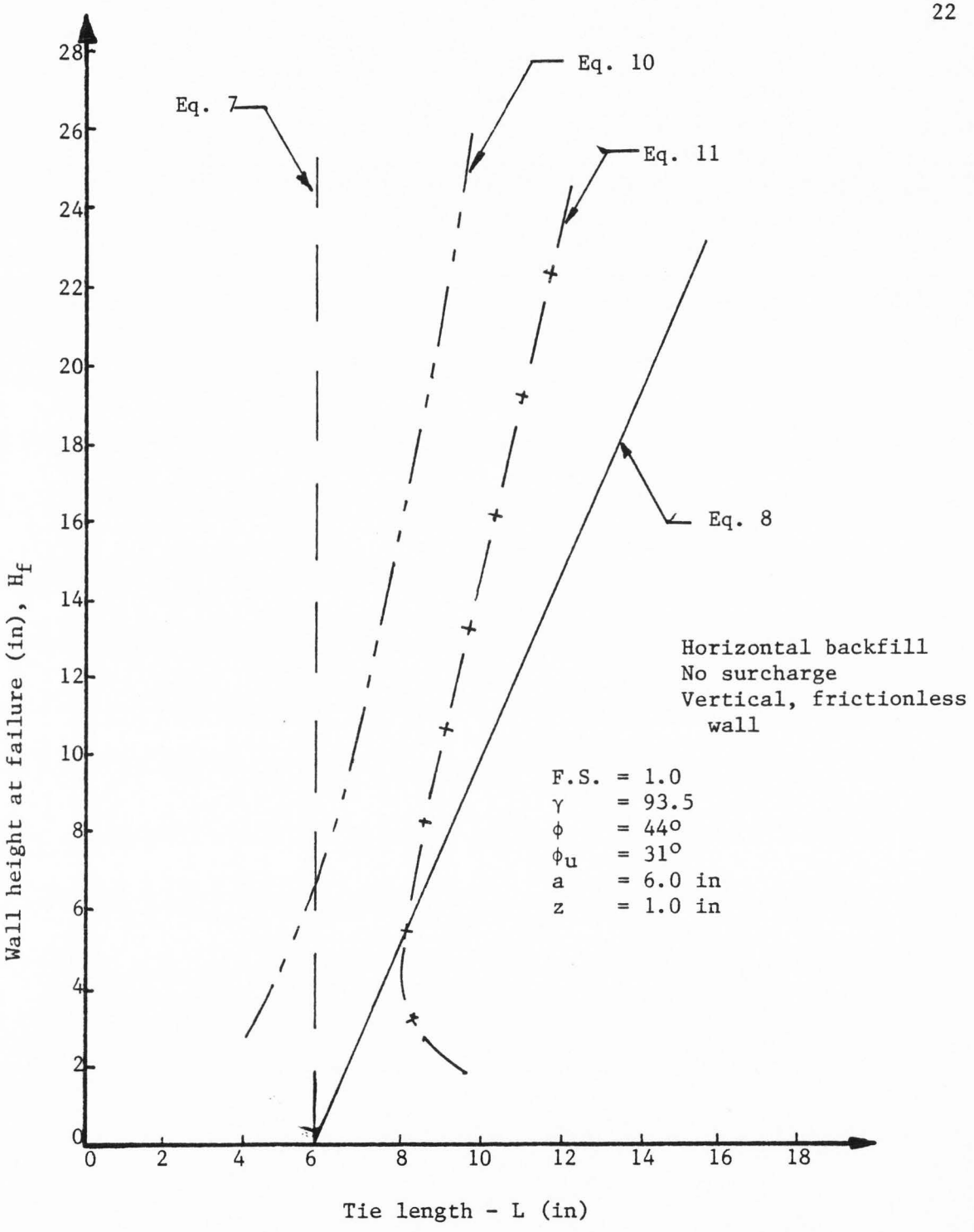

Figure 9. Comparison of different methods of analyzing pullout.

UCLA laboratory studies

Lee, Adams and Vagneron (1972) conducted a study on reinforced earth retaining walls that consisted of metal straps embedded longitudinally in a granular backfill (the basic reinforcing scheme used by the Reinforced Earth Company). Their study was broken into a theoretical and experimental phase.

The theoretical investigation involved the development of equations to design the various component parts for reinforced earth walls. This involved the application of the Coulomb earth pressure theory in two methods; summation of moments and summation of forces. The results of this phase have already been briefly discussed and the equations for tension failure and pullout failure were presented in the previous section.

To further evaluate the behavior of reinforced earth walls as well as the proposed design equations, an extensive experimental program was carried out. Over sixty model walls were build in a box 30" x 48" x 24" and allowed to fail in different modes. Reinforcing consisted of narrow, precision cut strips of aluminum foil which were varied in length from test to test. The backfill was dry Ottawa sand. Several straps were instrumented with strain gages to monitor tension stress. Earth pressure cells were installed to measure pressures. Construction procedures followed closely those used by the Reinforced Earth Company. Two different soil densities were employed to evaluate the effect of loose versus medium dense backfill. The construction was allowed to continue until the wall reached an unstable height and failed, at which time the location of the failure plane and the tension in the straps was carefully noted.

The UCLA study confirmed the prediction of lateral earth pressure theory in locating the failure plane. The formation of the active case of plastic equilibrium was shown to occur as theory predicted. The stresses were shown to be in agreement with predictions based on the active earth pressure condition. For the case of reinforcement breaking, the three methods of analysis (Equations 3, 4, and 5) showed the same solution, which was in good agreement with test data. In the case of reinforcement pullout the analysis by the Rankine method (Equation 8) was confirmed to be conservative. Pullout resistance based on the Coulomb force equilibrium method gave the best agreement with test data. Finally, the UCLA tests showed that the internal angle of friction of the backfill material was essentially unaffected by the presence of reinforcement.

Studies by California Department of Transportation

The California Department of Transportation (CalTrans) conducted an instrumentation, and evaluation program on the first Reinforced Earth wall built in the United States. In a later study CalTrans conducted field and laboratory tests to study reinforcement tension and pullout resistance.

In 1972 construction was started on the first Reinforced Earth project in the United States (Chang, Forsyth, and Smith, 1972). This project was a highway embankment (retaining wall) constructed as part of a landslide correction scheme that allowed the reopening of California Highway 39 (Figure 1). A series of drains and a toe buttress were constructed to stabilize the slide. The final maximum dimensions of the wall were 55 feet high and 528 feet long. The backfill material was native material, consisting primarily of decomposed granite.

At two different stations along the length of the wall the entire cross-section was instrumented. Additionally, several points on the slide below and along the face of the wall were instrumented. The total instrumentation program consisted of:

1. Slope indicators to measure internal movement;
2. Brass monuments on the wall face to show horizontal, vertical, and tilting movements;
3. Settlement plates to show settlement at different levels;
4. Extensometers to measure differential movements within the wall;
5. Soil pressure cells to measure internal stresses developed in the soil mass;
6. Strain gages to allow measurement of the stresses in the steel reinforcement.

Monitoring the instruments was on a daily basis during construction, and thereafter at intervals of two to four weeks for one year (Chang and Forsyth, 1977a).

The final evaluation (Chang and Forsyth, 1977a) of the test data showed, in general, good agreement with theoretical predictions. Actual vertical soil stresses were essentially as calculated. The measured strains in the steel and soil were reasonably consistent with each other. The computed stresses in the steel straps were generally smaller than, but approached, the theoretical active stress predicted. However, in some instances steel stresses approached the at-rest state of soil pressure. Essentially the monitored performance of the wall showed the validity of the design equations used as well as the applicability of this type of construction.

Coupled with the Route 39 project was an investigation on the pull-out resistance of different types of reinforcement (Chang, Hannon, and Forsyth, 1977). Two series of pullout tests were performed. The first used a group of fifteen dummy straps placed in the Highway 39 construction. These straps varied in length from 5 to 46 feet and were placed with overburden heights from 7 to 38 feet. All of the straps were of the standard type used by the Reinforced Earth Company. The field pullout tests confirmed that:

1. The soil does not strain significantly until the proportional limit (of either the steel or the soil) is reached. Thereafter the load deformation curve becomes non-linear.
2. For a pullout force, the maximum stress in a strap occurs near the wall face.

A group of large scale laboratory pullout tests were performed in a hydraulic soil pressure cell (allowing the simulation of an overburden height of up to 50 feet). These were done with four types of possible reinforcing materials:

1. Steel straps (the same type as used in the field)
2. A solid steel plate
3. Longitudinal smooth rebars (Number 3)
4. Number 3 rebars welded into a rectangular 4 x 6 inch mesh.

The same conclusions obtained from the field pullout tests were reached from the laboratory tests on steel straps. In addition, the bar mesh samples showed that:

1. For an equivalent surface area the bar mesh shows nearly six times the pullout resistance of longitudinal bars or steel straps.

2. Bar mesh embedded in a silty clay soil showed slightly higher pullout resistance than when buried in a looser gravelly soil.
3. An increase in bar mesh openings significantly reduces pullout resistance.

These conclusions indicated that mesh is superior to individual straps for providing pullout resistance. The tests appear to conclude that a mesh can be used in a cohesive soil of low plasticity, which is considered to be a very undesirable backfill material in Reinforced Earth construction.

Finite element analysis

It is beyond the scope of this paper to consider a detailed review of the finite element method. However, analysis of reinforced soil retaining walls by the finite element method is receiving increasing attention. The Reinforced Earth wall constructed and studied by the California Department of Transportation has been analyzed by the finite element method (Chang and Forsyth, 1977b). Another study at the University of California at Davis, California, considered an instrumented field prototype reinforced soil wall. This was studied analytically by the finite element method (Shen, Romstad, and Herrman, 1976).

Alternative reinforcing schemes

In concluding this review of literature, it is appropriate to discuss a few closely related alternative schemes for the reinforcement of soil. These schemes are generally in the form of a tied back retaining wall. This is essentially a flexible retaining wall with prefabricated facing pieces anchored through ties to an anchorage system. The anchor system could take the form of continuous anchors (metal strips placed

vertically) (Shroeder, Schwarzhoff and Hansen, 1976), double wall sections, anchor blocks, or rock bolts (Anderson and Selvage, 1976).

The type of construction described by Anderson and Selvage (1976) places the entire wall force against the facing pieces on the front of the earth wall. These pieces must be structurally sound and capable of transmitting the wall force to the anchor rods and hence to the anchor system. Very little if any frictional reinforcement by the horizontal tie rods occurs. Tension in the tie rod is essentially constant and it acts primarily as a link between the facing and the anchor system. However, the basic criteria for the internal stability of a conventional Reinforced Earth wall, failure of the tie rods in tension and pullout of the anchor system, still applies.

Failure of the tie rods in tension is avoided by simply providing a large enough cross-section in the rod. Pullout of the anchor system is somewhat more difficult to evaluate. Anchors near the surface are designed much as a conventional deadman. Primarily, this design is based on the passive resistance of the soil. For anchors buried deep it is theorized (Anderson and Selvage, 1976) that the anchor pushes the soil in front of it as a long horizontal column. The dimensions of this column are considered to be the area of the anchor by the length of the anchor rods. Resistance to pullout is obtained along the boundaries of this soil column by soil against soil resistance. In principle then, this is very similar to the more common reinforced soil retaining wall utilizing longitudinal straps. Alternately, Anderson and Selvage (1976) propose that the resistance for deep anchors should be determined by treating deep anchors as a spread of continuous footing whose depth is located at a depth equal to that of the anchor rod.

CHAPTER III

METHODOLOGY

Introduction

The purpose of this study was to examine a type of reinforced soil construction, referred to as a welded wire retaining wall. This examination was conducted with two objectives in mind:

1. To evaluate the structural performance of the welded wire retaining wall;
2. To develop a general design procedure for this type of construction.

A two phase experimental approach was used to accomplish these objectives. Phase one was devoted to the instrumentation and monitoring of a welded wire retaining wall constructed in the San Gabriel Mountains of Southern California. The second phase involved laboratory studies of welded wire mat as a soil reinforcing agent. The laboratory studies included pull-out tests and the construction of a wall section in an earth pressure cell.

Instrumentation and Monitoring Program

General

The welded wire retaining wall was constructed in the San Gabriel Mountains, northeast of Los Angeles, in Southern California. Southern California Edison Power Company maintains several improved dirt roads in these mountains for easy access to high voltage lines. The site for this construction was along one of these roads. A large slip out had occurred for approximately 75 feet along the road, and the wall was to

serve as a correction scheme. Slide debris was removed, and an excavation was made to a firm foundation below the failure plane of the slide. The wall was constructed from this level and continued until the top was 1 to 2 feet under the roadway at each end. A roadbase was then placed over the wall and the road placed back in service.

Measurements taken

The retaining wall was designed as a reinforced soil structure, with the mats of welded wire mesh serving as the reinforcement as shown in Figures 2 and 3. To evaluate the walls structural performance, measurements of four different types were taken during and after construction. These measurements were to provide a time history of:

1. Overall horizontal and vertical movements of the wall;
2. Differential vertical settlement within the wall;
3. Horizontal soil strain;
4. Stress in the wire mesh.

Instrumentation

Survey monuments. To measure overall wall movement, survey monuments were placed at four points on the face of the wall as shown on Figure 10a. Four control points were placed away from the construction area at the locations shown in Figure 10b. A one second theodelite (Kern DKM II) was placed at point C, and using the line B-C (Figure 10b) as a reference, angles were measured to each survey monument. This was to provide a record of horizontal movements. Overall vertical movement was to be read by using the vertical angle from the level plane of the instrument to the survey monument and correcting for the height of the insturment. However, poor anchorage of the survey monuments caused these measurements to be in question.

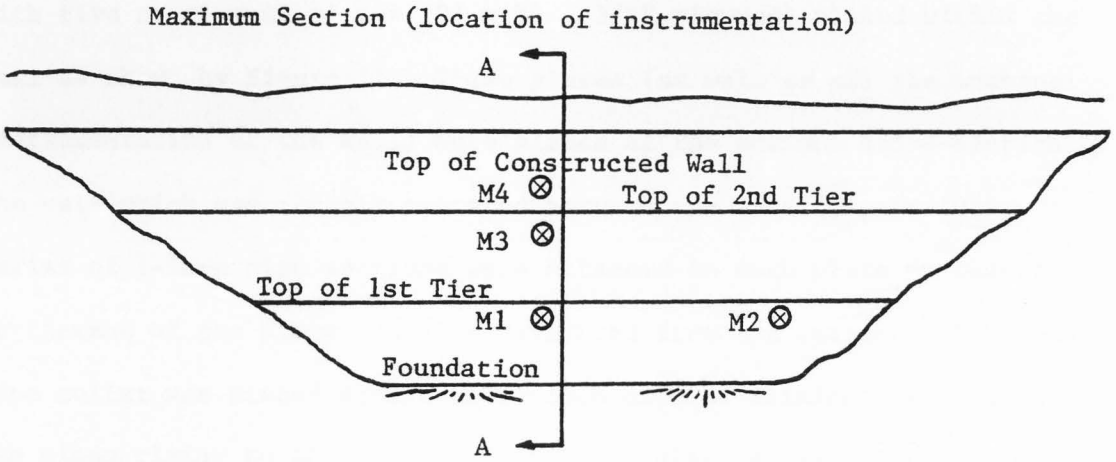

(a) front elevation of constructed wall showing surve monuments (M1 - M4)--N.T.S.

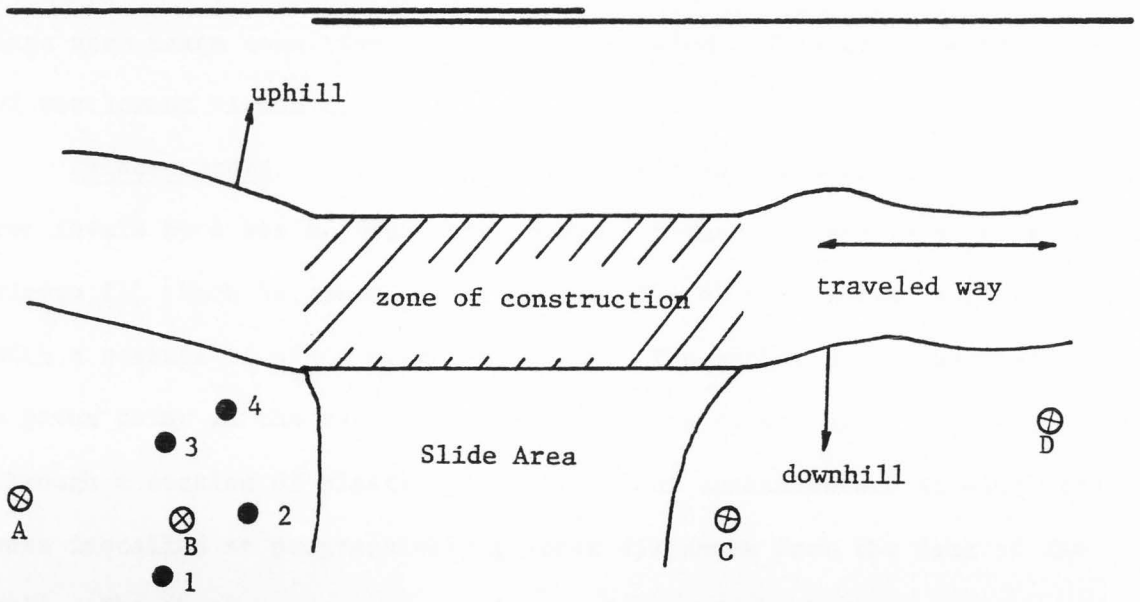

(b) diagrammatic sketch (plan view) showing locations of vertical control (BM 1-4) and horizontal control (transit points A-D)

Figure 10. Plan and elevation sketches of constructed welded wire wall.

Settlement plates. Differential vertical settlement was measured with five settlement plates (2' x 2' x 3/4" plywood) placed within the wall as shown by Figure 11. These plates (as well as all the internal instrumentation of the wall) were placed at the maximum cross-section of the wall which was roughly centered between the ends (Figure 10a). A series of 1-inch pipe sections were attached to each plate so that the settlement of the plate could be monitored from the surface. A 2-inch pipe collar was placed around the 1-inch pipe to eliminate soil drag. The pipes rising to the surface in the traveled way were cut off and capped about 18 inches below the proposed final grade. A series of reference benchmarks were set beyond the zone of construction. The settlement of each plate was then monitored using a standard automatic level. Readings were taken each time a lift was completed. This gave the time history of settlement within the wall.

Extensometers. Horizontal movement within the wall was measured at two levels by a set of four extensometers placed at each level as shown in Figure 11. Each extensometer consisted of a 4" x 6" x 1/8" anchor plate with a section of piano wire tied to it. The anchor plate was placed at a given point in the wall with the piano wire extending to the face through a section of plastic pipe. The four extensometers at each level were installed at progressively greater distances from the face of the wall. The shortest was at roughly two feet and the longest was just beyond the end of the welded wire mat. The wall movement was measured by notching the piano wire just outside the face and observing the movement of this notch with respect to a fixed plate on the wall face. This gave a measure of the average soil strain between the anchor plate and the face of the wall.

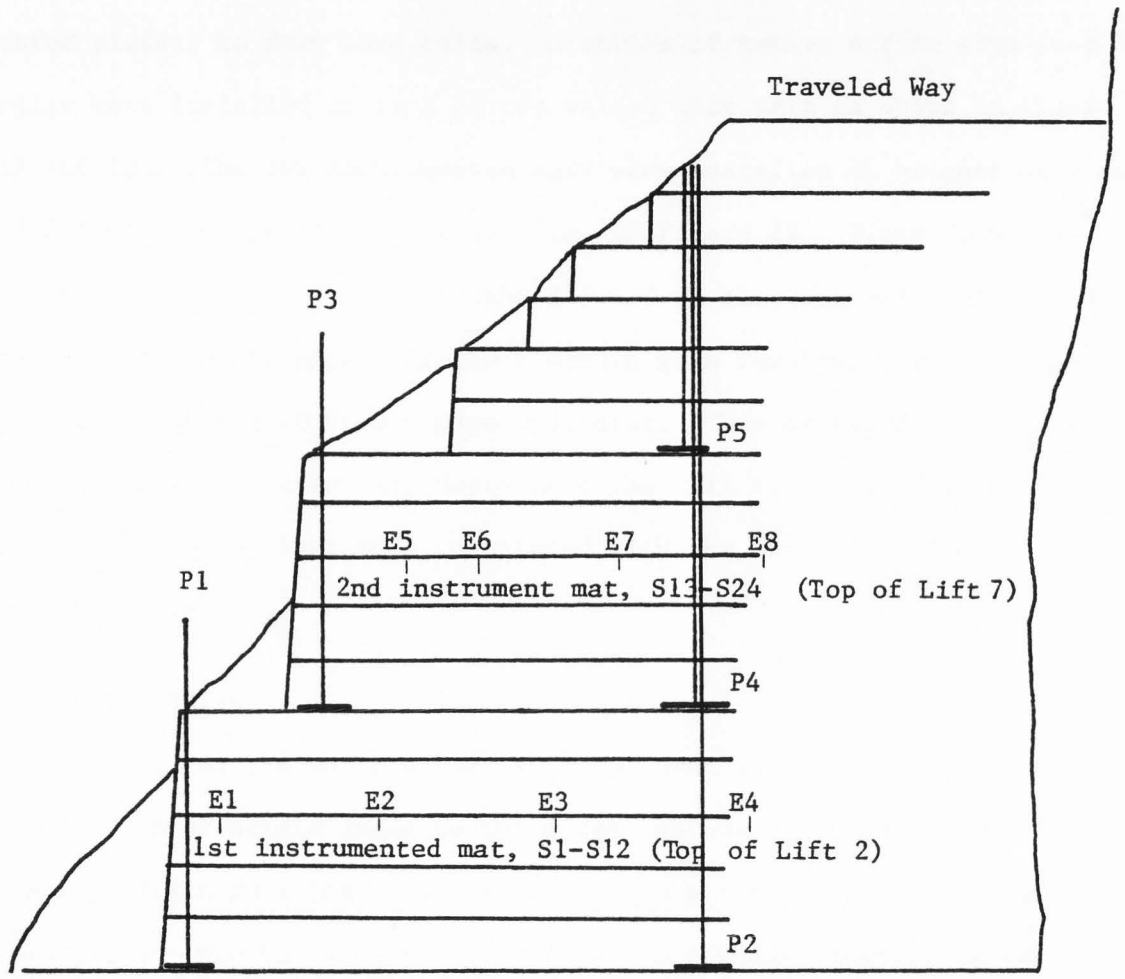

Figure 11. Cross-section of wall showing location of instrumentation. (Section A-A of Figure 10a.)

Strain gage load cells. The stresses in the longitudinal wires were measured by electrical resistance strain gages mounted on prefabricated plates, to form load cells. A series of twelve strain gage load cells were installed on each of two welded wire mats as shown in Figure 12 and 13b. The two instrumented mats were installed at heights of 3 and 10.5 feet from the foundation as shown in Figure 11. Wires from each strain gage load cell were brought forward to the face and housed in a section of plastic pipe. Frequent strain gage readings were then made with a portable BUDD strain gage indicator. This provided a complete time history of wire stress with depth into the wall at two different elevations. These readings were correlated with the movements shown by the extensometers.

Load cell design

Because of the small wires (9 gage) used in the wire mats, direct application of strain gages to the wires was not practical. Therefore, a special strain gage load cell was used. This was prefabricated and then placed into the wire mat just prior to placing backfill material.

To measure axial tension (or compression) in the longitudinal wires it was necessary to mount two strain gages on opposite sides of the load cell as shown on Figure 13a. The two gages were wired together in a series circuit. Thus, if the plate was subjected to bending the equal and opposite stress changes cancelled each other in the series circuit. Consequently, only the axial tension or compression was measured.

A standard Wheatstone Bridge circuit (Figure 14) was used to monitor the strain gages. The active gages were the strain gages mounted on the

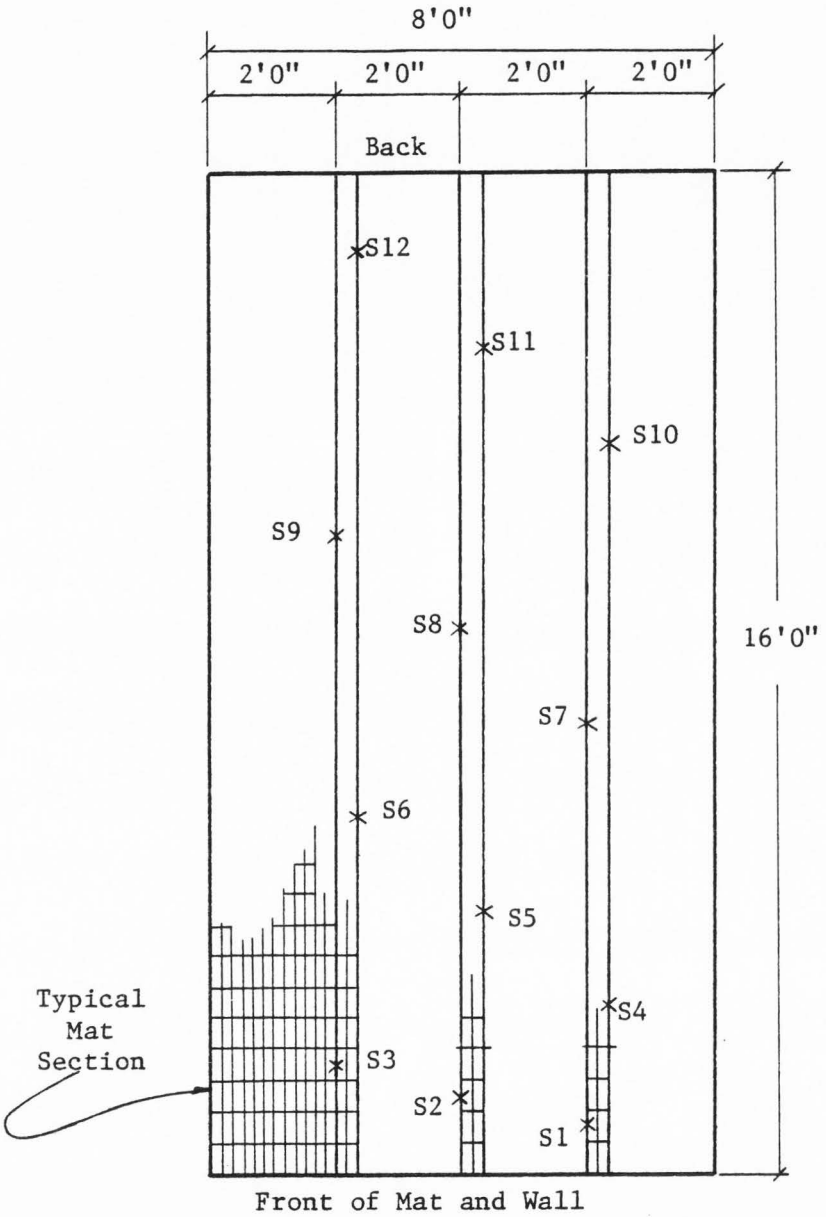

Figure 12. Strain gage load cell distribution for the first of two instrumented layers of wire mesh (placed at the top of lift #2). Distribution on the second mat was similar, though the mat was only 13'0" deep.

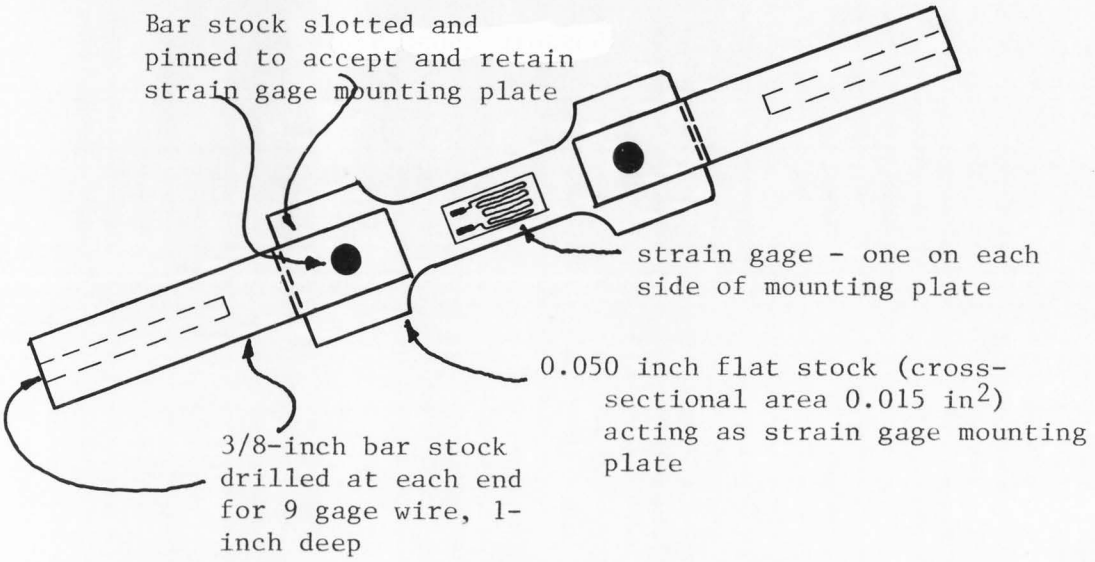

(a) load cell sketch (actual size)

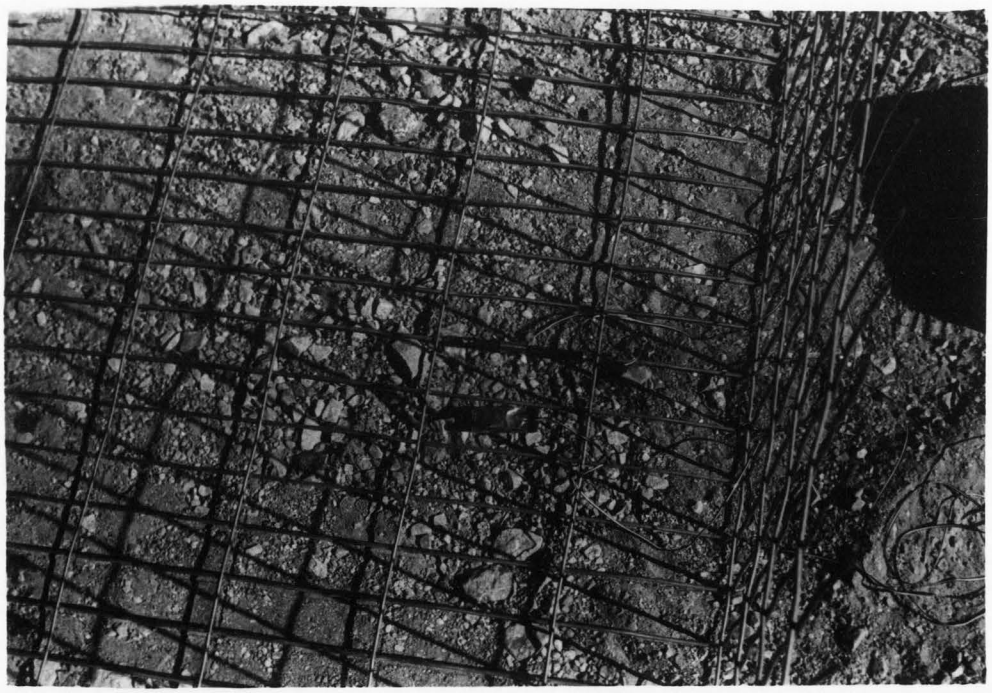

(b) load cell and temperature compensator prior to backfill in California wall

Figure 13. Load cell design and installation.

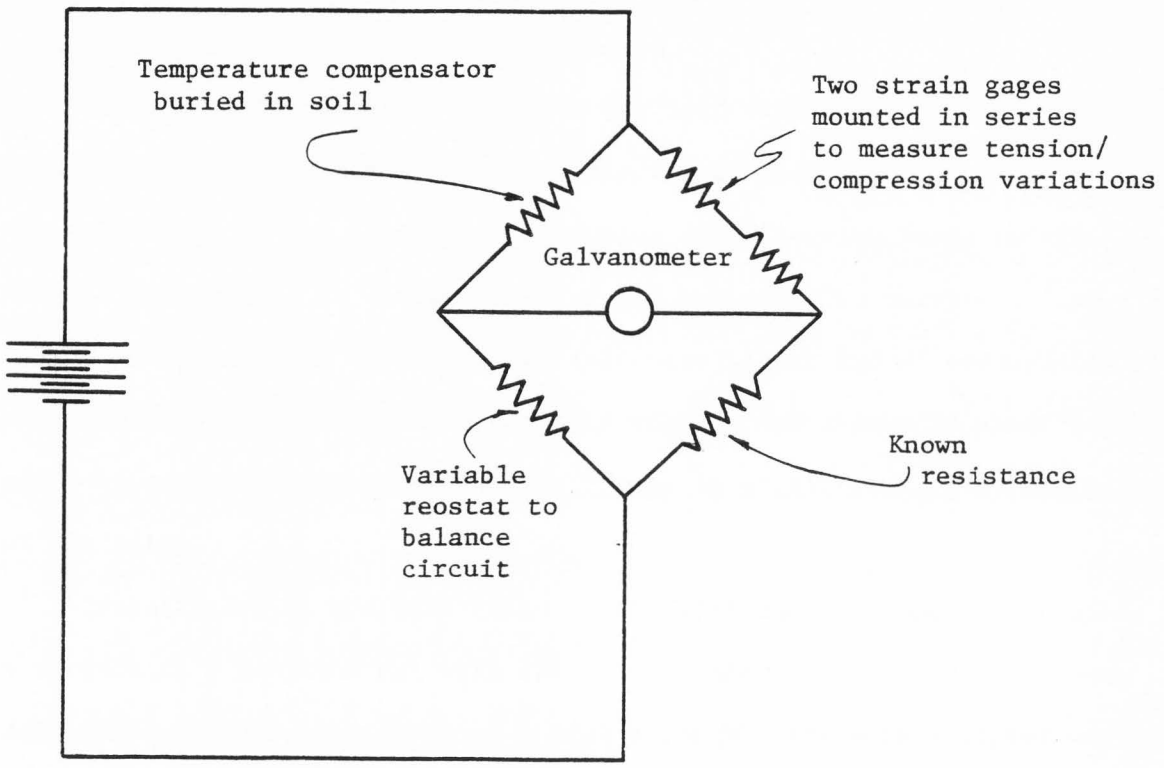

Figure 14. Wheatstone Bridge schematic.

load cell. As tension in the wire increased, the gage resistance increased and required the bridge to be balanced. To compensate for temperature changes two compensating gages wired in series were mounted on a small plate and buried in the backfill. The bridge circuit balanced the active and compensating strain gages against each other, thereby eliminating variations due to temperature changes.

All of the strain gages for both the load cells and the temperature compensators were mounted and completely weatherproofed. Each load cell was calibrated in the laboratory by adding axial tension loads to the cell in increments, to a total load of 250 pounds. The curves of load versus strain reading for each load cell were linear and of essentially the same slope. By establishing a zero reading the change in axial load could be computed by multiplying the change in strain reading by the slope of the curve.

Installation of the load cells in the wire mat was done at the site. A section of a longitudinal wire was cut out and the mounting tubes were soldered onto the cut ends using a high strength, low strain silver solder. Proper alignment and spacing of the tubes was achieved before soldering by using a dummy load cell pinned in place between the tubes as a spacer. As the mounting tubes cooled from the soldering process the dummy spacer load cell was placed under a slight tensile load. The load cells were installed after placing the mat in the wall and they were placed under this same slight tension load. This preload eliminated any unaccountable slack in the load cells after installation. Initial readings of all gages were taken with 8 to 10 inches of backfill on the mat. This acted as a zero base for subsequent readings.

Field and laboratory soil tests

In evaluating the welded wire retaining wall, a knowledge of the engineering properties of the backfill material was necessary. Two different soils were used for backfill. The first soil was a native decomposed granite. The second soil was a gravelly silt and was imported from a nearby borrow area.

During construction, sand cone inplace density tests were performed to monitor compaction of the backfill material. These tests were compared with standard Proctor compaction tests (AASHTO T-99 Method C) to determine the relative compaction. The results are presented in Appendix A.

A grain size analysis of both soils was performed and the grain size distribution curves are shown in Appendix A. The decomposed granite had 3 percent passing the #200 sieve (0.075 mm) and 29 percent passed the #200 sieve for the gravelly silt. Atterberg limits tests were performed on the gravelly silt and showed that it was non-plastic. The decomposed granite was classifed as GP by the Unified soil classification system and the gravelly silt classified as SM.

To determine the shear strength of the soils a series of direct shear tests were run on material passing the #4 sieve (4.75 mm). For a compaction to 90 percent of maximum dry unit weight (AASHTO T-99 Method C) at a moisture content just dry of optimum, the decomposed granite had a ϕ of 33^{o} and a cohesion of 450 psf. For similar conditions the gravelly silt had a ϕ of 33^{o} and a cohesion of 500 psf. The Mohr-Coulomb strength envelopes for the soils at various placements and long term conditions are shown in Figure 37 of Appendix A. Saturating the SM caused a significant strength loss.

Laboratory Studies

Pullout tests

Introduction. One of the failure modes for reinforced soil structures of this type is that of the reinforcement pulling out. This takes place as the face of the retaining wall yields toward the active case of plastic equilibrium. Reinforcement extending beyond the Coulomb failure plane is necessary to maintain the integrity of the wall as the active wedge develops. If there is not a sufficient amount of reinforcement beyond the failure plane, the existing reinforcement will pull out under the load, and the wall will fail. It is therefore necessary to determine the length of reinforcement required to prevent a pullout failure. To do this, the pullout strength of the welded wire mat needs to be established.

Equipment. To determine the pullout strength of the wire mat a series of pullout tests were performed utilizing the earth pressure cell shown in Figure 15. The use of an earth pressure cell allowed the simulation of different overburden pressures on a section of wire mat embedded in compacted soil. The section could then be subjected to a pullout force. Various mat sizes were investigated under laboratory controlled conditions.

The earth pressure cell was a reinforced concrete box open on the top and on one side. The inside dimensions were 6 feet wide by 5 feet long by 4 feet high. Four 1-foot high steel gates on the open side provided complete closure for the cell. After the cell was filled to capacity a 1/2 inch steel plate was placed on top of the soil. Four heavy steel arms with four hydraulic jacks mounted on each arm were positioned over the

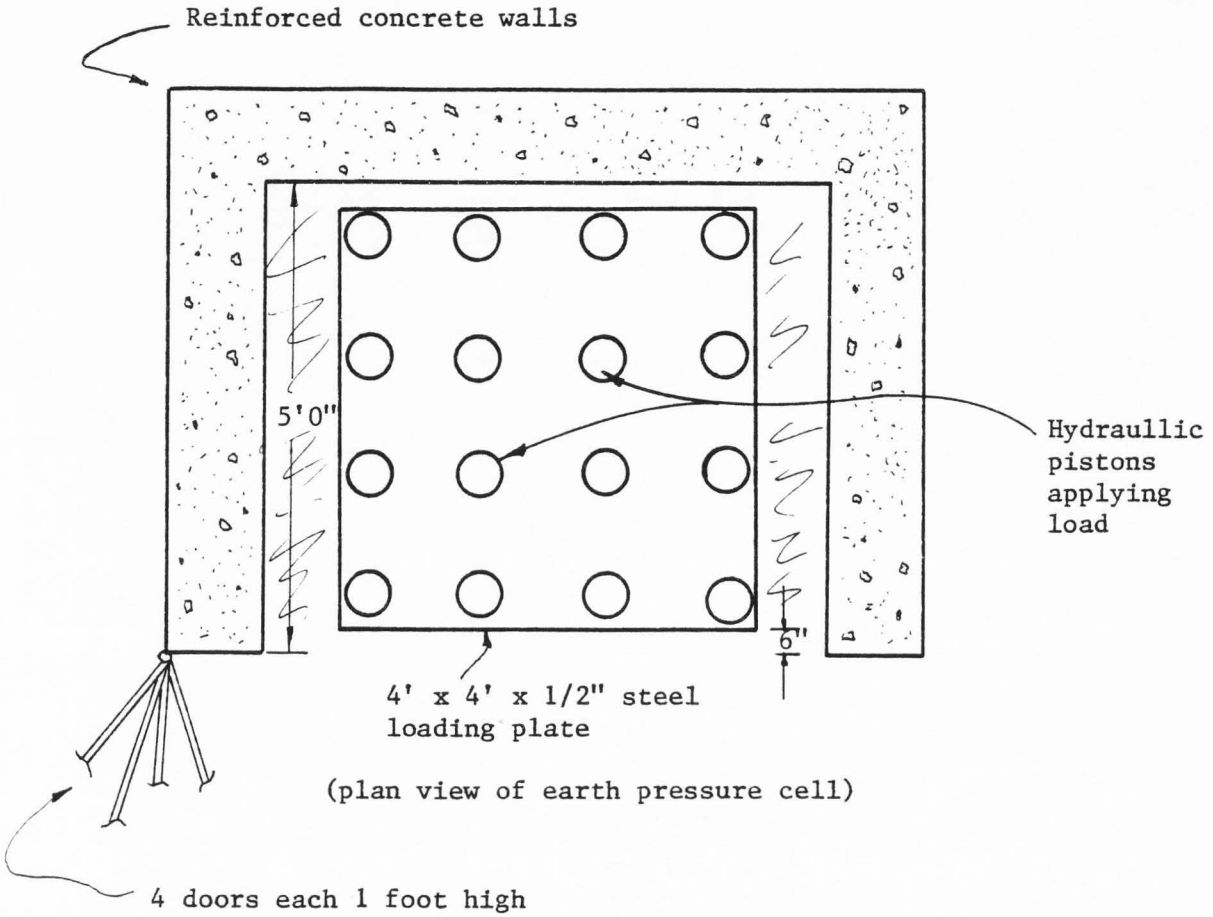

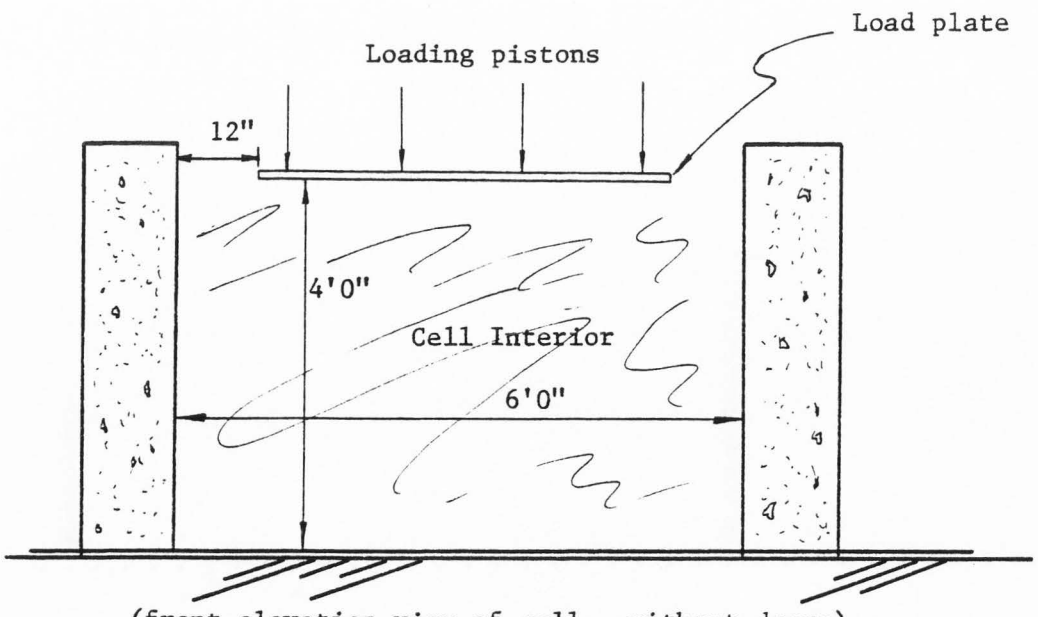

Figure 15. Plan and elevation sketches of earth pressure cell.

top of the cell as shown in Figure 16b. The sixteen hydraulic rams, activated by a common hydraulic pump system, were used to load the steel plate. This provided a vertical pressure to the soil inside the cell capable of simulating up to 100 feet of overburden.

Procedure. To perform the pullout tests, sections of mat were pulled out of the cell while loaded with different vertical pressures. The mat was pulled through a 2-inch slot between the top two gates of the cell. A permanent base of soil was compacted in the cell to the top of the third gate. The soil was scarified and the sections of mat were placed on the soil with the longitudinal wires extending out of the cell just above the third gate as shown in Figure 16b. The top gate was closed and the last foot of soil was compacted in place. The loading plate was put on top of the cell and loaded. To insure a complete loading of the wire mat, the experimental sections were placed directly under the load plate and at least 10 inches from the side walls of the cell. The longitudinal wires protruding between the top two gates were used to apply a pullout force to the wire mat sections. To measure the pullout force strain gage load cells, similar to the type used in the instrumentation of the retaining wall, were attached to the ends of the longitudinal wires as shown in Figure 16a. The load cells were larger to accommodate higher loads. Force was applied to the load cells by jacking wire cable through a continuous pull device.

Using this method of testing the experimental sections of wire mat were placed in the test cell and specific vertical pressure was then applied to the cell providing a simulated overburden weight over the test sections. Each test section was subjected to a pullout force in

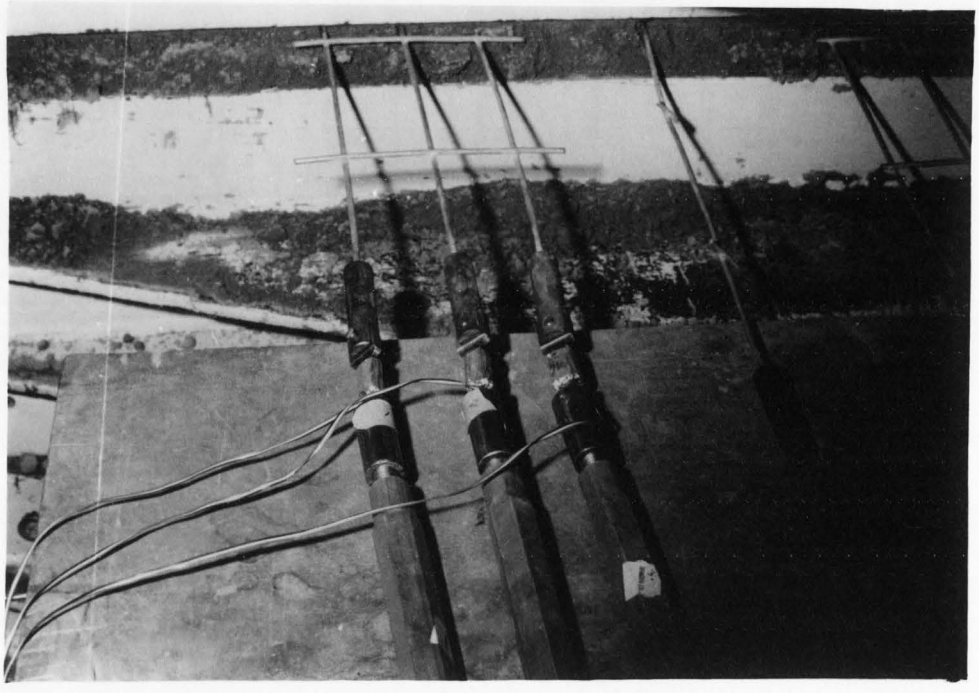

(a) load cells attached to mesh section for pullout test

(b) pullout test in progress

Figure 16. Pullout tests in earth pressure cell.

a continuous pull. Using turnbuckles (Figure 16a) the pullout force was initially distributed evenly to all the wires in the test section. The load cells provided a means of measuring the force in each longitudinal wire during the test. As the test section yielded outward, measurements of the displacement were taken. A graph of displacement versus pullout force applied was then plotted and the peak pullout force for each test section was established.

Test schedule. An initial series of tests were run using arbitrarily selected sections of mat. A lack of knowledge concerning the wire mat pullout strength and the limitations of the laboratory equipment made it difficult to establish a rational experiment design. Thus in the initial series of tests the sections used as well as the controlling experimental parameters were chosen from an intuitive understanding of the problem. From these tests data concerning the pullout strength of the mesh was obtained. While this data was very valuable, by itself it was inconclusive. Further testing was considered necessary. The initial data did provide an indication of the order of magnitude for the mat pullout strength, a clearer understanding of the behavior of the mat during pullout, and a knowledge of the limitations of the laboratory equipment.

Dimensional analysis techniques were used to develop a second group of tests to determine the pullout resistance. By limiting the study to a specific wire size, to one soil type, and to the same soil density for all tests, the amount of pertinent variables was reduced to a manageable number. Table 1 summarizes the test schedule with the conditions imposed on each test.

Table 1. Schedule of pullout tests.

	L_o	b: 6"	b: 12"
a	2"	3' - Test Series A* 5' - Test Seires B*	3' - A 5' - B
	4"	3' - A 5' - B	3' - A 5' - B
	6"	3' - A 5' - B	3' - A 5' - B

where: a = spacing between longitudinal wires
b = spacing between transverse wires
L_o = depth test section is buried

*Test Procedure: begin both test series with the overburden pressure equal to a 10 foot column of soil. Pull test section through peak pullout resistance a total of 6 inches (if possible). L_o then equals 2 1/2 and 4 1/2 feet for tests A and B respectively. Increase pressure to 15 feet of soil and pull another 6 inches. L_o then equals 2 and 4 feet. Increase overburden pressure to 20 feet and pull for peak pullout resistance.

Laboratory test wall

A small welded wire retaining wall was constructed in the test cell. It was built with a 9-inch lift on the bottom, two 15-inch lifts, and a 9-inch lift on top as shown in Figure 17b. The purpose of this test was to measure the stress in the longitudinal wires and compare the results with the measurements taken on the instrumented retaining wall constructed in the San Gabriel Mountains. The wire mat between the two 15-inch lifts was instrumented with strain gage load cells as shown in Figure 17a. The wall was constructed with the backfill placed at a dry unit weight of approximately 90 percent of the ASSHTO T-99 maximum dry unit weight.

Zero readings of the ten strain gage units were taken before soil was placed on the mat. Readings were again taken with 15 inches of soil on top and thereafter with each 5 feet of overburden applied by the hydraulic rams. After each 10 feet of hydraulic loading, the wall was allowed to stand for 45 minutes to determine any creep within the wall. With 30 feet of overburden the wall was allowed to stand for 8 hours. At the end of 8 hours it was concluded that little or no creep was occurring and the wall was loaded to an overburden of 100 feet (taking readings every 5 feet). Calculations indicated that the wall should have failed under 94 feet of overburden. Side friction along the walls of the test cell may have prevented the failure. After reaching this peak in the loading, the wall was unloaded and dismantled, and the wire mats were examined.

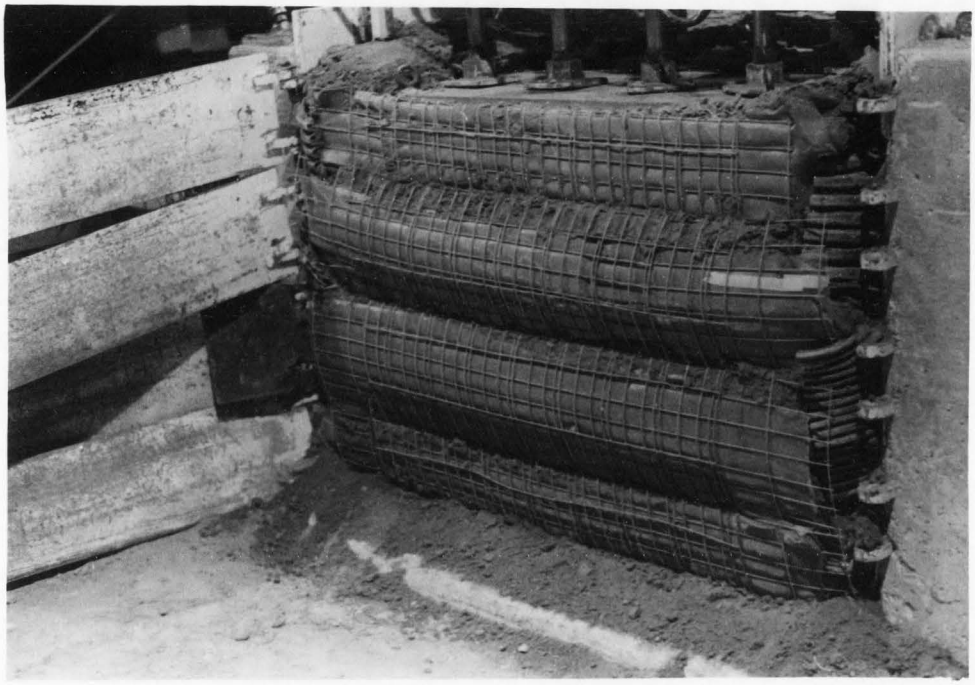

(a) test in progress

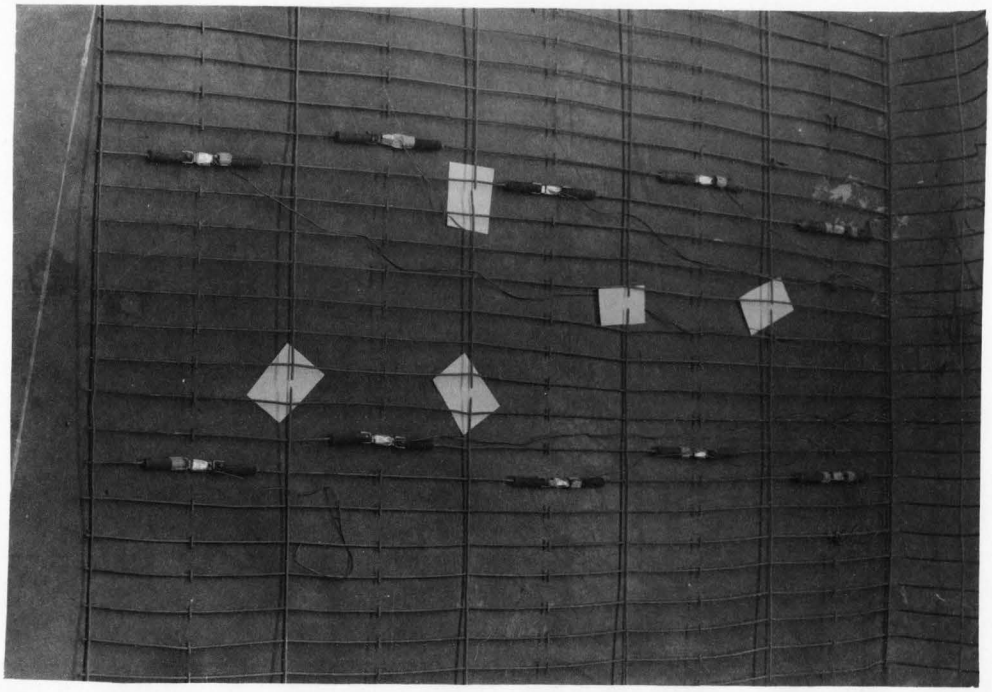

(b) instruments on center mat section (shown after test)

Figure 17. Laboratory test wall.

CHAPTER IV

RESULTS

Welded Wire Wall

Monitoring schedule

During the construction of the welded wire wall in California, all of the instrumentation was monitored as frequently as practical. During the construction of the first 11 lifts, the strain gages were monitored at the completion of each lift above their level of installation. Additionally, they were monitored before and after four days of rain and snow which occurred after completion of the tenth lift. Installation of the extensometer reference plate for the first set of extensometers was not completed until the completion of two lifts above the extensometers. Thereafter they were monitored at the completion of each lift, to the top of the tenth lift. For the same reason, monitoring of the second level of extensometers did not begin until the second lift above the extensometers was completed. The settlement plates were monitored after each lift from the time of installation to the eleventh lift. After enough fill had been placed over each survey monument to insure their permanence, they were monitored at irregular intervals sufficient to provide a time history of movements. At the completion of the eleventh lift a second construction slowdown made it impractical to continue a day by day monitoring of the instrumentation. No readings were taken until after the wall was completed. Seven weeks after the wall was finished and the road on top was placed in use, final readings of the instruments were obtained.

Force in longitudinal wires

Figures 18 - 23 provide a summary of the data from measurements of the force in the longitudinal wires. A compilation of all data obtained is presented in Appendix B. Figures 18 - 21 provide a record for each of the 24 load cells installed in the wall and show the force in the wire as a function of overburden height. To provide a reference for analysis, lines showing the theoretical wire force as a function of overburden height for different coefficients of lateral pressure (K) are also shown. The theoretical wire force was calculated by the equation:

$$F_t = K \sigma_v a z$$

The lines are plotted for values of K equal to 0.3, 0.5 and 0.7. Figures 22 and 23 show the variation of wire force with distance into the wall for representative heights of overburden. For reference, the theoretical Coulomb failure plane for the active case is shown where it would pass through the instrumented mats.

Horizontal strain and vertical settlement

Figure 24 shows the horizontal movement of the wall face relative to anchors placed within the wall, as a function of the overburden height. Figure 25 indicates overall settlement of the wall foundation as measured by P1 and P2 and settlement of the backfill material plus the foundation settlement as measured by P3 and P4. The difference between the readings (P1 - P3 and P2 - P4) is the compression of the backfill material.

Problems with the monitoring system

Because of problems incurred with the survey monuments, it is felt that the extensometers and the settlement plates provide a more accurate

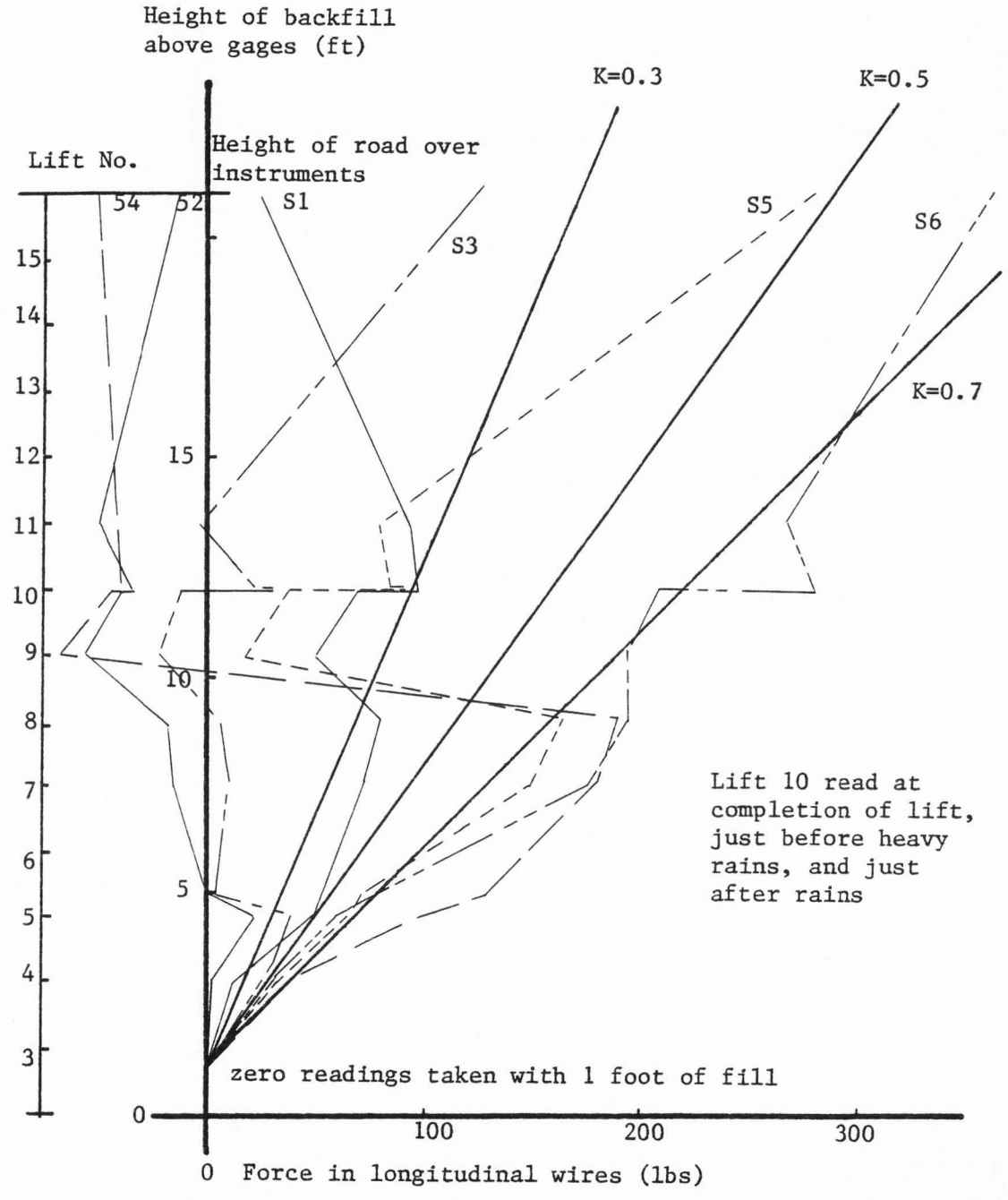

Figure 18. Height of backfill versus force in longitudinal wires. (S1-S6, 1st layer of instrumentation)

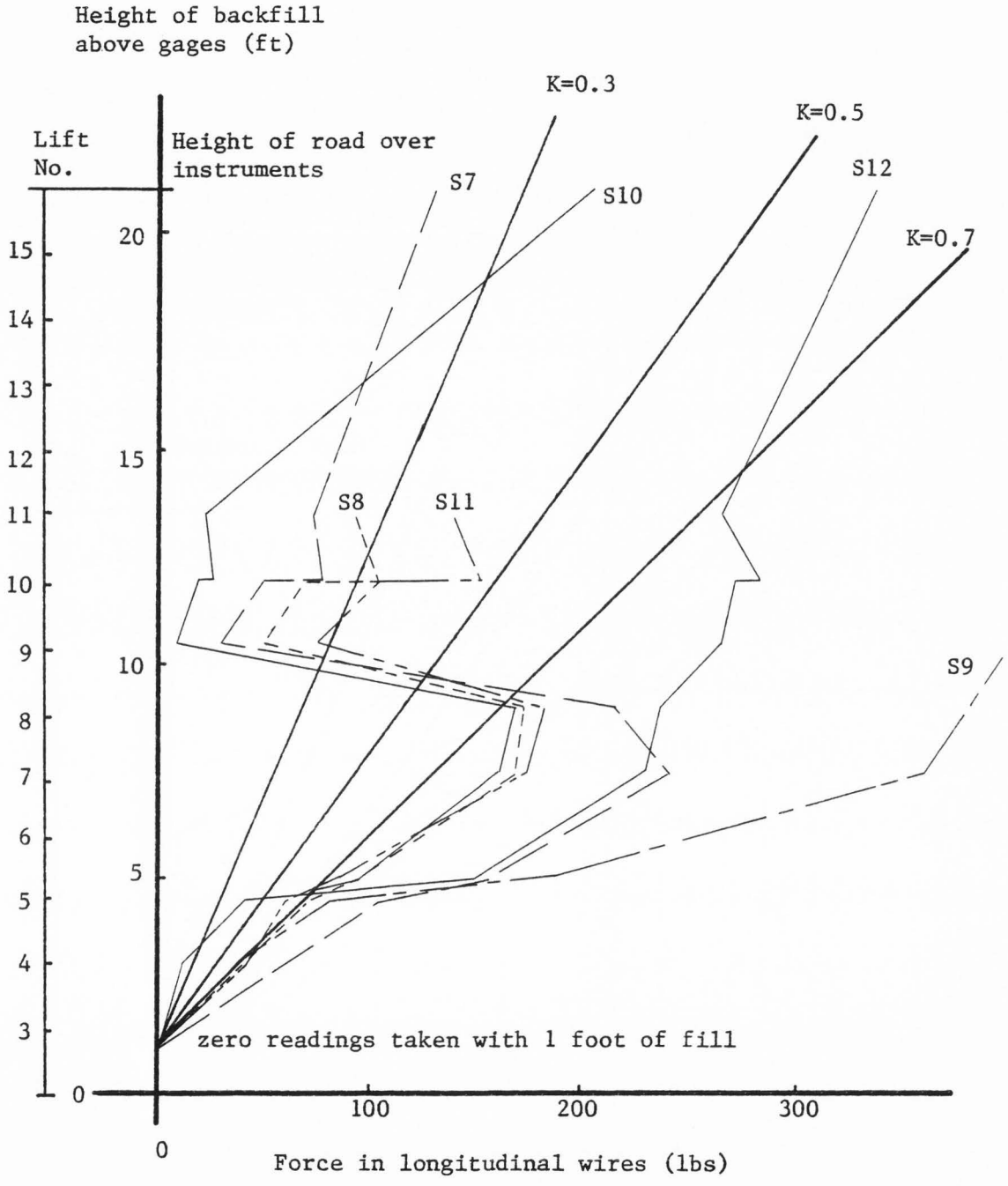

Figure 19. Height of fill versus force in longitudinal wires. (S7 - S12, 1st layer of instrumentation.)

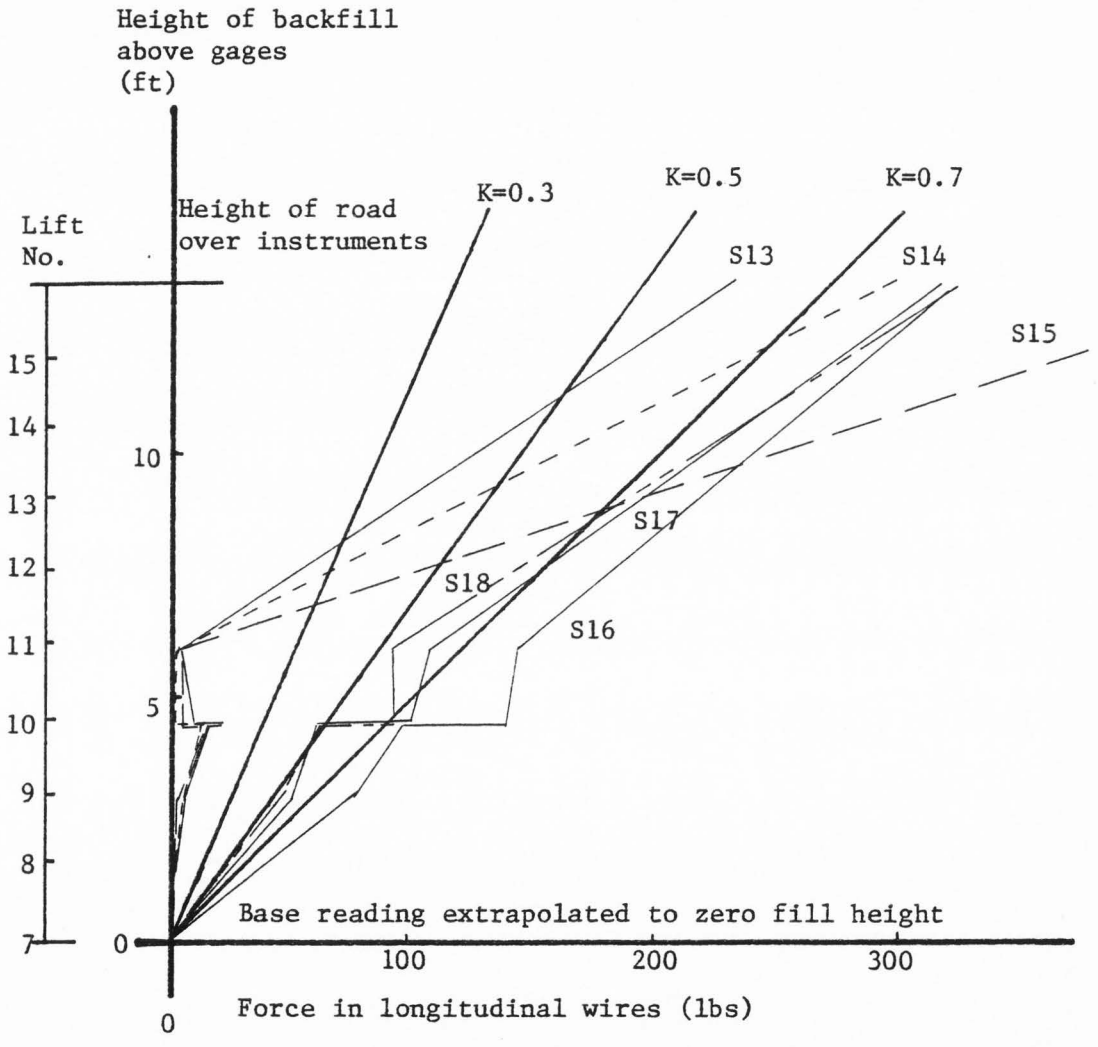

Figure 20. Height of fill versus force in longitudinal wires. (S13-S18, 2nd layer of instrumentation.)

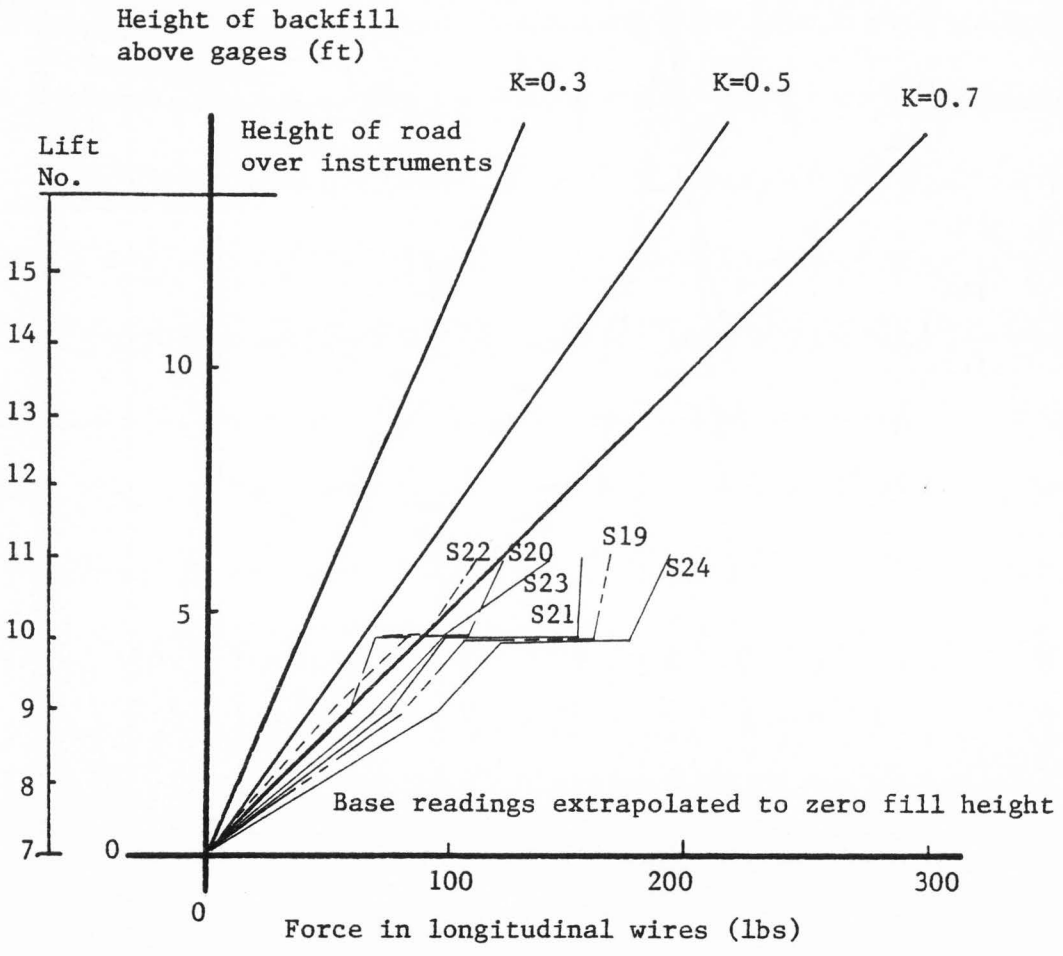

Figure 21. Height of fill versus force in longitudinal wires. (S19-S24, 2nd layer of instrumentation.)

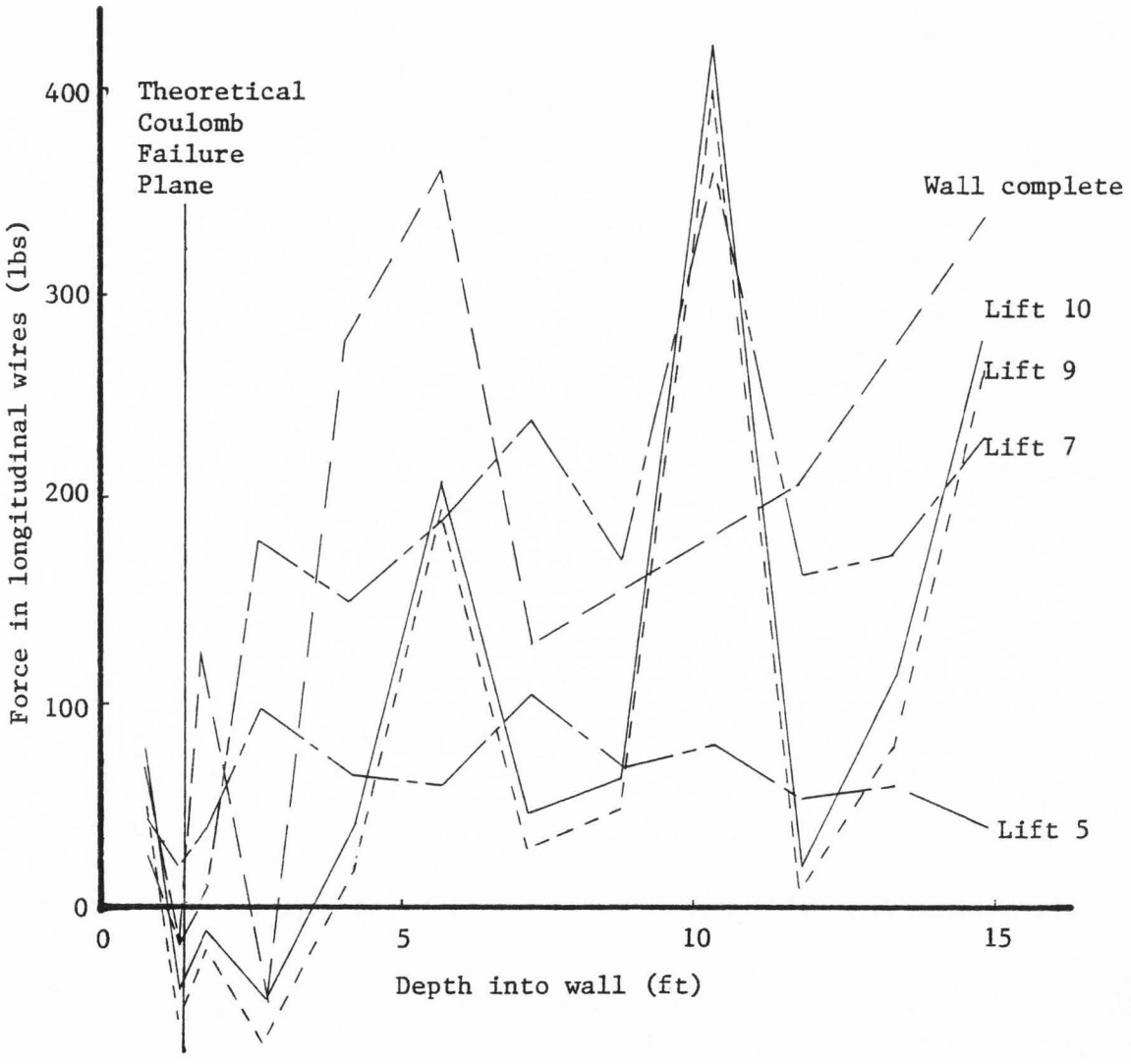

Figure 22. Force in longitudinal wires versus depth into wall. (S1 - S12, 1st layer of instrumentation.)

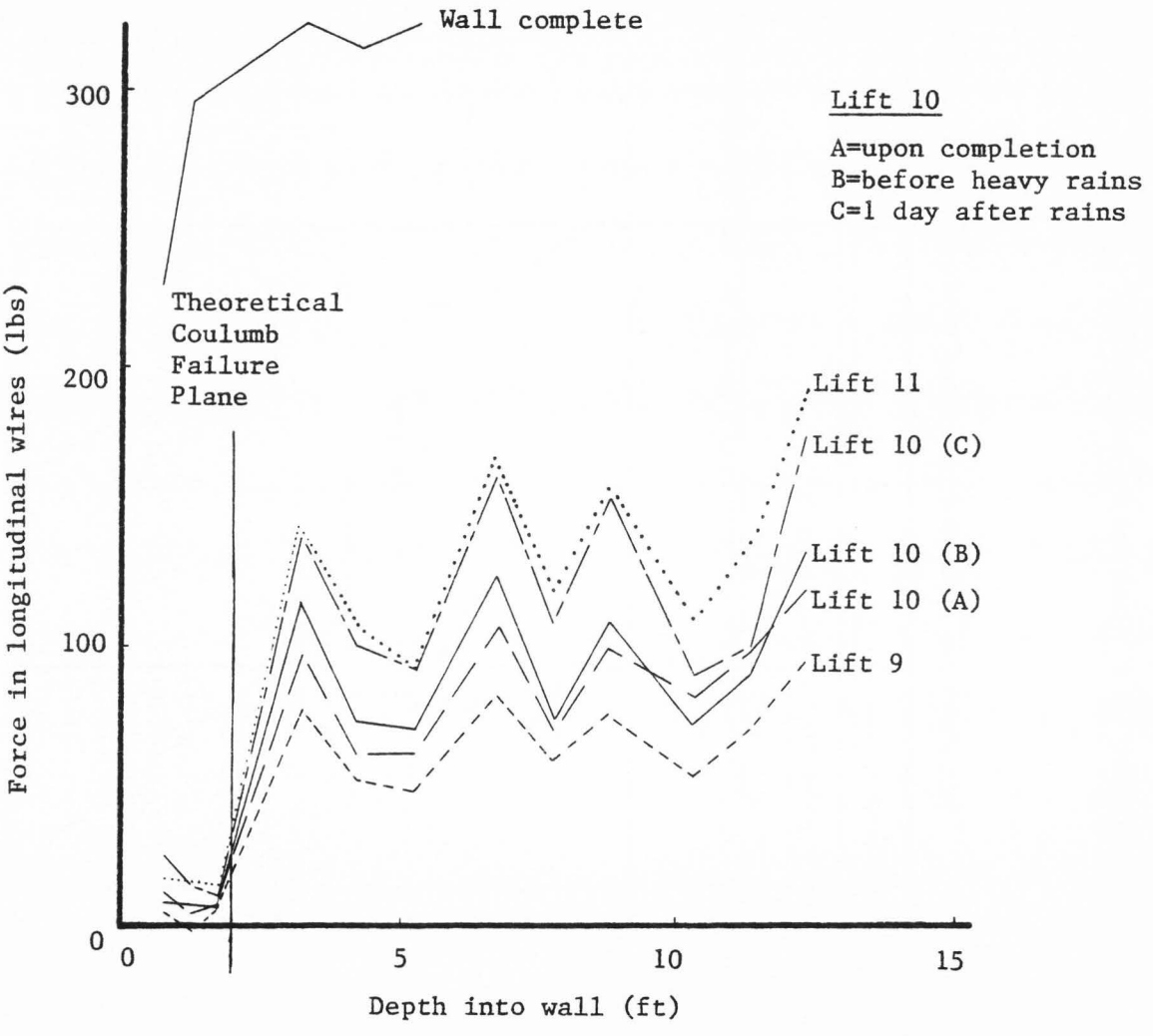

Figure 23. Force in longitudinal wires versus depth into wall. (S13 - S24, 2nd layer of instrumentation.)

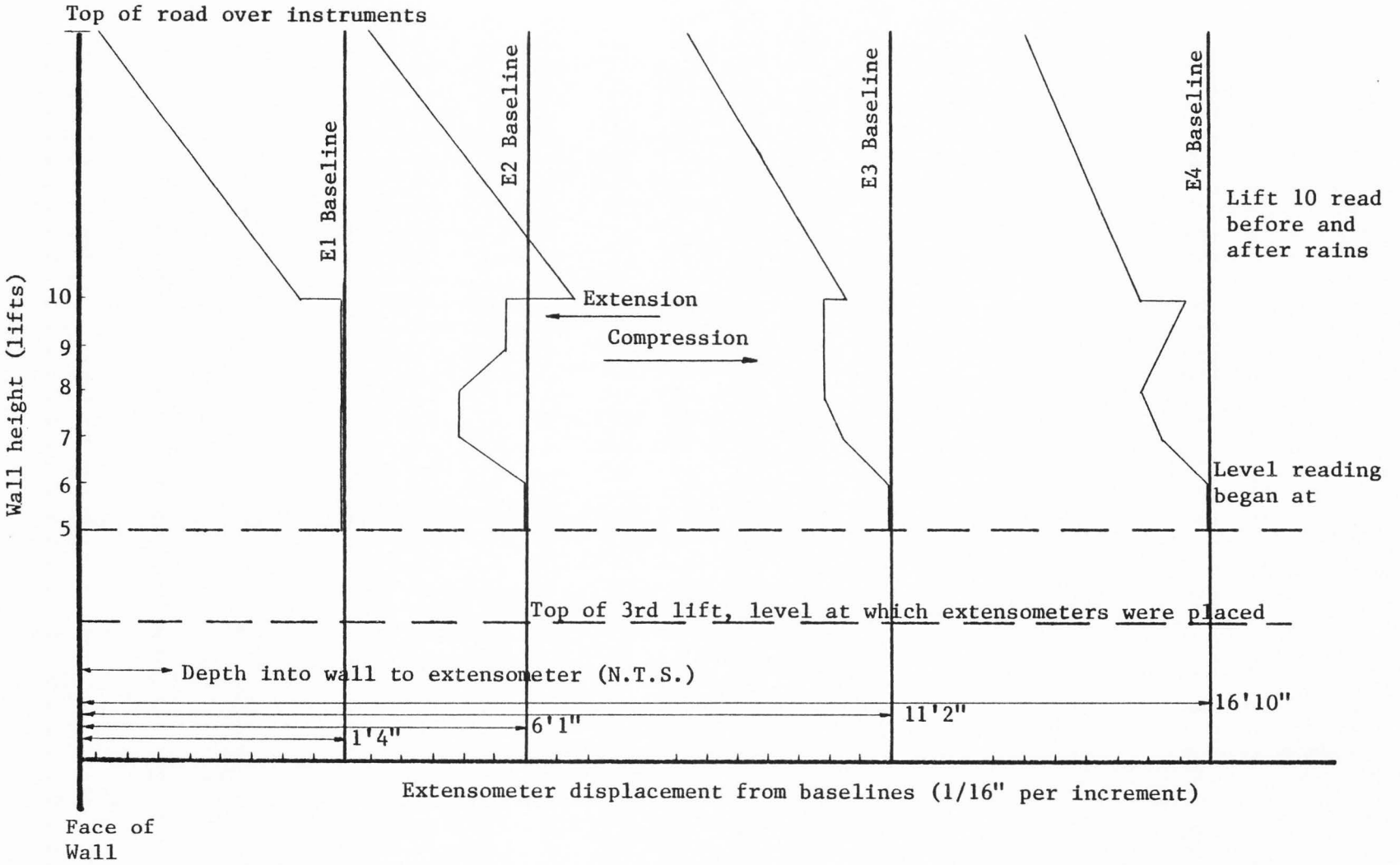

Figure 24. Extensometer displacement as a function of wall height.

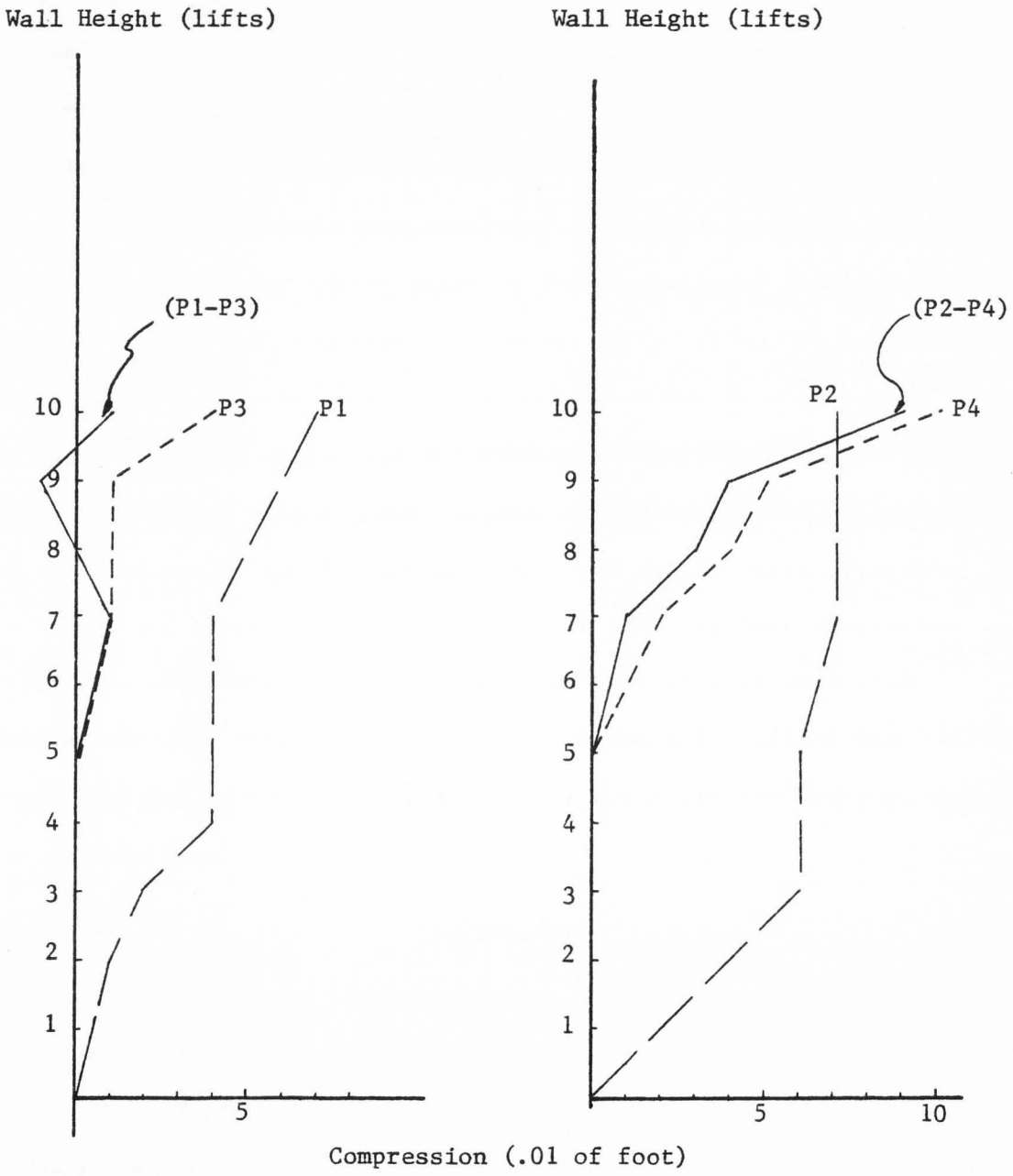

Figure 25. Settlement plate displacement.

picture of horizontal and vertical movement. The survey data is presented in Appendix B but is not presented here and will not be used to evaluate the wall movement. The upper layer of extensometers (E6 - E8) is not included because only two sets of readings were taken before heavy rains occurred which caused a pronounced outward movement of the reference plate. This movement rendered the third set of readings (taken seven weeks after construction concluded) useless. A problem with the data obtained from the strain gages on the second level should be noted. Following the initial readings taken after installation, an unaccountable jump of several hundred micro inches/inch of strain read occurred. This was observed in the second set and subsequent readings. After some time it was felt that a single change in the electrical circuit had occurred and that all the following readings were in a steady state situation. Therefore, all gages were plotted with wire force against overburden height, and extrapolated back to the force read with no overburden. These values were taken as the correct base and all readings were referenced from them. Therefore all graphs for S13 - S24 are based on this extrapolated base.

Pullout Tests

Appendix C lists all raw data obtained from the pullout tests. Figure 26 shows a summary of data for tests involving single longitudinal wires. The frictional force per unit length is shown as a function of the overburden height.

In presenting the data for the mesh pullout tests, several approaches were used to show the best relationship of the pullout force (F_p) to the variables considered. Figure 27 shows F_p as a function of the total

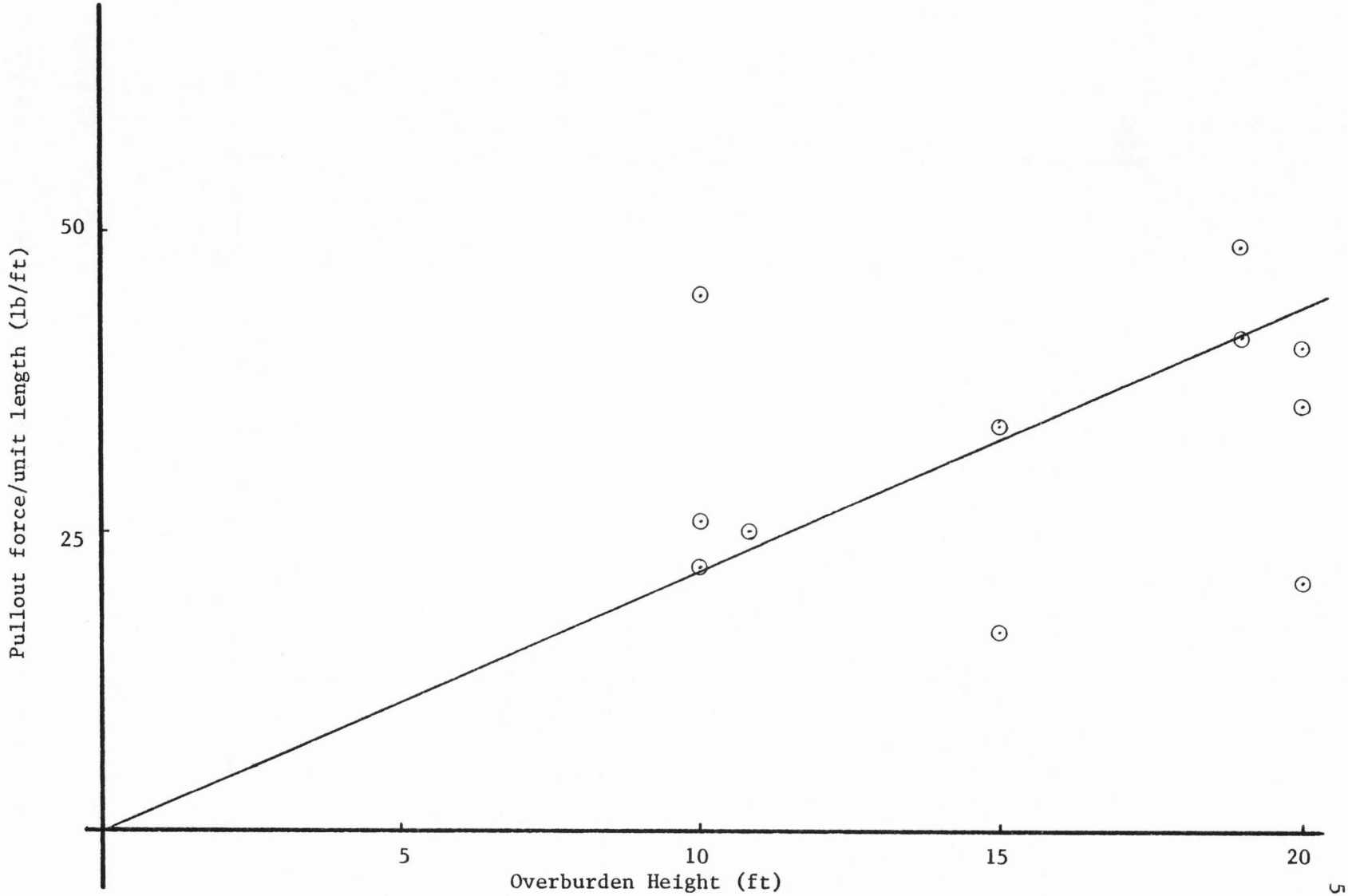

Figure 26. Single wire pullout force.

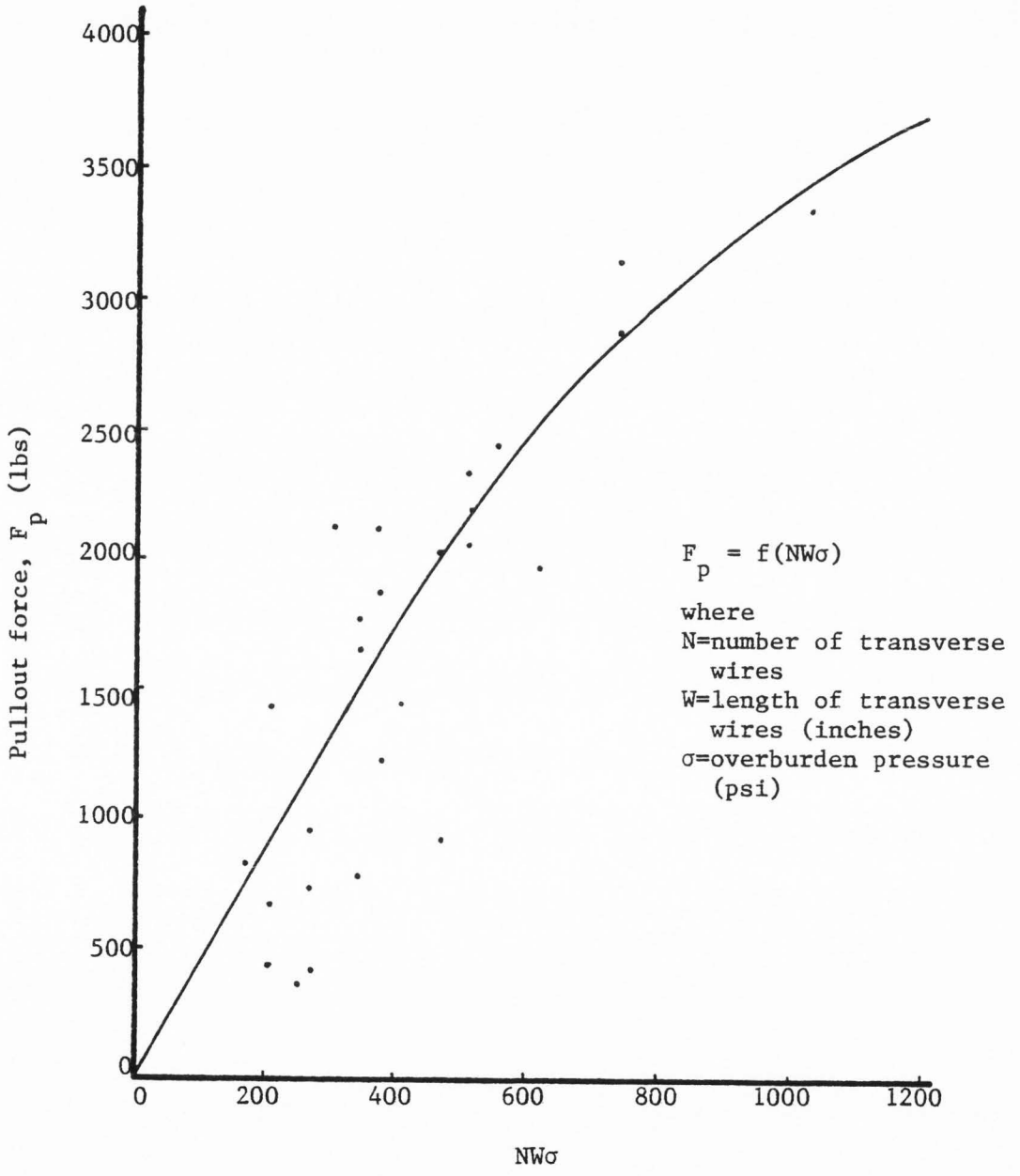

Figure 27. Pullout force as a function of NWσ.

length of buried transverse wires and the overburden pressure. The frictional resistance to pullout is not included in F_p; F_p only represents the resistance to pullout provided by the transverse wires. Figure 28 shows the force, F_p, per number of transverse wires buried as a function of the area of the mesh pulled.

Model Wall

Appendix D presents the raw data from the tests on the model wall. Figure 29 shows the force in the longitudinal wires as a function of similated overburden height. Theoretical values of wire force for K = 0.3, 0.5, 0.7 are also shown. The wall was instrumented with two parallel lines of strain gage load cells and the forces shown in Figures 29 and 30 are the average of load cell pairs. Figure 30 shows the wire force with depth into the wall for representative heights of similated overburden. The location of the theoretical failure plane on the instrumentation levels is also shown in Figure 30.

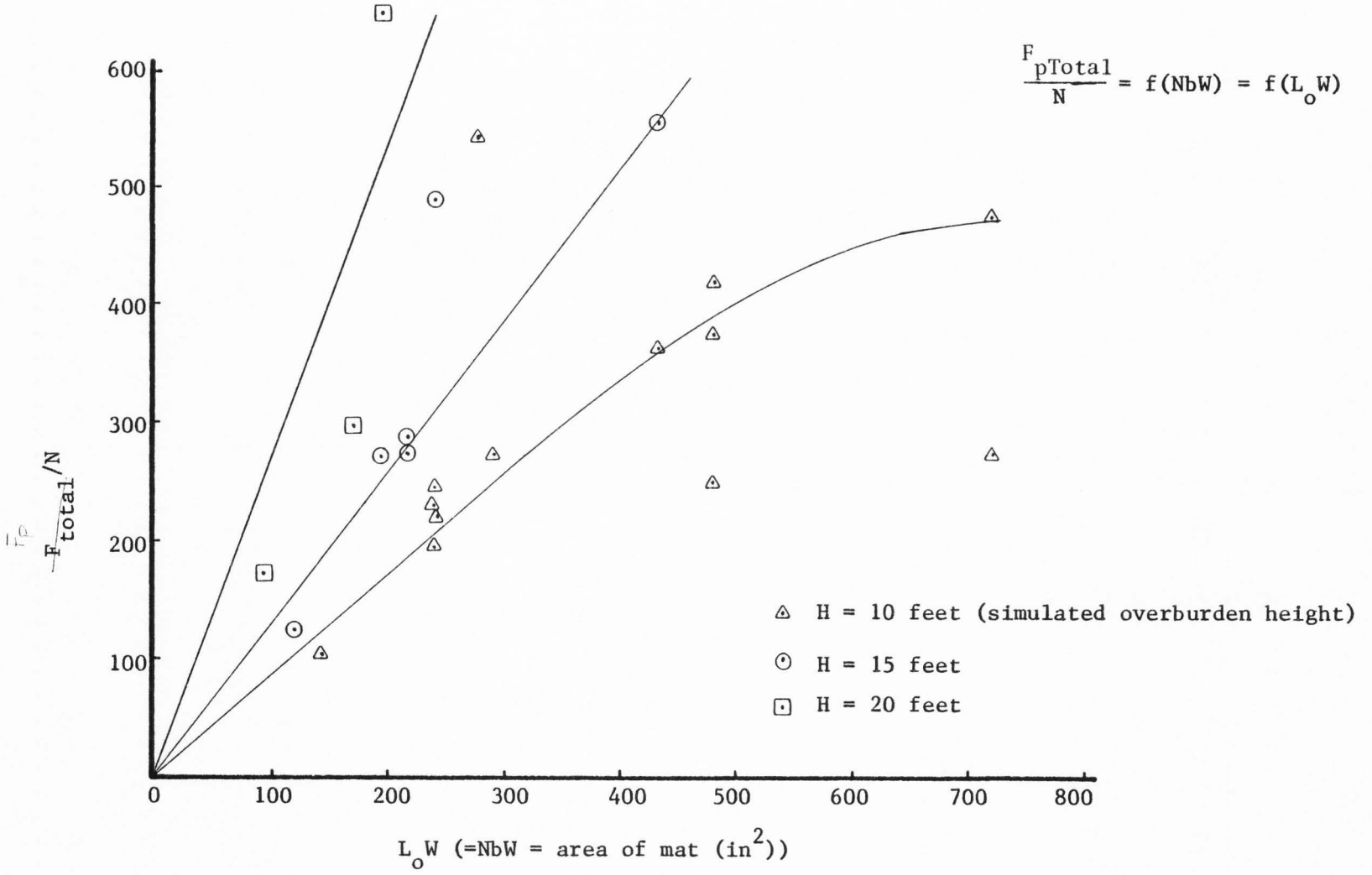

Figure 28. Pullout force as a function of NbW.

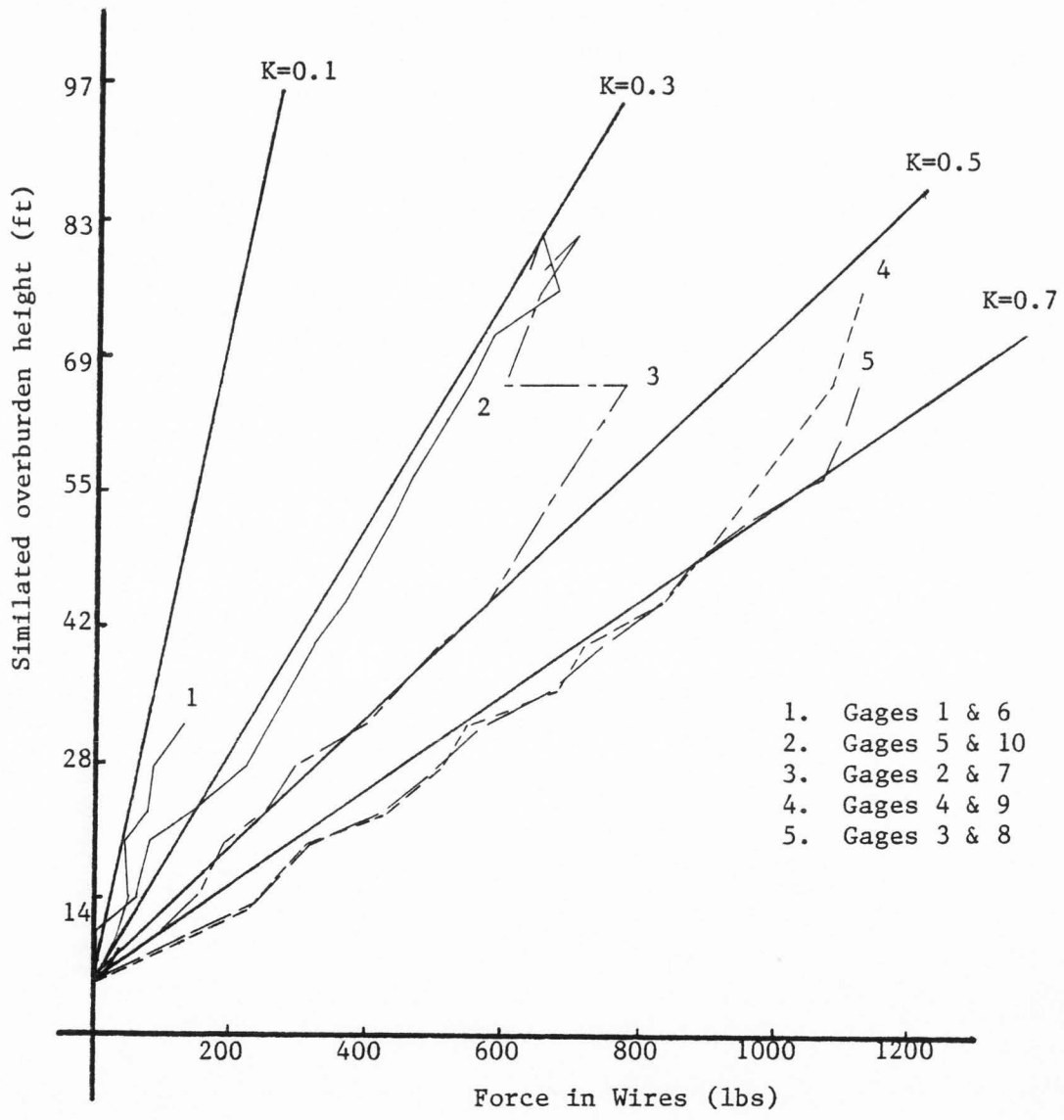

Figure 29. Force in the longitudinal wires versus height of backfill above instrumented mat--laboratory test wall.

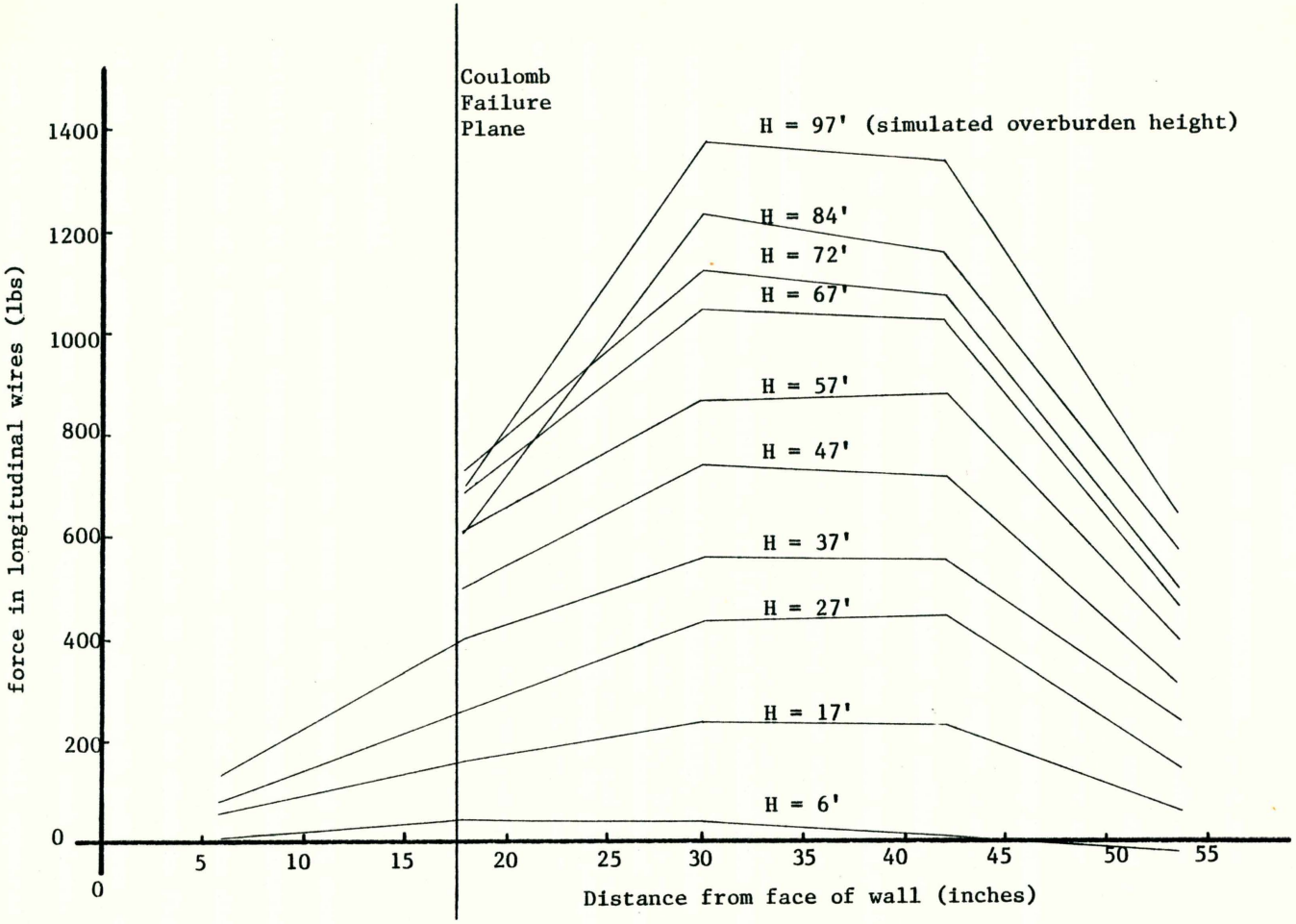

Figure 30. Force in wires versus depth into wall - laboratory test wall.

CHAPTER V

CONCLUSIONS AND RECOMMENDATIONS

Introduction

Purpose of the study

The purpose of this study was to evaluate the adequacy of welded wire mesh as a soil reinforcement. The objectives were:

1. To evaluate the performance of a welded wire wall;
2. To develop design recommendations for the welded wire wall.

Method of procedure

To accomplish these objectives, a 22 1/2 foot high welded wire wall was instrumented and its performance monitored. Additionally, a series of laboratory tests were made to evaluate the pullout resistance of the welded wire mesh and to confirm the stress distribution in the longitudinal wires.

Evaluation of Results

Welded wire wall

As the wall was constructed the force in the wires did not show any definite peak at a given distance from the face that could be considered an indication of a failure plane. However, yielding of the face did occur. The force versus wall height for load cells S1 - S12 as shown on Figures 18 and 19 and the extensometer record shown in Figure 24 indicate that between lifts six and nine significant lateral movement took place. Between lifts six and seven the outer 2 - 3 feet of the wall appeared to

relax slightly. An outward movement of about 1/8 inch was indicated by extensometers E2, E3 and E4. An accompanying drop in force in the longitudinal wires occurred at load cells S1 - S3 as shown on Figures 18 and 22. A more drastic relaxation occurred between lifts eight and nine. Both the force versus displacement curves (Figure 22) and the force versus height of fill curves (Figures 18 and 19) show a relaxation for all of the strain gages on the first level. This was accompanied by a movement of the extensometers showing E2 - E4 moving outward. This is interpreted as the interior of the wall relaxing and "catching up" with the face, in the completion of an accordian effect. This second movement showed the lateral pressure coefficient changing from about K = 0.70 down to $K \leq 0.3$ indicating that the active state occurred at this time. Hereafter the lateral pressures (as shown by the wire forces) began to build again and did not relax. Figures 18 - 21 all show that the lateral pressure coefficient averaged around K = 0.65. Figures 22 and 23 show no definite formation of a failure plane. This implies that the mesh holds the soil together tight enough to maintain the at-rest pressures. Therefore, for design purposes, the at-rest pressures should be used with K = 0.60 to 0.70.

Pullout tests

The test results to determine the frictional pullout resistance of a single longitudinal wire are shown in Figure 26. Using a best fit line, an average pullout force per unit length of wire was obtained. Calculating the frictional resistance based on a coefficient of frction of 0.31 ($\delta = 17^{o}$) gives approximately one half the values obtained using Figure 26. Until this discrepancy can be accounted for by more experimental data,

only the calculated frictional pullout force should be used for design purposes.

A silty sand to sandy silt was used in conducting the pullout tests. This soil represents one of the least desirable types of backfill material that would be used to construct a welded wire wall. Pullout resistance computed from the curves developed from these tests should therefore be on the conservative side for most acceptable backfill materials. From the pullout tests on the mesh sections several conclusions can be drawn. Considering the data obtained (Appendix C) it is apparent that the presence of a series of transverse wires welded to the longitudinal wires to form a mesh provides substantially greater resistance to pullout (on the order of four to six times) than do the longitudinal wires alone. Primarily, the pullout resistance is a function of the overburden pressure, soil density, number of transverse wires (N), and length of transverse wires (W). The pullout resistance may also be thought of as a combination of all the wires in a specific mesh size, or as the number of transverse wires, N, per area of mat. There are probably more variables in the problem than these mentioned.

In evaluating the different possible relationships between longitudinal force the the different variables several approaches were taken. The first involved showing the force, F_p, as a function of the overburden pressure and the total length of transverse wire resisting pullout. Figure 27 depicts this relationship. This relationship considered the transverse wires to act as a series of small line anchors providing resistance to pullout as some function of soil bearing capacity. This is different than the frictional resistance to pullout provided by the

longitudinal wires. Thus to define the pullout force (F_p) due to the transverse wires alone:

$$F_p = F_{\text{total resistance}} - F_{\text{frictional resistance}}$$

Figure 27 presents a possible relationship, and though it will need refining, it can be used for design in its present form. It is the most reasonably conservative approach considered to estimate the pullout resistance of the welded wire mesh.

A second approach considers the pullout force (F_p) as the total force required to pull out the mesh section:

$$F_p = F_{\text{total}}$$

This force, F_p, per number of transverse wires in the mesh (F_p/N) is shown in Figure 28 plotted as a function of the total mat area. This is done for each of the three overburden heights tested in the laboratory. This relationship can be used in the design of mats to resist pullout. However more tests should be performed to confirm the results. The pullout resistance is substantially greater (20 percent ot 50 percent) when determined by Figure 28 than by Figure 27.

When the unsupported length of the transverse wires (a) was greater than 2 inches (the tests also included 4-inch and 6-inch spacing) some of the welds failed and these abrupt weld failures caused a sudden drop in the pullout resistance. Also, when test specimens were removed from the pressure cell some of the transverse wires with the wider longitudinal spacing were bent backwards between longitudinal supports. This would probably be the condition just prior to weld failure. Observation of these conditions leads to the conclusion that the transverse wire strength

as well as the longitudinal wire strength must be considered in selecting the spacing of the longitudinal wires.

Laboratory tested wire wall

The wall constructed and loaded in the earth pressure cell provides confirmation of the data and conclusions from the instrumented wall in California. Figures 29 and 30 show high lateral pressures throughout the depth of the wall. Figure 29 shows that it is necessary to consider the at-rest pressures to govern, with K = 0.60 to K = 0.70. The records shown in Figures 29 and 30 confirm the tight, unyielding structure observed in California.

Conclusions

Based on all the laboratory and field data studied it is felt that the welded wire wall as designed and constructed in California is adequate. Considering the high pullout resistance of the mesh samples as demonstrated by the pullout tests, failure by pullout in such a wall should not be a problem. In both the field and laboratory studies with lateral pressures within the wall were typical of the at-rest condition with K = 0.60 to 0.70. For design of tension reinforcement (longitudinal wires) the lateral pressure coefficient should be 0.60 to 0.70. The force in the longitudinal wires should be calculated by:

$$F = K \sigma_v a z$$

where σ_v is the vertical pressure, a the horizontal wire spacing and z the vertical mat spacing. The spacing between longitudinal wires (a) should be no greater than about 4 inches. Spacing between layers of mesh in the wall (z) should be less than or equal to 24 inches, to insure

proper interaction between the layers. To design the mats for pullout, Figure 27 can be used. Though no failure plane is well defined in the experimental data, design against pullout failure is best accomplished by considering only that portion of the mats extending beyond the classic Coulomb failure plane. Considering the entire embedment depth as being effective against pullout would be unconservative. A factor of safety against pullout (FS_p) of 2.0 should be used.

Recommendations

Welded wire retaining wall design procedure

As in any retaining wall problem, exterior stability as well as internal stability must be satisfied (see Appendix E for an example design problem). To satisfy external stability, three conditions should be investigated:

1. Sliding (including deep stability)
2. Bearing capacity
3. Overturning

These are conventional criteria for the design of retaining walls. The external stability requirements should be used to establish the overall dimensions of the wall including the length of embedment of the mats.

With external stability satisfied, the design of the wall elements is considered. This is internal stability and with a welded wire wall two failure mechanisms must be considered:

1. Failure of longitudinal wires fail in tension,
2. Failure of the mesh fails in pullout.

It is proposed to design for these two conditions as follows:

1. Design for tension in the longitudinal wires

   a. Establish an idealized lateral pressure diagram for design. Use K = 0.65.

   b. Based on the lateral pressure diagram select a wire spacing and size. The force in each wire can be computed using

   $$F = K \sigma_v a z \qquad (2)$$

   as previously defined. The walls that were tested in this study used 9 gage galvanized steel wire (diameter = 0.149 inches) and a horizontal wire spacing of 2 inches. The vertical spacing between mats was 18 inches for the field wall and 15 inches for the laboratory wall. In selecting the wire size both corrosion and the ability to field bend the wire must be considered. Nine gage wire is the largest size that can be efficiently bent using hand tools. A vertical spacing of 18 inches between mats seems practical.

2. Check the pullout resistance of the mats

   a. The embedment length of the mats are generally established by considering sliding at any level of the wall (an external stability criteria).

   b. Only the extension of the mats behind the Coulomb failure plane as shown in Figure 31 should be considered as effective in providing resistance to pullout.

   c. The required extension of the mats behind the Coulomb failure plane will depend on the force in the wire, the vertical stress, and the spacing of the transverse wires in the mat. The resistance of the mats to pullout can be determined from Figure 27.

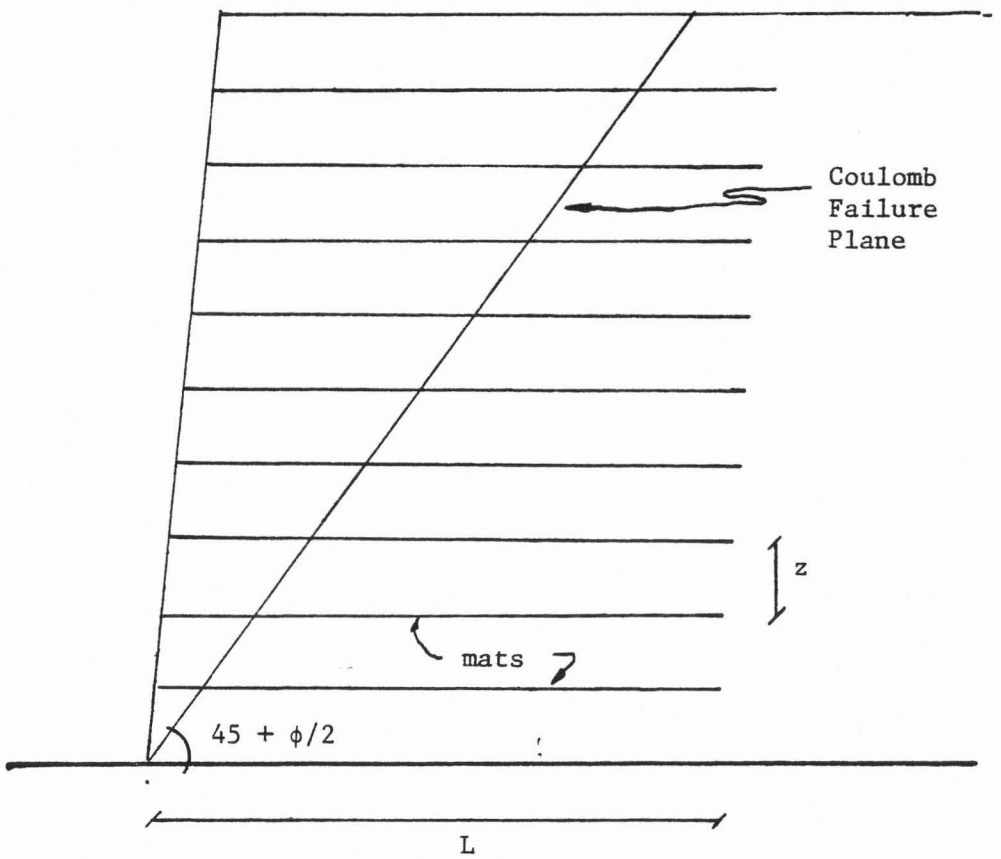

Figure 31. Generalized cross-section of welded wire wall showing the Coulomb failure plane.

d. Compare the resistance to pullout computed in (c) with the tension in the longitudinal wires. The pullout resistance can be adjusted by changing either the mat length of the spacing of the transverse wires. A factor of safety of 2.0 or greater (against pullout failure) should be used, where

$$FS_p = \frac{F_p}{F} \geq 2.0$$

e. In some cases it may be desirable to reduce the length of the mats near the top of the wall. It is not necessary to extend the mats near the top of the wall beyond the Coulomb failure plane if the mats in the lower portion provide enough pullout resistance to withstand the full Coulomb lateral force with an adequate factor of safety. The mats at the top must extend deep enough into the wall to maintain the integrity of the wall at the top. This concept is discussed in Chapter Two and illustrated by Figure 32.

Construction recommendations

A suggested construction sequence is detailed in Figure 33. The beginning of the sequence is shown with the placement of a typical mat section on Figure 33a. Backfill material is placed to the full height of the lift to within 1/2 to 2 feet of the face as shown. The next mat is placed and tied to the face of the lower mat as shown on Figure 33b. Backfill is placed to the rear of the second mat to hold this mat in place and preserve the batter on the face of the lower mat. The void at

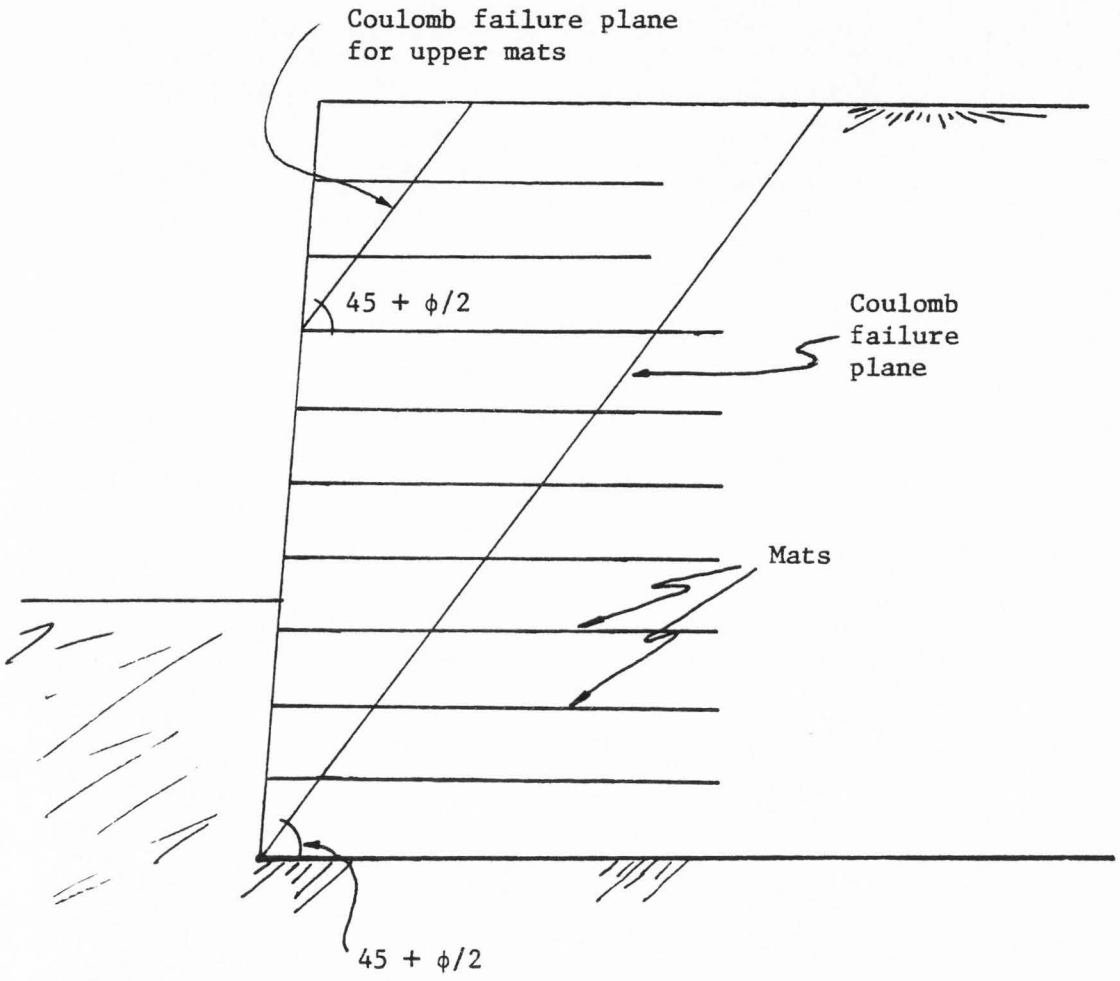

Figure 32. Upper mats shown cut off inside Coulomb failure plane.

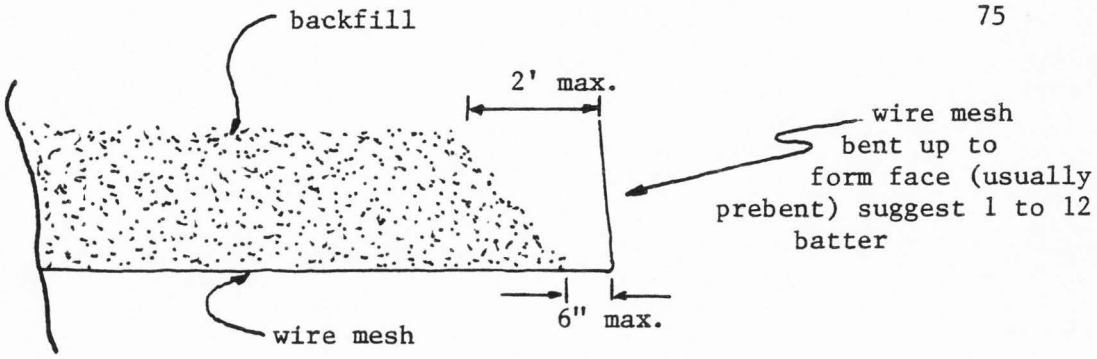

(a)

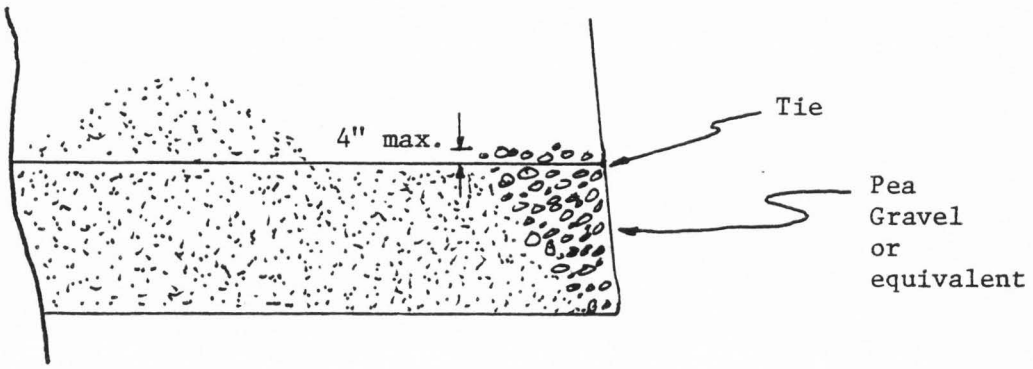

(b)

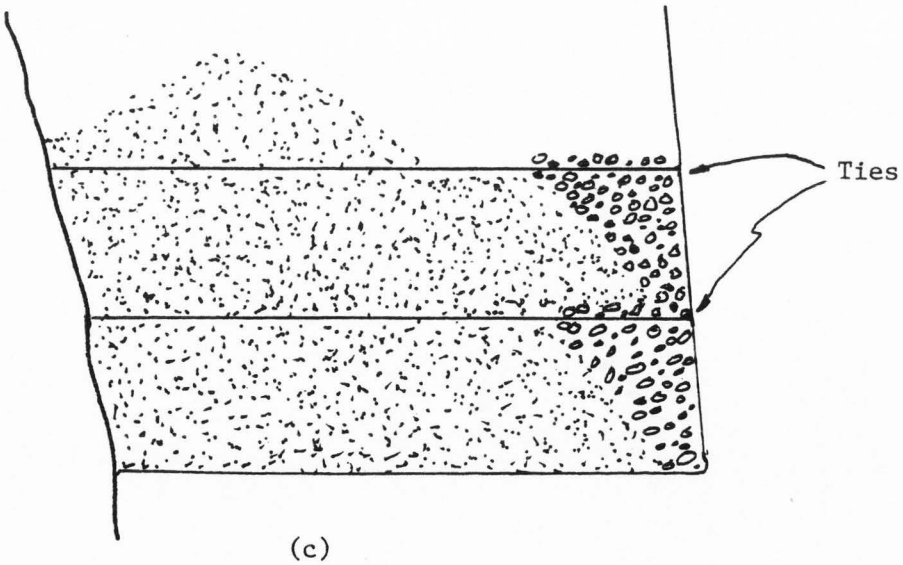

(c)

Figure 33. Proposed construction sequence.

the face of the lower mat is then filled with a coarse granular material (pea gravel) poured through the mesh of the upper mat. This material is rodded to avoid arching and to achieve a high in place density. This pea gravel will prevent settlement due to poorly compacted material at the face (as occurred on the instrumented wall studied in California) and will act as a filter to prevent migration of the fines from the backfill material. This procedure is then repeated throughout the remainder of the construction (Figure 33c).

Alternately the face of the lower mat in Figure 33a can be temporarily supported by boards along the face and tied back as originally devised by the designer or by backfill placed in front, if there is room (a procedure successfully used on the lower lifts of the wall in California). These two techniques allow the placement of the backfill up to the face and eliminate the need to import and place the pea gravel.

Granular material is the most desirable backfill material because it is easy to place, it has a low compressibility, it is free draining, and it has good strength characteristics. Silty or clayey sands and gravels are also acceptable provided no more than 40 percent of the material passes the #200 sieve. Clay soils should be avoided because of their shrink-swell characteristics, poor drainage capabilities, and somewhat lower shear strengths. For the construction sequence in Figure 33, pea gravel or 3/4-inch minus concrete aggregate should be used at the face.

As with any retaining wall, groundwater control should be maintained. If necessary an underdrain system should be installed.

It was established by a test in the earth pressure cell that elaborate ties to tie the face to the next upper mat (see Figure 33b) is not

needed. A welded wire wall was built and loaded to 100 feet of overburden pressure. The tie used was done simply by bending the wire from the face once around the corresponding wire on the next lift. No problem was encountered during the initial loading. The face was then cut open and the wall remained in place. It can be concluded that the tie is not subject to large stress and a simple tie is quite adequate.

Recommended additional research

More pullout data are needed to more clearly define the pullout failure mechanism. Control of soil density should be maintained during the test, and varied to see its effect. Soil type should also be varied.

Additional information and confirmation (if possible) should be obtained from the field. This should be in the form of another instrumented welded wire wall. In doing this instrumentation, some improvements should be made. Additional temperature compensators should be installed to assure a fixed base to compare installed strain gages. The extensometers should use an improved reference point at the face of the wall, and the survey targets and control should be more firmly anchored.

LITERATURE CITED

Anderson, Loren R., and Selvage, John R. 1976. Prefabricated tie back walls. New Horizons in Construction Materials. Envo Publishing Company, Inc., Lehigh Valley, Pennsylvannia. 682 p.

Amesbury, H. C. 1935. Final report for the construction of a portion of primary state highway in Del Norte County, between Last Chance Slide and Flannigans. Road I-DN-1-B Contract 61TC1, Division of Highways, State of California, Sacramento, California.

Chang, J. C., and Forsyth, R. A. 1977a. Design and field behavior of reinforced earth wall. Journal of the Geotechnical Engineering Division, ASCE 103:677-691.

Chang, J. C., and Forsyth, R. A. 1977b. Finite element analysis of reinforced earth wall. Journal of the Geotechnical Engineering Division, ASCE 103:711-724.

Chang, J. C., Forsyth, R. A. and Smith, T. 1972. Reinforced earth highway embankment -- Road 39. Highway Focus, Federal Highway Administration, U. S. Department of Transportation, Washington, D.C. Vol. 4, No. 1.

Chang, J. C., Hannon, J. B., and Forsyth, R. A. 1977. Pull resistance and interaction of earthwork reinforcement and soil. Presented at the 56th Annual Meeting of the Transportation Research Board, January 1977 (not published).

Doran, W. E. 1948. Stabilization of river banks. Proceedings of the 2nd International Conference on Soil Mechanics 2:60-63.

Dunn, I. S., Anderson, L. R. and Kiefer, F. W. 1976. Fundamentals of geotechnical analysis. Utah State University, Logan, Utah. 170 p.

Lee, K. L. 1976. Reinforced earth--An old idea in a new setting. New Horizons in Construction Materials. Envo publishing Company, Inc., Lehigh Valley, Pennsylvannia. 682 p.

Lee, K. L., Adams, B. D., and Vagneron, J-M. J. 1972. Reinforced earth retaining walls. Report No. 7233, University of California at Los Angeles School of Engineering and Applied Science, Los Angeles, California.

Schlosser, F. and Vidal, H. 1969. Reinforced Earth. Bulletin de Liason des Laboratories Routiers, Ponts et Chaussees.

Schroeder, W. L., Schwarzhoff, J. C. and Hanson, L. A. 1976. Performance of a thin metal retaining wall with multiple anchorage. Paper presented at the Annual Meeting of the Transportation Research Board, Washington, D.C.

Shen, C. K., Romstad, K. M. and Herrmann, L. R. 1976. Integrated study of Reinforced Earth--II: Behavior and design. Journal of the Geotechnical Engineering Division, ASCE 102:577-590.

Vidal, H. 1969. The principle of Reinforced Earth. Highway Research Record, Washington, D. C. No. 282, pp. 1-16.

Vidal, H. 1966. La Terre Armee. Annales de 1'Institute Technique du Batiment et des Travaux Publics, Paris, Frances, Nos 223-229, pp. 888-938.

APPENDICES

Appendix A

Soil Data

The welded wire wall in California utilized two separate soil types. The first was native material, a decomposed granite (S1). The second was imported from a nearby borrow area and was a gravelly silt (S2).

Figure 34 shows the results of the standard Procter compaction tests (AASHTO T-99, Method C). Table 2 records the sand cone in-place density tests run during construction.

A grain size analysis was performed on both soils and the grain size distribution curves are shown on Figure 35 (S1) and Figure 36 (S2). An attempt to run Atterberg Limit tests on S2 showed it to be non-plastic.

Figure 37 shows the Mohr-Coulomb strength envelopes for the four direct shear tests and long term condition on the shear strength is illustrated.

Unified soil classification system classified the decomposed granite (S1) as a GP and the gravelly silt (S2) as SM.

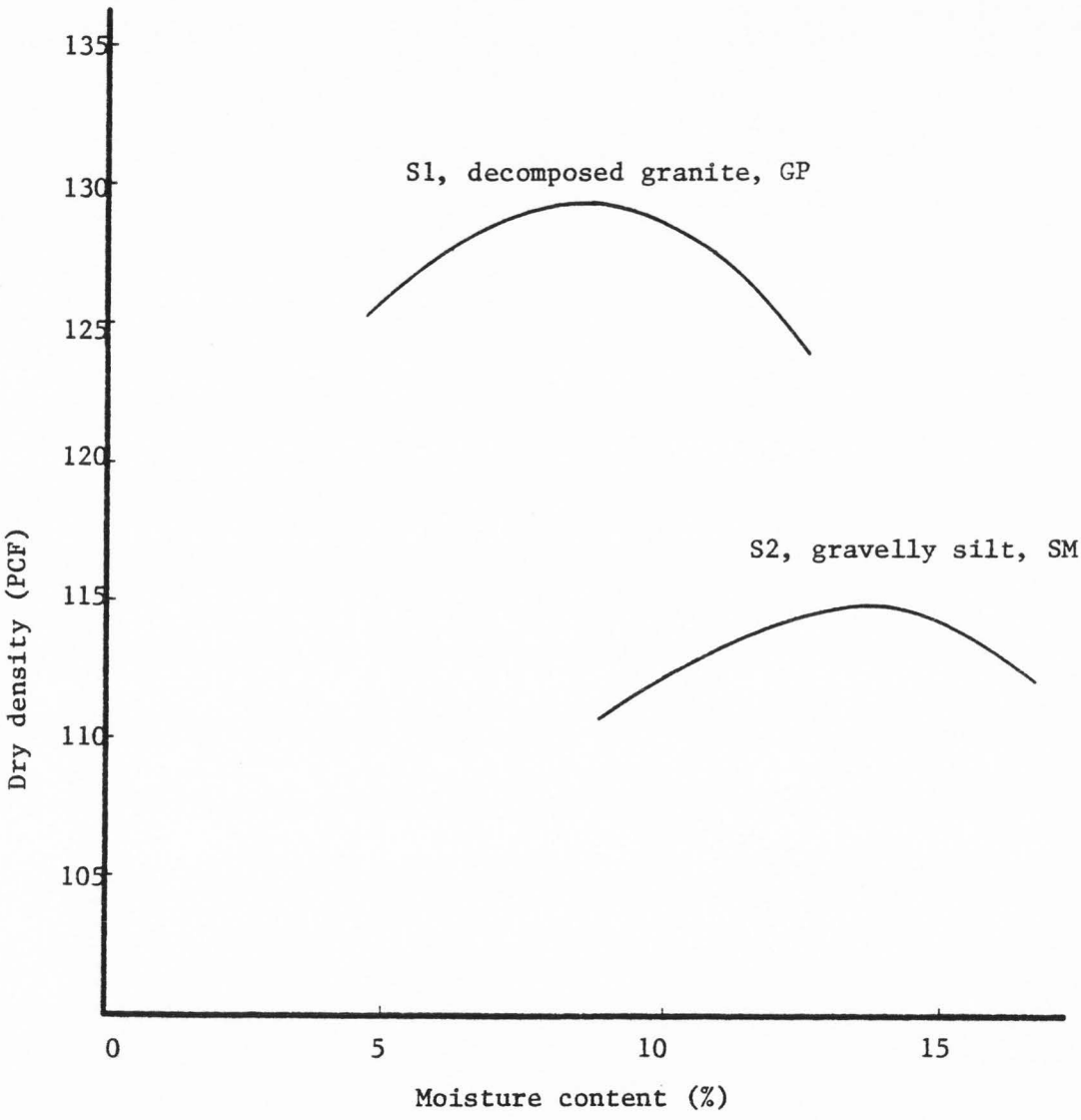

Figure 34. Moisture/density relationships (AASHTO T-99 Method C) for soil used in construction of California wall.

Table 2. Sand cone density tests for San Gabriel wall.

Location of Test	Soil Type	% Relative Compaction
Foundation	GP	71
Foundation Fill	GP	79
Foundation Fill	GP	78
2nd Lift	GP	78
7th Lift	SM	70
8th Lift	SM	68
9th Lift	SM	97
10th Lift	SM	95

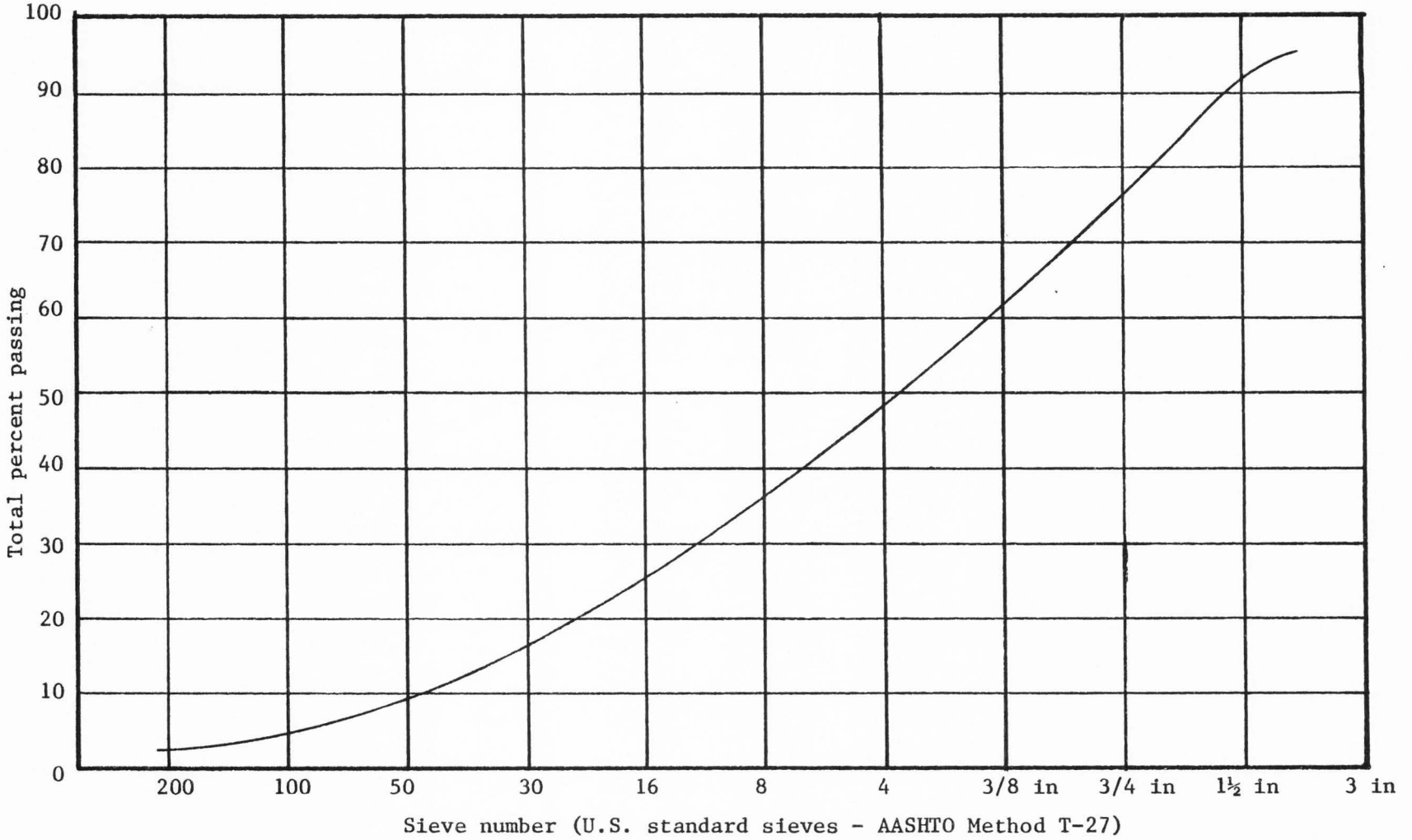

Figure 35. Grain size distribution-sample 1 (GP).

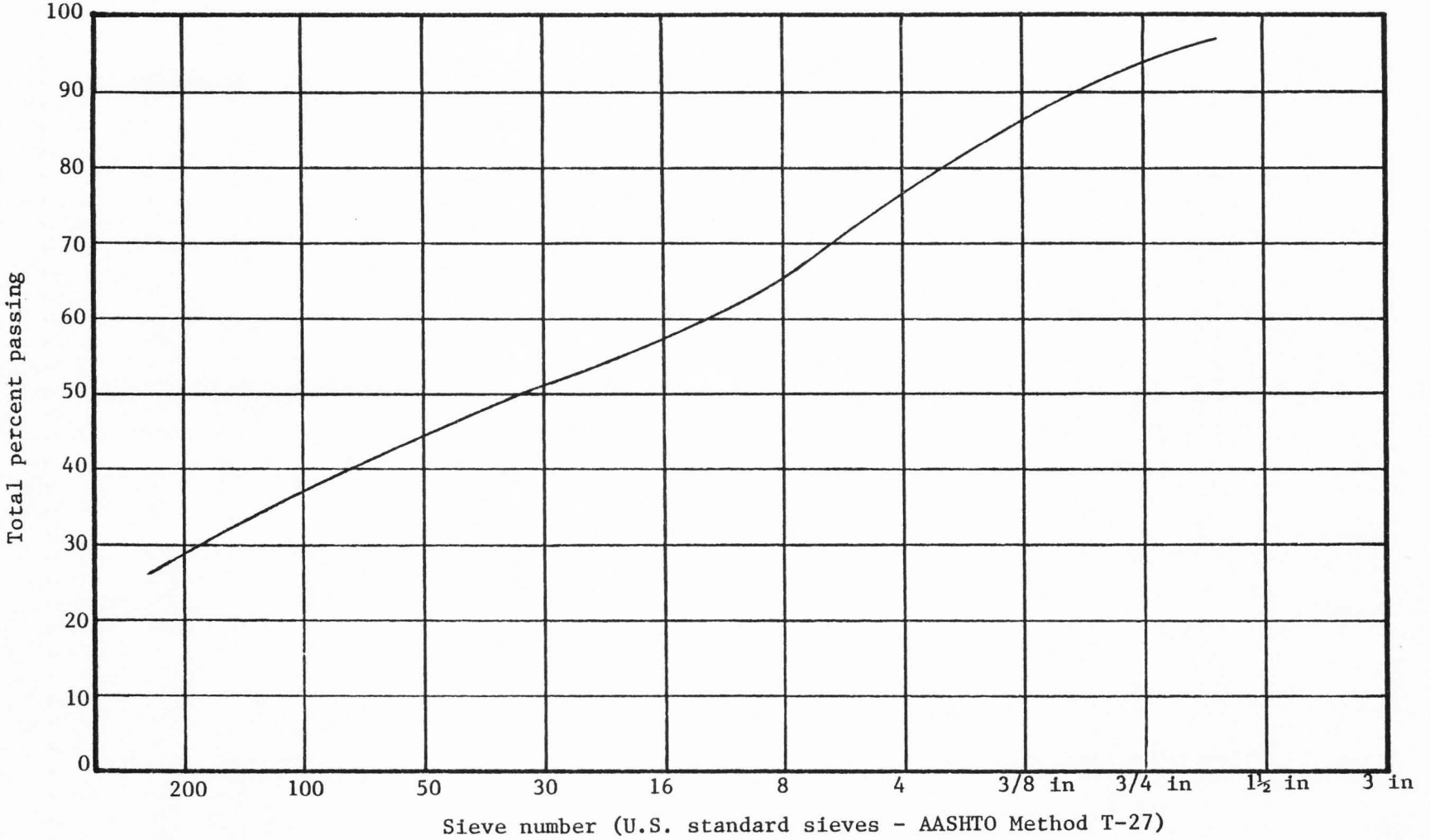

Figure 36. Grain size distribution-sample 2 (SM).

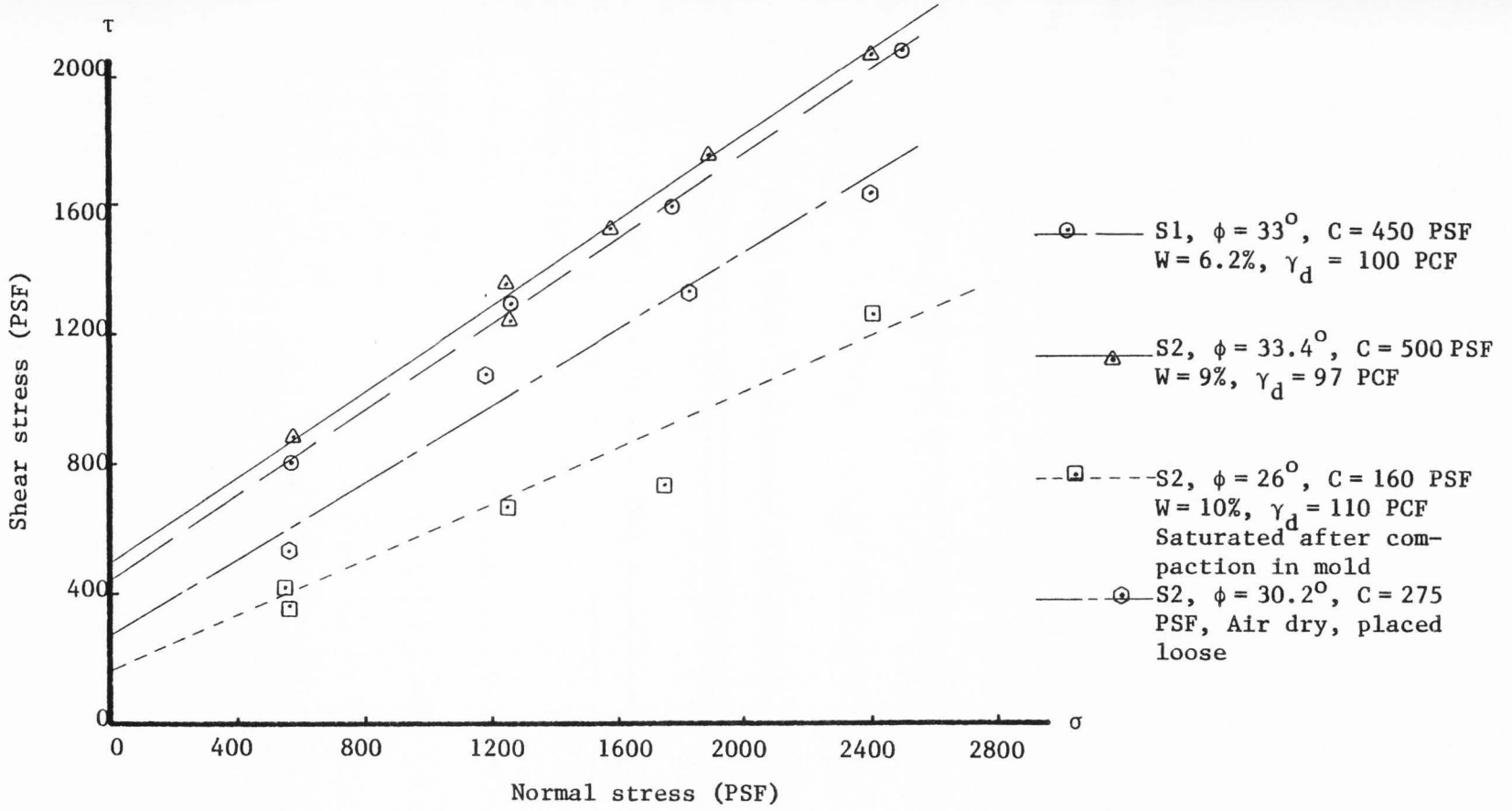

Figure 37. Direct shear tests, S1 and S2.

Appendix B

Field Data

The data from the instrumentation of the Welded Wire Wall in California was taken from four types of instruments: settlement plates, strain gages, extensometers, and survey monuments. For each instrument a zero or base reading was taken at or soon after installation. Thereafter the instruments were monitored as successive lifts were placed over them.

Table 3. Settlement plate data. (relative elevations in feet)

Completed Lift No.	P1	P2	P3	P4	P5	
Foundation Level (zero reading)	159.66	159.40				
2nd	159.65	159.36				
3rd	159.64	159.34				
4th	159.62	159.34				
5th	159.62	159.34	167.01.	166.64	(zero readings for P3,P4)	
7th	159.62	159.33	167.00	166.62		
8th	159.61	159.33	167.00	166.60		
9th	159.60	159.33	167.00	166.59		
10th	159.59	159.33	166.98	166.54	174.75	(zero reading)
Completed Wall	159.54	159.21[a]	166.95	--[a]	--[a]	

[a]Some vandalism had apparently occurred which rendered P2 in question and P4 and P5 useless.

Table 4. Strain gage data, S1 - S12. (S1 - S12; 1st layer placed on top of 2nd lift, see Figure 11.)

Completed Lift No.	S1	S2	S3	S4	S5	S6
Zero reading with 1' of fill	1091	1274	1173	472	-29	603
4th	1109	1277	1209	540	37	661
5th	1159	1305	1230	649	93	710
5th plus 8"	1161	1274	1178	681	49	748
7th	1198	1244	1190	800	244	925
8th	1210	1240	1182	814	268	954
9th	1178	1173	1133	349	6	953
10th	1220	1203	1153	388	42	985
10th (just before heavy rains	1237	1224	1221	452	128	1087
10th (after rains)	1233	1225	1206	406	127	1112
11th	1230	1200	1170	398	114	1087
Wall Complete	1129	1253	1361	386	478	1259

Completed Lift No.	S7	S8	S9	S10	S11	S12
Zero reading with 1' of fill	1260	1324	1442	2342	2232	1523
4th	1372	1396	1510	2391	2308	1608
5th	1452	1450	1589	2444	2339	1665
5th plus 8"	1540	1495	1745	2516	2382	1859

Table 4. Continued.

Completed Lift No.	S7	S8	S9	S10	S11	S12
7th	1695	1627	2096	2640	2548	2007
8th	1715	1640	2126	2655	2563	2017
9th	1312	1411	2168	2362	2376	2066
10th	1347	1446	2206	2392	2421	2095
10th (just before heavy rains)	1400	1497	2270	2382	2435	2089
10th (after rains)	1401	1512	2320	2390	2512	2100
11th	1390	1492	2292	2382	2484	2071
Wall Complete	1494	375	3057	2715	8950	2201

Note: To determine the force in the gage, multiply the net gage reading by: S1 - S3 - .674
S4 - S12 - .552
This will give the force in pounds.

Table 5. Strain gage data, S13 - S24. (S13 - S24; 2nd layer on top of lift #7, see Figure 11)

Completed Lift No.	S13	S14	S15	S16	S17	S18
Zero readings	329	446	854	342	227	331
9th	897	988	1409	1676	1390	1427
10th	914	1002	1422	1712	1408	1513
10th (just before heavy rains)	926	999	1415	1745	1429	1528
10th (after rains)	903	980	1412	1788	1478	1566
11th	563	523	552	1454	1265	1236
Wall Complete	971	1066	1374	1782	1641	1658
Completed Lift No.	S19	S20	S21	S22	S23	S24
Zero readings	590	440	966	1473	1448	1273
9th	1906	1638	2204	2704	2549	2527
10th	1951	1656	2243	2758	2599	2578
10th (just before rains)	1965	1665	2263	2739	2523	2599
10th (after rains)	2048	1727	2343	2770	2642	2674
11th	1472	1308	1384	1333	1223	1427
Wall Complete	2382	1986	2860	3179	2656	2834

Note: To determine force on the gage, apply a corrected zero base (see Chapter 4) and multiply net gage reading by .552 to get force in pounds.

Table 6. Extensometer data (relative movements). (See Figures 11 for locations.)

Completed Lift No.	E1	E2	E3	E4	E5	E6	E7	E8
Zero reading 5th lift	67 9/16	65 15/16	66 1/4	66 3/8				
5th lift plus 8"	67 9/16	65 15/16	66 1/4	66 3/8				
7th	67 9/16	65 3/4	66 1/8	66 1/4				
9th	67 9/16	67 7/8	66 1/16	66 1/4				
10th	67 9/16	65 7/8	66 1/16	66 5/16	60 9/16	60 7/8	60 1/4	60 1/16
10th (after rains)	67 7/16	66 1/16	66 1/8	66 3/16	60 15/32	60 13/16	60 3/32	59 15/16
Wall Complete	66 7/8	65 1/2	65 11/16	65 7/8	59 3/16[a]	59 11/16[a]	58 11/16[a]	58 5/16[a]

[a]Reference plate appears to have been moved and so these readings are in question.

Table 7. Survey monument data. (Horizontal angles measured from a fixed baseline. See Figure 10 for monument location.)

Completed Lift No.	M1	M2	M3	M4
7th (Begin M1 and M2)	10.1650 (H.A.)[a] 83.4150 (V.A.)[a] 4.60 (H.I.)[a]	17.5417° (H.A.) 79.5067 (V.A.) 4.60 (H.I.)		
8th (Begin M3)	10.1667 (H.A.) 4.25 (H.I.)	17.5458 (H.A.) 4.25 (H.I.)	16.9050 (H.A.) 88.5547 (V.A.) 4.25 (H.I.)	
10th	10.1639 (H.A.) 4.20 (H.I.)	17.5458 (H.A.) 4.20 (H.I.)	16.8936 (H.A.) 4.20 (H.I.)	
10th (after rains)	10.1666 (H.A.) 4.30 (H.I.)	17.5511 (H.A.) 4.30 (H.I.)	16.8986 (H.A.) 4.30 (H.I.)	
10th (Plus 6")	10.1898 (H.A.) 4.25 (H.I.)	17.5342 (H.A.) 4.25 (H.I.)	16.8744 (H.A.) 4.25 (H.I.)	
Wall Complete (Begin M4)	10.1361 (H.A.) 83.4061 (V.A.) 4.55 (H.I.)	17.5539 (H.A.) 79.2492 (V.A.) 4.55 (H.I.)	16.8667 (H.A.) 87.3725 (V.A.) 4.55 (H.I.)	17.2511 (H.A.) 91.9017 (V.A.) 4.55 (H.I.)

[a]H.A. = Horizontal angle, V.A. = Vertical angle, H.I. = Height of instrument. Angles in degrees.

Note: Slope distance from instrument to monuments: M1 - 51'5", M2 - 30'6", M3 - 43'7", M4 - not determined.

Appendix C

Pullout Tests Data

Pullout tests

Two series of pullout tests were performed. The first was run with single longitudinal wires, single transverse wires, and sections of mesh with constant mesh openings (2" x 6"). This first series showed the need for additional testing which varied the mesh opening, embedment depth, and overburden pressure.

Table 8. Pullout test data, preliminary tests.

Wire No.	Overburden Height (ft)	Peak Pullout Force (lbs)	Comments
T1 (3 longitudinal wires)	11	2466	
	21	2903	Load cell solder joint broke, test inconclusive
T2 (3 longitudinal wires	11	2236	
	21	3246	Test incomplete - 2 longitudinal wires broke
T3 (5 longitudinal wires)	11	3751	
	21	5026	Shear pins on pullout device broke before test completed
T4	11	3485	
3 longitudinal wires with 1 transverse	11	435	Questionable due to very large displacement before peak pullout force
	19	782	
	11	861	
	21	1253	

Table 8. Continued.

Wire No.	Overburden Height (ft)	Peak Pullout Force (lbs)	Comments
Single	11	125	
longitudinal	19	195	
wire	19	231	

The second series was done with mat sections of 3 longitudinal wires and varied mesh openings, embedment depths, and overburden heights. Two groups (A and B) were run, with the A group having an initial embedment of 3 feet and the B group having an initial embedment of 5 feet.

Table 9. Pullout test data, varied mesh sizes.

Wire #	Longitudinal Spacing (a) (in)	Transverse Spacing (b) (in)	L_o (ft)	Peak Pullout Force (in)	Displacement At Peak Force (in)	Overburden Height (ft)	Comments
A1[a]	2	6	3	628	.94	10	
			2.5	625	1.50	15 -	Trans. wire hooked on
			2	666	1.19	20	grate
A2	4	6	3	1632	2.67	10	
			2.5	2448	1.12	15	
			2	2688	1.06	20	
A3	6	6	3	2180	2.5	10	
			2.5	3114	1	15 -	Could not reach peak
			2	--	--	No Pull	or wire would break[b]
A4	2	12	3	349	4.25	10	
			2.5	403	.313	15	
			2	277	1.513	20	
A5	4	12	3	1640	2.44	10	
			2.5	2378	2.12	15 -	Trans. wire broke
			2	1769	2.375	20 -	Another trans. wire broke
A6	6	12	3	1265	2.19	10	
			2.5	1122	2.44	15 -	Trans. wire broke
			2	783	1.94	20	
B1	2	6	5	1985	1.69	10	
			4.5	2484	1.50	15	
			4	3258	.25	20 -	Backed off before over-
							load

Table 9. Continued.

Wire #	Longitudinal Spacing (a) (in)	Transverse Spacing (b) (in)	L_o (ft)	Peak Pullout Force (in)	Displacement At Peak Force (in)	Overburden Height (ft)		Comments
B2	4	6	5	2740	.75	10	-	Backed off before overload
B3	6	6	5	3688	2.313	10	-	Peak force is approximate due to load cell failure
B4	2	12	5	1155	2.5	10		
			4.5	1410	1.62	15		
			4	1074	2.12	15		
			3.5	1191	1	20		
			3.25	1321	2.25	25		
			2.92	1924	2.5	37		
			2.58	1698	4	46	-	Trans. wire failed
B5	4	12	5	1830/ 2103	2.06/ 5.62	10	-	Showed two peaks
			4.5	2789	1.5	15	-	Trans. wire broke
B6	6	12	5	2392	2.88	10		

[a]The process of testing was to set the mesh in the cell at an initial embedment (3 or 5 feet), load the cell with 10 feet of equivalent soil pressure, and pull the mesh through a peak pullout resistance a total of 6 inches. The pressure was increased to 15 feet and the section pulled another 6 inches. Except in the case of B4 this process was only taken one more step, to 20 feet of pressure.

[b]The approximate tensile capacity of three longitudinal wires is 3200 lbs. The load cells were designed to handle about 1150 lbs each, for maximum sensitivity. It was occasionally necessary to end the test before the peak force was achieved to avoid damage to the equipment.

Table 10. Single wire pullout tests.

L_o (ft)	Overburden Height (ft)	Peak Force (lbs)
3	10	66
2.33	20	92
3	15	50
2.00	20	43
5	10	130
4.5	20	160
5	10	220
4.5	15	152

Appendix D

Laboratory Test Wall Data

Table 11. Laboratory test wall data. (Figure 38)

Soil Height (ft)	Gage Reading (Micro-inches/inch)[a] 1	2	3	4	5	6	7	8	9	10
0	0	0	0	0	0	0	0	0	0	0
1.25	10	13	10	19	19	14	4	26	31	33
1.8	6	2	14	-6	-16	-9	18	-14	-20	-14
4.6	25	27	43	14	1	-19	47	29	13	0
10.0	48	76	117	77	30	36	107	133	120	47
(After 10 min)	50	74	121	83	-11	33	107	131	128	43
(After 15 min)	39	66	101	67	-37	19	96	113	101	22
15.0	56	106	183	131	15	25	145	201	243	81
20.0	66	114	240	195	6	33	183	265	307	131
(After 10 min)	62	131	243	194	-9	8	179	260	303	126
25.0	79	176	314	261	51	48	222	344	396	177
30.0	95	211	388	317	82	56	263	420	470	217
(After 25 min)	100	210	392	330	111	41	271	420	477	220
(After 8 hours)	113	212	398	336	119	29	265	408	478	227
35.0	130	242	443	366	143	74	396	460	510	252
40.0	157	301	550	450	168	-	442	571	624	300
(After 40 min)	-	295	540	447	163	-	428	442	618	288
45.0	-	325	590	480	183	-	480	604	665	314
50.0	-	374	677	549	195	-	534	655	750	356
(After 40 min)	-	371	676	556	234	-	540	644	760	353
55.0	-	409	718	600	258	-	568	676	806	385
60.0	-	439	794	642	285	-	592	736	870	406
65.0	-	476	900	701	300	-	623	800	906	438
70.0	-	501	960	762	342	-	650	858	969	461
76.0	-	546	1020	794	392	-	704	894	1014	485
(After 10 min)	-	560	-	824	386	-	386	937	937	483
82.0	-	587	-	866	410	-	415	983	988	511
87.0	-	603	-	920	-	-	438	1040	1048	538
(After 10 min)	-	625	-	948	-	-	401	1061	1047	537

Table 11. Continued.

Soil Height (ft)	Gage Reading (Micro-inches/inch)[a] 1	2	3	4	5	6	7	8	9	10
95.0	-	694	-	1022	-	-	438	1104	1126	568
90.0	-	678	-	1027	-	-	360	1100	1128	560
(After 10 min)	-	690	-	1034	-	-	364	1104	1128	563
3.0	-	80	-	117	-100	-	70	32	120	94
0.0	-	37	-	-	-14	-	98	-50	82	-

[a]Multiply gage reading by 1.25 to get wire force in pounds.

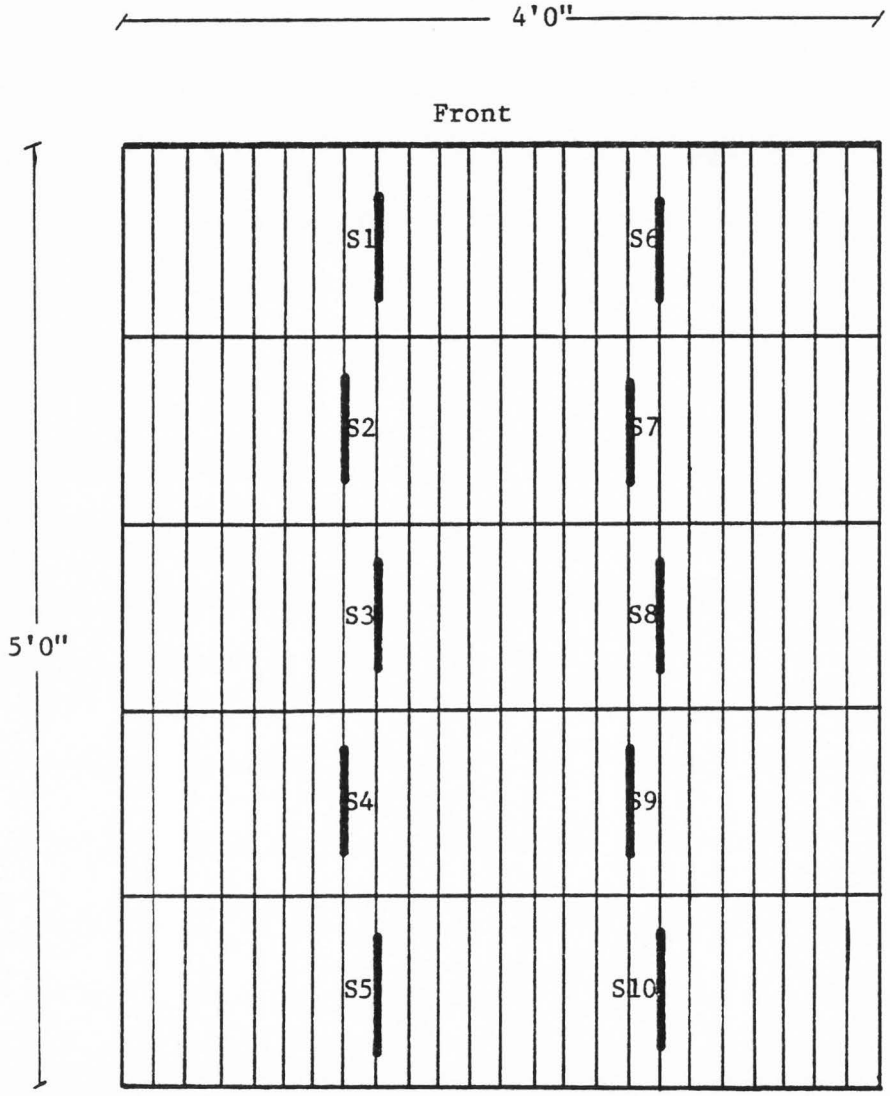

Figure 38. Plan view of instrumentation layout on wire mat for test wall.

Appendix E

Hypothetical Design Problem

To illustrate the design procedure, a hypothetical 20 foot high wall (Figure 40) with a 3 foot dead load surcharge and a level backfill will be designed. Consider the foundation and backfill material to be sand with a unit weight of 110 PCF and a friction angle of 33^{o}.

External stability

The overall dimensions of the wall will initially be selected on the basis of external stability requirements. Since the backfill and natural soil at the site are sand, base the lateral pressure for external stability requirement on the active case. Consideration of external stability should include sliding, overturning and bearing capacity.

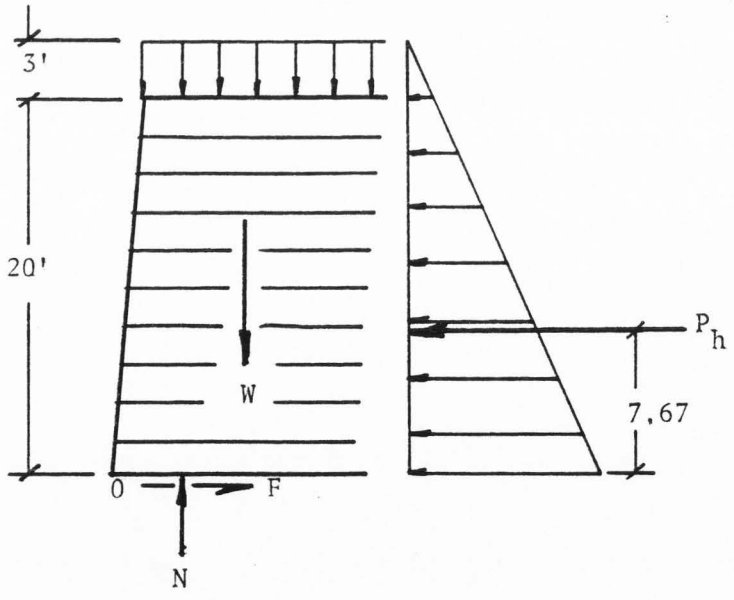

Figure 39. Freebody Diagram of Wall

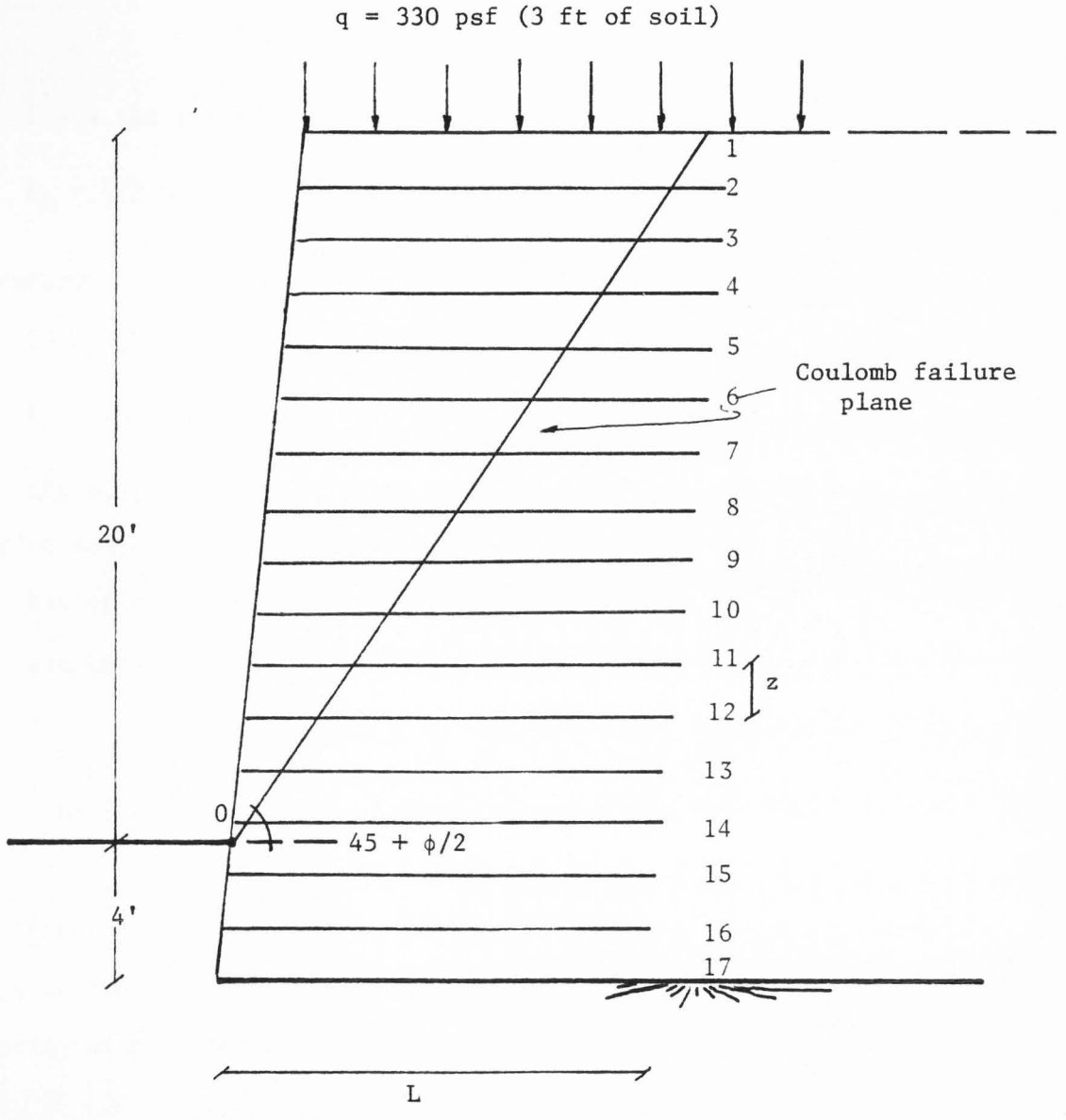

Figure 40. Cross-section for hypothetical design problem (N.T.S.).

Sliding. Use the sliding criteria with a factor of safety of 1.5 to select an initial trial length for the wire mats. From the freebody diagram of Fig. 39 the factor of safety can be expressed as,

$$F.S. = \frac{F}{P_h} = 1.5$$

or

$$F = 1.5\ P_h$$

$$F = N \tan \phi = 23\ L\ (110) \tan \phi$$

$$P_h = 1/2\ K_a\ \gamma H^2 = 1/2\ (0.3)\ 110\ (23)^2$$

therefore

$$23\ L\ 110 \tan 33^o = 1.5\ (1/2\ (0.3)\ 110\ (23)^2)$$

L = 8.0 feet minimum ---- use L = 10.0 feet

Check overturning. Taking moments about "O", the ratio of the resisting moment to the overturning moment should be 1.5 or greater.

Resisting moment = 1/2 L W = 1/2 L ($HL\gamma$)

Overturning moment = 7.67 P_h = 7.67 ($1/2\ K_a\ \gamma H^2$)

$$\frac{1/2\ L\ H\ L\ \gamma}{7.67\ (1/2\ K_a \gamma H^2)} = \frac{L^2}{7.67\ K_a H} = \frac{100}{7.67\ (0.3)\ 23} = 1.89 > 1.5$$

Check bearing capacity. Since settlement will take place during construction base the allowable bearing pressure on the ultimate bearing capacity with a factor of safety of 3.0.

$$q_{ult} = 1/2\ B\gamma N_\gamma + \gamma D(N_q - 1)$$

The width B in the bearing capacity equation is the length, L, of the longitudinal wires. However, since the base is loaded eccentrically an effective width B' must be used.

$$B' = L - 2e$$

$$e = \frac{M}{N} = \frac{H/3\ (1/2)\ K_a \gamma H^2}{H(L)\gamma}$$

$$e = \frac{K_a H^2}{6L} = \frac{0.3\ (27^2)}{6(10)} = 3.65 \text{ ft.}$$

$$B' = 10 - 2(3.65) = 2.70 \text{ ft.}$$

The ultimate bearing capacity can now be computed based on B'

$$q_{ult} = 1/2\ (2.7)\ (110)\ (35.6) + 110\ (4)\ (26.3 - 1)$$

$$q_{ult} = 5{,}287 + 11{,}132 = 16{,}520 \text{ psf}$$

$$q_a = \frac{q_{ult}}{3} = \frac{16520}{3} = \underline{5{,}510} \text{ psf}$$

Since the resultant is outside the middle third of the base the maximum bearing pressure must be calculated on the basis of a triangular pressure distribution. The base of the triangle will be

$$\text{base} = 3\ (\tfrac{L}{2} - e)$$

and the area of the triangular pressure distribution must equal the normal force N.

$$1/2 q_{max}\ (3)(\tfrac{L}{2} - e) = N$$

$$N = HL\gamma$$

$$q_{max} = \frac{2HL\gamma}{3(\frac{L}{2} - e)}$$

For a mat length of 10 ft.

$$q_{max} = \frac{2(27)(10)(110)}{3(\frac{10}{2} - 3.65)} = 14{,}670 \text{ psf} > 5{,}510 \text{ psf}$$

Since the maximum bearing pressure is greater than the allowable bearing pressure increase the length of the mat.

Try L = 12 ft

$$e = \frac{K_a H^2}{6L} = \frac{0.3(27^2)}{6(12)} = 3.04$$

$$B' = 12 - 2(3.04) = 5.92 \text{ ft}$$

$$q_{ult} = 1/2(5.92)\ (110)\ (35.6) + 110(4)\ (26.3-1)$$

$$q_{ult} = 22{,}700 \text{ psf}$$

$$q_{allow} = \frac{22{,}700}{3} = \underline{7{,}570 \text{ psf}}$$

Again, the resultant is outside the middle third

$$q_{max} = \frac{2(27)\ (12)110}{3(\frac{12}{2} - 3.04)} = 8{,}027 \text{ psf} > 7{,}570 \text{ psf}$$

Try L = 13 ft

$$e = \frac{K_a H^2}{6L} = \frac{0.3(27^2)}{6(13)} = 2.80$$

$$B' = 13\text{-}2\ (2.80) = 7.40$$

$$q_{ult} = 1/2(7.40)(110)(35.6) + 110(4)(26.3-1)$$

$$q_{ult} = 25{,}600$$

$$q_{allow} = \frac{25{,}600}{3} = 8{,}530 \text{ psf}$$

The resultant is again slightly outside the middle third

$$q_{max} = \frac{2(27)(13)(110)}{3(\frac{13}{2} - 2.80)} = 6{,}960 \text{ psf} < 8{,}530 \text{ psf}$$

Use L = 13.0 ft

Internal stability - design of wire mats

In order to facilitate field bending of the wires, use 9 gage wire.

Tension in wires. Establish the spacing of the longitudinal wires required to resist tension.

$f_y = 65{,}000$ psi

Dia = 0.150 in.

Area = 0.0177 sq. in.

Consider the corrosion rate to be 0.25 ounces per square foot of surface area, per year. For a 25 year structure life this would give the following design dimensions:

Dia = 0.130 in.

Area = 0.0132 in^2

Based on the AISC code, the allowable stress for a tension member is $F_t = 0.6\ f_y$. therefore,

$$F_t = 0.6\ (65{,}000) = 39{,}000$$

The allowable tension force, T_a, in each longitudinal wire becomes

$$T_a = (0.0132)\ 39{,}000 = 515 \text{ pounds}$$

Compute the tension force in the longitudinal wires based on a lateral pressure coefficient of K = 0.65.

From Equation 2

$$F = K\ \sigma_v\ a\ z$$

where

σ_v = vertical soil pressure = γH

z = vertical spacing of mats

a = horizontal spacing of wires

The required horizontal spacing can be obtained from the above equation. For a vertical spacing of z = 18 inches the required horizontal spacing becomes.

Depth below top	σ_v (PSF)	a (in)
20	2530	2.5
16	2090	3.0
12	1650	3.8
8	1210	5.2
4	770	8.2
0	330	19.2

At this point, it is pertinent to consider economics. The amount of money saved by optimizing the wire spacing and saving material could easily be offset by additional fabrication costs and handling costs. The single most important consideration will be the amount of material used, in other words, the length of the wall. Depending on economics there are three reasonable combinations of wire spacing that could be used. The first would be to use a uniform spacing of 2 inches throughout the construction. The second is:

Depth from top (ft)	a (in)
0 - 10	4
10 - 25	2

and the third is:

Depth from top (ft)	a (in)
0 - 8	4
8 - 16	3
16 - 24	2

Check pullout. With the wall essentially sized it is necessary to check the pullout resistance and compare it with the applied pullout force. Figure 27 can be used to determine the pullout resistance of each mat. Only that portion of the mat extending beyond the Coulomb failure plane, shown on Figure 40, should be considered effective in providing resistance to pullout. The table shown below illustrates a systematic evaluation of the pullout resistance for a one foot wide section of mat. Note that 4000 pounds per foot is used as a limiting value of the pullout resistance. Since this exceeds the allowable tension force per foot of wall for nine gage wire on two inch centers (25 year life) it does not create a severe limitation to the design. If a higher resistance is required the vertical spacing of the mats should be decreased. The variables used in the table are defined as follows:

L_{EFF} = Length of mat extending beyond the Coulomb failure plane

σ_v = Vertical stress at the level of the mat

N = Number of transverse wires beyond the Coulomb failure plane that are effective in providing pullout resistance

W = Width of mat being considered (12 inches for this example)

F_p = Pullout resistance per width W of mat as obtained from Figure 27. The upper limit is 4000 pounds per foot.

A wall batter of 1 horizontal to 12 vertical was used in computing L_{EFF}.

Mat #	L_{EFF} (ft)	σ_v (psi)	N (6" spacing)	$NW\sigma_v$	Fp/ft
1	3.7	2.29	8	220	960
2	4.4	3.44	9	372	1620
3	5.1	4.58	11	605	2500
4	5.8	5.73	12	825	3040
5	6.5	6.88	13	1073	3500
6	7.2	8.02	15	1444	3900
7	7.9	9.17	16	1761	4000
8	8.6	10.31	18	2227	4000
9	9.3	11.46	19	2613	4000
10	10.0	12.60	20	3024	4000
11	10.7	13.75	22	3630	4000
12	11.4	14.90	23	4112	4000
13	12.1	16.04	25	4812	4000
14	12.8	17.19	26	5363	4000
				ΣF_p	47520

The pullout resistance should now be compared with the computed tension force in the longitudinal wires. The table below shows the computed values of the tension force per foot of wall and compares these values with the pullout resistance, F_p, computed above. The following equation was used to compute the tension force in mats 2 through 14.

$$F = K\sigma_v Wz$$

where K = 0.65

Mat #	Tension Force/ft.	F.S.
1	503	1.91
2	483	3.35
3	644	3.88
4	804	3.78
5	965	3.63
6	1126	3.46
7	1287	3.11
8	1448	2.76
9	1609	2.49
10	1770	2.26
11	1931	2.07
12	2091	1.91
13	2252	1.78
14	2413	1.66
ΣF	19326	

The overall F.S. becomes,

$$F.S. = \frac{\Sigma F_p}{\Sigma F} = \frac{47520}{19326}$$

$$F.S. = 2.46$$

A factor of safety of 2.0 or greater should be adequate.

This problem considers a level backfill only. A sloping backfill would increase the horizontal pullout forces. It is also necessary to consider any water present (runoff or groundwater). Ditches to handle runoff and blanket drains to handle groundwater may be necessary as dictated by the situation. It should also be realized that the backfill material considered is ideal. Highly plastic soils may not have as great a resistance to pullout.